

AD _____

Award Number: DAMD17-02-1-0667

TITLE: Pathogenesis of Ovarian Serous Carcinoma as the Basis for Immunologic Directed Diagnosis and Treatment

PRINCIPAL INVESTIGATOR: Robert J. Kurman, M.D.
Ie-Ming, M.D., Ph.D.
Richard Roden, Ph.D.
T-C Wu, M.D., Ph.D.

CONTRACTING ORGANIZATION: The Johns Hopkins University
School of Medicine
Baltimore, Maryland 21205

REPORT DATE: August 2004

TYPE OF REPORT: Annual

PREPARED FOR: U.S. Army Medical Research and Materiel Command
Fort Detrick, Maryland 21702-5012

DISTRIBUTION STATEMENT: Approved for Public Release;
Distribution Unlimited

The views, opinions and/or findings contained in this report are those of the author(s) and should not be construed as an official Department of the Army position, policy or decision unless so designated by other documentation.

REPORT DOCUMENTATION PAGEForm Approved
OMB No. 074-0188

Public reporting burden for this collection of information is estimated to average 1 hour per response, including the time for reviewing instructions, searching existing data sources, gathering and maintaining the data needed, and completing and reviewing this collection of information. Send comments regarding this burden estimate or any other aspect of this collection of information, including suggestions for reducing this burden to Washington Headquarters Services, Directorate for Information Operations and Reports, 1215 Jefferson Davis Highway, Suite 1204, Arlington, VA 22202-4302, and to the Office of Management and Budget, Paperwork Reduction Project (0704-0188), Washington, DC 20503

1. AGENCY USE ONLY (Leave blank)		2. REPORT DATE August 2004	3. REPORT TYPE AND DATES COVERED Annual (1 Aug 2003 - 31 Jul 2004)	
4. TITLE AND SUBTITLE Pathogenesis of Ovarian Serous Carcinoma as the Basis for Immunologic Directed Diagnosis and Treatment			5. FUNDING NUMBERS DAMD17-02-1-0667	
6. AUTHOR(S) Robert J. Kurman, M.D., Ie-Ming, M.D., Ph.D. Richard Roden, Ph.D., T-C Wu, M.D., Ph.D.				
7. PERFORMING ORGANIZATION NAME(S) AND ADDRESS(ES) The Johns Hopkins University School of Medicine Baltimore, Maryland 21205 E-Mail: rkurman@jhmi.edu			8. PERFORMING ORGANIZATION REPORT NUMBER	
9. SPONSORING / MONITORING AGENCY NAME(S) AND ADDRESS(ES) U.S. Army Medical Research and Materiel Command Fort Detrick, Maryland 21702-5012			10. SPONSORING / MONITORING AGENCY REPORT NUMBER	
11. SUPPLEMENTARY NOTES Original contains color; all DTIC reproductions will be in black and white.				
12a. DISTRIBUTION / AVAILABILITY STATEMENT Approved for Public Release; Distribution Unlimited			12b. DISTRIBUTION CODE	
13. ABSTRACT (Maximum 200 Words) See abstracts in respective projects 1-3.				
14. SUBJECT TERMS etiology, pathways, early detection, tumor antigen, antigen-specific tumor immunity, murine model			15. NUMBER OF PAGES 115	
			16. PRICE CODE	
17. SECURITY CLASSIFICATION OF REPORT Unclassified	18. SECURITY CLASSIFICATION OF THIS PAGE Unclassified	19. SECURITY CLASSIFICATION OF ABSTRACT Unclassified	20. LIMITATION OF ABSTRACT Unlimited	

Table of Contents

Cover	1
SF 298	2
Table of Contents	3
Introduction	
See Project 1: "Molecular Characterization of Ovarian..."	
See Project 2: "Identification of Autologous Antigens..."	
See Project 3: "Development of Antigen-Specific Cancer..."	
Body	
Key Research Accomplishments	
Reportable Outcomes	
Conclusions	
References	
Appendices	

PROJECT 1 – MOLECULAR CHARACTERIZATION OF OVARIAN SEROUS
TUMORS DEVELOPING ALONG DIFFERENT PATHWAYS

Ie-Ming Shih, M.D., Ph.D.

ABSTRACT:

The purpose of this study is to elucidate the pathogenesis of serous carcinoma by identifying the molecular genetic changes and preferentially expressed genes of different histological types of serous neoplasms. We hypothesize that the development of serous carcinoma proceeds along two main pathways: one is rapid progression from ovarian surface epithelium to high-grade serous carcinoma without well-established morphological precursors ("de novo" pathway) and the other is a gradual development from borderline tumors, to non-invasive micropapillary serous carcinomas then to low-grade carcinomas (stepwise pathway). The first pathway results in a high-grade neoplasm (conventional serous carcinoma) and the second leads to the development of a low-grade indolent tumor. Both types of carcinomas and the putative precursor lesions of invasive MPSC are characterized by distinctive molecular genetic alterations and specific gene expression. We identified that mutations in *KRAS* and *BRAF* genes characterized the development of low-grade serous carcinomas. Expression of HLA-G, apoE and membralin molecules were confined to high-grade serous carcinomas. This project, designed to test our proposed model of diverse pathways in the pathogenesis of ovarian serous carcinoma, provides an etiologic basis for the other two projects.

Table of Contents

Cover.....	1
Abstract.....	2
Table of Contents.....	3
Introduction.....	4
Body.....	5
Key Research Accomplishments.....	7
Reportable Outcomes.....	8
Conclusions.....	9
References.....	10
Appendices.....	11

INTRODUCTION

The objective of this proposal is to elucidate the pathogenesis of serous carcinoma by identifying the molecular genetic changes and preferentially expressed genes of different histological types of serous neoplasms. We hypothesize that the development of serous carcinoma proceeds along two main pathways: one is rapid progression from ovarian surface epithelium to conventional serous carcinoma without well-established morphological precursors ("de novo" pathway) and the other is a gradual development from serous borderline tumor (atypical proliferative tumor), to non-invasive micropapillary serous carcinoma then to invasive micropapillary serous carcinoma (stepwise pathway). The first pathway results in a high-grade neoplasm (conventional serous carcinoma) and the second leads to the development of a low-grade indolent tumor (invasive micropapillary serous carcinoma). Both types of carcinomas and the putative precursor lesions of invasive micropapillary serous carcinoma are characterized by distinctive molecular genetic alterations and specific gene expression. This project, designed to test our proposed model of diverse pathways in the pathogenesis of ovarian serous carcinoma, provides an etiologic basis for the other two projects in this proposal. Although many genes are altered during tumorigenesis, only a few are truly critical for tumor progression. Identifying these genes holds promise for the development of new diagnostic assays and immunology-directed treatment for patients with different types of serous carcinoma.

BODY

There are no substantial changes or modifications of the original statements. The accomplishments associated with each task outlined in the approved statement of work are detailed, point by point in the followings.

Task 1: To characterize the molecular genetic alterations of ovarian serous tumors developing along two different pathways.

In the past several years, we have conducted a systematic clinicopathologic and molecular analysis of a large number of SBTs and invasive epithelial ovarian tumors of all histologic types in an effort to delineate their pathogenesis and behavior¹. By careful examination of histopathology of SBT, we identify a unique "variant" of SBTs- non-invasive micropapillary serous carcinoma (or intraepithelial low-grade serous carcinoma) which are more frequently associated with extraovarian disease (implant) and poor clinical outcome as compared to the conventional SBT (called atypical proliferative tumor)²⁻⁵. We define the morphological criteria of "good" versus "bad" implants to predict the clinical outcome in SBT patients⁶. Based on mutational analysis and the patterns of allelic imbalance, we provide the molecular evidence of tumor progression from cystadenoma to atypical proliferative tumor, intraepithelial low-grade serous carcinoma (or non-invasive micropapillary serous carcinoma) then to invasive low-grade serous carcinoma⁷. We demonstrate that mutations in BRAF and KRAS characterize SBT and low-grade serous carcinoma^{7,8} and that mutations in both genes occur early in the tumor progression, i.e., the cystadenoma stage, preceding the development of SBTs⁹. We show that mutations of BRAF and KRAS correlate with the activation of mitogen activated protein kinase (MAPK), the downstream target of KRAS-BRAF signaling pathway, in SBT and low-grade serous carcinomas¹⁰ and have defined the downstream molecular targets regulated by activated MAPK in SBT using serial analysis of gene expression (Pohl, unpublished data). We further show that in contrast to BRAF and KRAS, mutations in p53 gene are significantly less frequent in SBTs and low-grade serous carcinoma than in conventional high-grade serous carcinoma^{11,12}. We have studied the chromosomal imbalance in SBTs using CGH and demonstrated that the pattern of chromosomal imbalance was similar between APST and non-invasive MPSC (intraepithelial low-grade serous carcinoma) but distinct from conventional high-grade serous carcinoma¹³. Based on our studies, we have extended our "dualistic pathway" model into a modified hypothesis in the development of ovarian cancer¹.

Task 2: To identify the genes preferentially expressed in the serous carcinomas.

We have continued to perform serial analysis of gene expression (SAGE) to characterize differential genes expressed in either low-grade (micropapillary) or high-grade serous carcinomas. We have finished SAGE library construction, sequencing and analysis in 2 high-grade and 2 low-grade ovarian serous carcinomas in the second year of the funding period. We then combined the SAGE results and cDNA microarray analysis (as an alternative approach to complement SAGE as described in the original aim), we have identified several high-grade associated and low-grade associated genes in ovarian cancer. More specifically, we have identified HLA-G, membralin and apolipoprotein E overexpression in high-grade but not in low-grade serous carcinoma. This part of study has been published in *Clin Cancer Res*¹⁴ and has been submitted for publication (including a research paper pending revision in *Cancer Res*). The validation and clinical application of HLA-G and apolipoprotein E expression will be described in the next section (Task 3). Besides, we have identified two low-grade associated genes, p21 and anti-trypsin, based on analysis of SAGE data we have collected.

Task 3: To validate the candidate genes and assess their biological significance in the development of serous carcinoma.

We have validated three of the candidate genes, HLA-G, apolipoprotein E and membralin in high-grade ovarian serous tumors and sought for the clinical application and biological functions of these markers¹⁴. The summary of these three studies are summarized as follows.

HLA-G molecule is a MHC class II molecule involved in immune response. The HLA-G immunoreactivity ranging from focal to diffuse was detected in 45 of 74 (61%) high-grade ovarian serous carcinomas but in none of the 18 low-grade serous carcinomas or 26 serous borderline tumors (atypical proliferative tumors and non-invasive micropapillary serous carcinomas) that were studied. The differential expression of HLA-G in high-grade but not low-grade serous carcinomas may have biological significance as HLA-G appears to facilitate tumor cell evasion of the immune system by protecting the malignant cells from lysis by natural killer cells. This finding is similar to the HLA-G expression observed in large cell carcinoma of the lung that is associated with a poor outcome as compared with absence of expression in carcinomas with a better prognosis. HLA-G staining was not detected in a wide variety of normal tissues including ovarian surface epithelium and normal breast tissue. RT-PCR demonstrated the presence of HLA-G5 isoform in all tumor samples expressing HLA-G. ELISA was performed to measure the sHLA-G in 42 malignant and 18 benign ascites supernatants. sHLA-G levels were significantly higher in malignant ascites than in benign controls ($p < 0.001$). We found that the area under the receiver-operating characteristic (ROC) curve for sHLA-G was 0.95 for malignant versus benign ascites specimens. At 100% specificity, the highest sensitivity to detect a malignant ascites was 78% (95% CI, 68% - 88%) at a cutoff of 13 ng/ml. In summary, our findings suggest that measurement of sHLA-G is a useful molecular adjunct to cytology in the differential diagnosis of malignant versus benign peritoneal ascites.

Apolipoprotein (Apo) E has been recently identified as a potential tumor-associated marker in ovarian cancer by serial analysis of gene expression. ApoE has long been known to play a key role in lipid transport and its specific isoforms participate in the atherosclerogenesis. However, its role in human cancer is not known. In this study, apoE expression was frequently detected in ovarian serous carcinomas, the most common and lethal type of ovarian cancer. It was not detected in serous borderline tumors and normal ovarian surface epithelium. Inhibition of apoE expression using an apoE specific siRNA led to G₂ cell cycle arrest and apoptosis in an apoE expressing ovarian cancer cell line, OVCAR3, but not in an apoE negative cell line, SKOV3. Furthermore, the phenotype of apoE-siRNA treated OVCAR3 cells was not reversed by exogenous apoE in the culture medium. Expression of apoE in nuclei was significantly associated with a better patient survival who had advanced stage serous carcinomas at the 5-year follow-up ($p = 0.004$). This study suggests a new role of apoE in cancer as apoE expression is important for the survival in apoE expressing ovarian cancer cells and its expression is associated with a favorable clinical outcome in ovarian cancer patients.

A novel gene, membralin, was cloned from a human ovarian cancer cell line in the DoD 2nd year funding period. Human membralin is unique without significant sequence homology to other human genes except the membralin from the other species. The gene contains 11 exons which encodes at least two spliced variants in human cancer. The long form of membralin is composed of 11 exons, encoding a protein of 620 amino acids and the short form contains all exons except the exon 10, encoding a protein of 408 amino acids. Expression of different membralin isoforms depends on the tissue type. Long form of membralin is expressed in ovarian and colorectal carcinomas but not in breast or pancreatic carcinomas which express only the short form. Membralin-GFP fusion protein demonstrates its exclusive cytoplasmic localization. Based on quantitative real-time PCR, in situ hybridization and Western blot analysis, membralin was highly expressed in ovarian serous carcinomas as compared to serous borderline tumors and ovarian surface epithelium ($p < 0.001$). Furthermore, the expression level of membralin correlated with a worse 5-year survival in patients with previously untreated stage III ovarian serous carcinomas ($p < 0.05$). In conclusion, these findings provide the first characterization of human membralin and suggest that membralin is a novel tumor-associated marker in ovarian serous carcinomas with potential prognostic significance.

KEY RESEARCH ACCOMPLISHMENTS

- Continue providing molecular genetic evidence to support the hypothesis of the dualistic pathway in the development of ovarian serous carcinoma. We further modify and extend our hypothesis to include all the major types of ovarian carcinomas.
- Mutations of *KRAS* and *BRAF* characterize the development of low-grade (invasive micropapillary) serous carcinomas based on mutational analysis of 186 ovarian serous tumors.
- Demonstration of mutations of *KRAS* and *BRAF* occur very early in the tumor progression of serous borderline tumors, suggesting “gate-keeper” roles of both genes in the development of serous borderline tumors.
- HLA-G, apoE and membralin overexpression is associated with high-grade (conventional) serous carcinomas and p21 and anti-trypsin overexpression is associated with low-grade serous tumors. Further studies reveal their clinical relevance and biological functions in ovarian serous carcinomas.
- Completion in the generations of ovarian tumor tissue arrays including a whole spectrum of lesions and normal tissues that could serve as an important research tool for this program project and others in ovarian cancer research. The tissue microarray set is currently ready to be used in the entire program project.

REPORTABLE OUTCOMES

Articles published in the 2nd year of funding period (September, 2003-August 2004):

Ho C-L, Kurman RJ, Dehari R, Wang T-L, Shih IM. Mutations of BRAF and KRAS precede the development of ovarian serous borderline tumors. *Cancer Res*, in press.

Shih IM and Kurman RJ. Ovarian tumorigenesis - a proposed model based on morphological and molecular genetic analysis. *Am J Pathol*, 164: 1511-1518, 2004.

Cheng EJ, Kurman RJ, Wang M, Oldt III R, Wang BG, Berman DM, Shih IM. Molecular genetic analysis of ovarian serous cystadenoma. *Lab Invest*, 84:778-784, 2004.

Singer G, Rebmann V, Chen Y-C, Cheng C-C, Liu H-T, Ali SZ, Reinsberg J, McMaster MT, Pfeiffer K, Chan DW, Wardelmann E, Grosse-Wilde H, Cheng CC, Kurman RJ, Shih I-M. HLA-G is a potential tumor marker in malignant effusion. *Clin Cancer Res*, 9: 4460-4466, 2003.

Hsu C-Y, Bristow R, Cha MS, Wang BG, Ho C-L, Kurman RJ, Wang TL, Shih IM. Characterization of Active Mitogen-activated Protein Kinase in Ovarian Serous Carcinomas. *Clin Cancer Res*, in press.

Shih IM and Wang TL. Exploring cancer genome using innovative technologies. *Curr Opin Oncol*, in press.

Singer G, Stohr R, Cope L, Dehari R, Hartmann A, Cao D-F, Wang TL, Kurman RJ, Shih IM. Patterns of p53 mutations separate ovarian serous borderline tumors, low and high-grade carcinomas and provide support for a new model of ovarian carcinogenesis. *Am J Surg Pathol*, in press.

Article submitted for review:

Research resource:

Ovarian tumor tissue microarrays- TMA 64, 65, 66, 209, 210, 211, 212, 213, 311, 312.

Trainees who received awards using this funding resource:

Brant G. Wang, MD, PhD, research fellow, Johns Hopkins University, recipient of the HERA Ovarian Cancer Research Award, 2003 (advisor: I-M Shih).

CONCLUSIONS

Summary of the accomplished research findings: Ovarian epithelial tumors are the most common type of ovarian cancer and are the most lethal gynecologic malignancy. The main purpose of the Project 1 is to delineate the molecular basis of ovarian serous tumors and identify the genes that are associated with tumors that develop along different pathways in tumor progression. The 2nd year of DoD project has made progress toward this goal as we have finished many of the tasks proposed in the specific aims. Based on clinicopathological and molecular observations, we propose a new model for their development. In this model, ovarian serous tumors are divided into two categories designated low-grade and high-grade tumors which correspond to two main pathways of tumorigenesis. Low-grade neoplasms arise in a stepwise fashion from borderline tumors whereas high-grade tumors arise from ovarian surface epithelium or inclusion cysts for which morphologically recognizable precursor lesions have not been identified, so-called “de novo” development. Low-grade tumors are associated with distinct molecular changes that are rarely found in high-grade tumors, such as *BRAF* and *KRAS* mutations. Gene expression profiling has shown that the two types of ovarian serous tumors are characterized by distinct gene expression patterns. Some of the genes have been selected for further studied to reveal their clinical and biological significance.

Implications and significance of the accomplished research findings: Our proposed model of carcinogenesis in ovarian serous tumors reconciles the relationship of borderline tumors to invasive carcinoma and provides a morphologic and molecular framework for studies aimed at elucidating the pathogenesis of ovarian cancer. Identification and characterization of the panoply of molecular changes associated with ovarian carcinogenesis will facilitate development of diagnostic tests for early detection of ovarian cancer and for the development of novel therapies aimed at blocking key growth-signaling pathways.

REFERENCES

1. Shih I-M, Kurman RJ: Ovarian tumorigenesis- a proposed model based on morphological and molecular genetic analysis. *Am J Pathol* 2004, 164:1511-1518
2. Burks RT, Sherman ME, Kurman RJ: Micropapillary serous carcinoma of the ovary. A distinctive low-grade carcinoma related to serous borderline tumors. *Am J Surg Pathol* 1996, 20:1319-1330.
3. Riopel MA, Ronnett BM, Kurman RJ: Evaluation of diagnostic criteria and behavior of ovarian intestinal- type mucinous tumors: atypical proliferative (borderline) tumors and intraepithelial, microinvasive, invasive, and metastatic carcinomas. *Am J Surg Pathol* 1999, 23:617-635.
4. Seidman JD, Russell P, Kurman RJ: Surface epithelial tumors of the ovary. *Blaustein's Pathology of the Female Genital Tract*. Edited by Kurman RJ. New York, Springer Verlag, 2002, pp 791-904
5. Seidman JD, Kurman RJ: Subclassification of serous borderline tumors of the ovary into benign and malignant types. A clinicopathologic study of 65 advanced stage cases. *Am J Surg Pathol* 1996, 20:1331-1345
6. Sehdev AES, Sehdev PS, Kurman RJ: Noninvasive and invasive micropapillary serous carcinoma of the ovary: a clinicopathologic analysis of 135 cases. *Am J Surg Pathol* 2003, 27:725-736
7. Singer G, Kurman RJ, Chang H-W, Cho SKR, Shih I-M: Diverse tumorigenic pathways in ovarian serous carcinoma. *Am J Pathol* 2002, 160:1223-1228
8. Singer G, Oldt R, 3rd, Cohen Y, Wang BG, Sidransky D, Kurman RJ, Shih I-M: Mutations in BRAF and KRAS characterize the development of low-grade ovarian serous carcinoma. *J Natl Can Inst* 2003, 95:484-486.
9. Ho C-L, Kurman RJ, Dehari R, Wang T-L, Shih I-M: Mutations of BRAF and KRAS precede the development of ovarian serous borderline tumors. *Cancer Res* 2004, in press.
10. Hsu C-Y, Bristow R, Cha M, Wang BG, Ho C-L, Kurman RJ, Wang T-L, Shih I-M: Characterization of active mitogen-activated protein kinase in ovarian serous carcinomas. *Clin Cancer Res* 2004, in press.
11. Singer G, Stöhr R, Cope L, Dehari R, Hartmann A, Cao D-F, Wang T-L, Kurman R, Shih I-M: Patterns of p53 mutations separate ovarian serous borderline tumors, low and high-grade carcinomas and provide support for a new model of ovarian carcinogenesis. Submitted 2004
12. Katabuchi H, Tashiro H, Cho KR, Kurman RJ, Hedrick Ellenson L: Micropapillary serous carcinoma of the ovary: an immunohistochemical and mutational analysis of p53. *Int J Gynecol Pathol* 1998, 17:54-60
13. Staebler A, Heselmeyer-Haddad K, Bell K, Riopel M, Perlman E, Ried T, Kurman RJ: Micropapillary serous carcinoma of the ovary has distinct patterns of chromosomal imbalances by comparative genomic hybridization compared with atypical proliferative serous tumors and serous carcinomas. *Hum Pathol* 2002, 33:47-59.
14. Singer G, Rebmann V, Y-C C, Liu H-T, Ali SZ, Reinsberg J, McMaster M, Pfeiffer K, Chan DW, Wardelmann E, Grosse-Wilde H, Kurman RJ, Shih I-M: HLA-G is a potential tumor marker in malignant ascites. *Clin Cancer Res* 2003, in press.

APPENDICES

Representative Publications in the 2nd year of project:

Ho C-L, Kurman RJ, Dehari R, Wang T-L, Shih IM. Mutations of BRAF and KRAS precede the development of ovarian serous borderline tumors. *Cancer Res*, in press.

Shih IM and Kurman RJ. Ovarian tumorigenesis - a proposed model based on morphological and molecular genetic analysis. *Am J Pathol*, 164: 1511-1518, 2004.

Cheng EJ, Kurman RJ, Wang M, Oldt III R, Wang BG, Berman DM, Shih IM. Molecular genetic analysis of ovarian serous cystadenoma. *Lab Invest*, 84:778-784, 2004.

Singer G, Rebmann V, Chen Y-C, Cheng C-C, Liu H-T, Ali SZ, Reinsberg J, McMaster MT, Pfeiffer K, Chan DW, Wardelmann E, Grosse-Wilde H, Cheng CC, Kurman RJ, Shih I-M. HLA-G is a potential tumor marker in malignant effusion. *Clin Cancer Res*, 9: 4460-4466, 2003.

Review

Ovarian Tumorigenesis

A Proposed Model Based on Morphological and Molecular Genetic Analysis

Ie-Ming Shih and Robert J. Kurman

From the Departments of Pathology, Oncology and Gynecology and Obstetrics, Johns Hopkins University School of Medicine, Baltimore, Maryland

The pathogenesis of ovarian carcinoma, the most lethal gynecological malignancy, is unknown because of the lack of a tumor progression model. Based on a review of recent clinicopathological and molecular studies, we propose a model for their development. In this model, surface epithelial tumors are divided into two broad categories designated type I and type II tumors that correspond to two main pathways of tumorigenesis. Type I tumors tend to be low-grade neoplasms that arise in a stepwise manner from borderline tumors whereas type II tumors are high-grade neoplasms for which morphologically recognizable precursor lesions have not been identified, so-called *de novo* development. As serous tumors are the most common surface epithelial tumors, low-grade serous carcinoma is the prototypic type I tumor and high-grade serous carcinoma is the prototypic type II tumor. In addition to low-grade serous carcinomas, type I tumors are composed of mucinous carcinomas, endometrioid carcinomas, malignant Brenner tumors, and clear cell carcinomas. Type I tumors are associated with distinct molecular changes that are rarely found in type II tumors, such as *BRAF* and *KRAS* mutations for serous tumors, *KRAS* mutations for mucinous tumors, and β -catenin and *PTEN* mutations and microsatellite instability for endometrioid tumors. Type II tumors include high-grade serous carcinoma, malignant mixed mesodermal tumors (carcinosarcoma), and undifferentiated carcinoma. There are very limited data on the molecular alterations associated with type II tumors except frequent p53 mutations in high-grade serous carcinomas and malignant mixed mesodermal tumors (carcinosarcomas). This model of carcinogenesis reconciles the relationship of borderline tumors to invasive

carcinoma and provides a morphological and molecular framework for studies aimed at elucidating the pathogenesis of ovarian cancer. (*Am J Pathol* 2004, 164:1511-1518)

Ovarian cancer is the most lethal gynecological malignancy and surface epithelial tumors (carcinomas) are the most common type of ovarian cancer. Despite considerable efforts aimed at elucidating the molecular mechanisms of ovarian carcinoma, its pathogenesis is still unknown, because unlike colorectal carcinoma,¹ a progression model has not been described. Ovarian carcinomas are heterogeneous and are primarily classified by cell type into serous, mucinous, endometrioid, clear cell, and Brenner (transitional) tumors corresponding to different types of epithelia in the organs of the female reproductive tract.²⁻⁴ The tumors in each of the categories are further subdivided into three groups, benign, malignant, and intermediate (borderline tumor) to reflect their behavior. Mucinous and endometrioid borderline tumors are often associated with invasive carcinomas but serous borderline tumors are rarely associated with serous carcinomas.² This latter observation as well as recent molecular genetic studies showing a very different frequency of p53 and *KRAS* mutations in serous carcinoma as compared to serous borderline tumors have led most investigators to conclude that serous borderline tumors and serous carcinomas are unrelated.⁵⁻⁹ The uncertainty about the nature of the borderline group of tumors, reflected by the ambiguous term "borderline," is a major shortcoming of the current classification. Here we review recent histopathological and molecular genetic

Supported by the United States Department of Defense (research grant no. OC010017).

Accepted for publication December 22, 2003.

Address reprint requests to Robert J. Kurman or Ie-Ming Shih, Department of Pathology, Johns Hopkins Medical Institutions, Weinberg Cancer Center, Room 2242, 401 N. Broadway, Baltimore, MD 21231. E-mail: rkurman@jhmi.edu (RJK). E-mail: shihie@yahoo.com (IS).

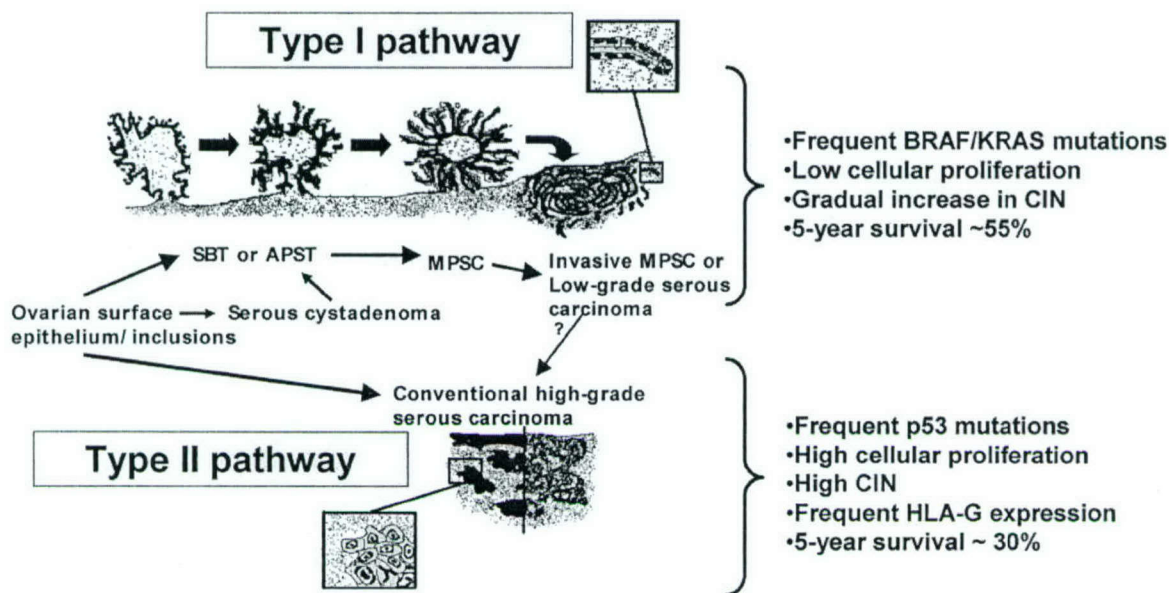


Figure 1. Schematic representation of the dualistic model depicting the development of ovarian serous carcinomas, the most common type of ovarian cancer. Low-grade serous carcinoma (MPSC) represents the prototypic type I tumor and develops in a stepwise manner from an atypical proliferative tumor through a noninvasive stage of MPSC (both of these tumors qualified as borderline) before becoming invasive. These tumors are associated with frequent *KRAS* or *BRAF* mutations. High-grade serous carcinoma represents the prototypic type II tumor and develops from the ovarian surface epithelium or inclusion cysts without morphologically recognizable intermediate stages. *KRAS* and *BRAF* mutations have been rarely found in these neoplasms. CIN, chromosomal instability.

studies to re-examine this issue and propose a model of ovarian carcinogenesis that integrates clinical, histopathological, and molecular genetic findings.

Clinical and Pathological Observations that Provide the Basis for the Proposed Model

Throughout the last 10 years, we have conducted a systematic microscopic and clinical analysis of a large number of noninvasive and invasive epithelial ovarian tumors of all histological types in an effort to delineate their pathogenesis and behavior.^{2,10-12} These studies drew attention to a subset of low-grade serous tumors designated "micropapillary serous carcinoma (MPSC)" with characteristic histopathological features, low proliferative activity, and an indolent behavior that contrasts dramatically with the conventional type of serous carcinoma, an aggressive neoplasm that is high-grade and has high proliferative activity.^{2,10-12} The term "MPSC" was originally proposed to distinguish the noninvasive form of this tumor from the more common noninvasive tumor, termed an "atypical proliferative serous tumor," both of which have been included under the rubric "borderline" or "low malignant potential."^{10,12} Histological transitions from adenofibromas and atypical proliferative serous tumors to noninvasive MPSCs are observed in nearly 75% of cases.¹³ In addition, areas of infiltrative growth (stromal invasion) immediately adjacent to the noninvasive component are found in a significant proportion of cases (Figure 1).¹³ These invasive MPSCs are synonymous with low-grade serous carcinoma. The former term describes its histopathological features and the latter its clinical behavior. The histopathological findings strongly suggest that

there is a morphological and biological spectrum beginning with a benign serous cystadenoma/adenofibroma, through a proliferative tumor (atypical proliferative serous tumor) to a noninvasive carcinoma (noninvasive MPSC) ending with an invasive low-grade serous carcinoma (invasive MPSC).

Low-grade serous carcinomas typically pursue an indolent course that may last more than 20 years.^{12,13} Approximately 50 to 60% of patients ultimately succumb because of widespread intra-abdominal carcinomatosis but the tumor maintains its low-grade appearance and low proliferative index throughout its course (Silva et al, 1997 and unpublished data).¹³ This contrasts with conventional high-grade serous carcinoma that presents as a clinically aggressive neoplasm that spreads rapidly and is associated with a poor outcome. Analysis of mucinous, endometrioid, clear cell carcinomas, and malignant Brenner tumors reveals that they are often associated with cystadenomas, borderline tumors, and intraepithelial carcinomas.² Furthermore, it has been long recognized that endometrioid carcinoma and clear cell carcinoma are associated with endometriosis in the ovary or pelvis in 15 to 50% of cases^{14,15} leading investigators to propose that endometriosis is a precursor of these tumors. Rarely, a high-grade serous carcinoma is associated with ovarian endometriosis but this is viewed as an independent, coincidental finding; a causal relationship of endometriosis and serous carcinoma has never been proposed. A recent clinical study using serial transvaginal ultrasonography has shown that ~50% of ovarian carcinomas develop from pre-existing cystic lesions whereas the remaining 50% develop in ovaries without apparent abnormality on ultrasound.¹⁶ The former group

Table 1. Precursors and Molecular Genetic Alterations of Type I Tumors of the Ovary

Type I tumors	Precursors*	Known molecular genetic alterations
Low-grade serous carcinoma (invasive MPSC)	Serous cystadenoma/adenofibroma Atypical proliferative serous tumor Noninvasive MPSC	<i>BRAF</i> and <i>KRAS</i> mutations (~67%)
Mucinous carcinoma	Mucinous cystadenoma Atypical proliferative mucinous tumor Intraepithelial carcinoma	<i>KRAS</i> mutations (>60%)
Endometrioid carcinoma	Endometriosis Endometrioid adenofibroma Atypical proliferative endometrioid tumor Intraepithelial carcinoma	LOH or mutations in <i>PTEN</i> (20%) β -catenin gene mutations (16–54%) <i>KRAS</i> mutations (4–5%) Microsatellite instability (13–50%)
Clear cell carcinoma	Endometriosis Clear cell adenofibroma Atypical proliferative clear cell tumor Intraepithelial carcinoma	<i>KRAS</i> mutations (5–16%) Microsatellite instability (~13%) TGF- β RII mutation (66%) [†]
Malignant Brenner (transitional) tumor	Brenner tumor Atypical proliferative Brenner tumor	Not yet identified

Abbreviation: MPSC, micropapillary serous carcinoma; LOH, loss of heterozygosity; TGF, transforming growth factor.

*Atypical proliferative serous tumors and noninvasive MPSC have been termed "borderline" tumors in the literature. Similarly for mucinous, endometrioid, clear cell, and Brenner tumors, atypical proliferative tumor and intraepithelial carcinoma have been combined and designated "borderline tumor" in the literature.

[†]Based on preliminary results analyzing three cases.⁵⁷

was composed mainly of mucinous, endometrioid, clear cell carcinomas, and borderline tumors whereas the latter group was composed almost exclusively of high-grade serous carcinomas. This distribution corresponds to the type I and II tumors described below.

A Proposed Model of Ovarian Carcinogenesis

Our clinicopathological and molecular genetic studies provide the basis for a proposed model of ovarian carcinogenesis in which there are two main pathways of tumorigenesis, corresponding to the development of type I and type II tumors (Tables 1 and 2). It should be emphasized that the terms, type I and type II, describe pathways of tumorigenesis and are not specific histopathological terms. Type I tumors (low-grade serous carcinoma, mucinous carcinoma, endometrioid carcinoma, malignant Brenner tumor, and clear cell carcinoma) develop in a stepwise manner from well-recognized precursors, namely borderline tumors that in turn develop from cystadenomas and adenofibromas (Figure 1 and Table 1).⁵ The latter benign tumors appear to develop from the surface epithelium or inclusion cysts in the case of serous and mucinous tumors and from endometriosis or endometriomas in the case of endometrioid and clear cell tumors. Type I tumors are slow growing as evidenced by the observation that they are large and

often confined to the ovary at diagnosis. In contrast, type II tumors are high-grade at presentation. Type II carcinomas include what are currently classified as high-grade serous carcinoma (moderately and poorly differentiated), malignant mixed mesodermal tumors (carcinosarcomas), and undifferentiated carcinoma (Figure 1 and Table 2). In addition, it is likely that some high-grade serous and undifferentiated carcinoma containing cells with clear cytoplasm have been classified as clear cell carcinoma and would be included in this group. Although malignant mixed mesodermal tumors (carcinosarcomas) were once thought to be mixed tumors comprised of carcinoma and sarcoma, recent studies have demonstrated that they are monoclonal.^{17,18} Accordingly, these tumors are now regarded as high-grade carcinomas with metaplastic sarcomatous elements. Type II carcinomas are rarely associated with morphologically recognizable precursor lesions and it has been proposed that they develop *de novo* from the surface epithelium or inclusion cysts of the ovary.⁷ They evolve rapidly, metastasize early in their course, and are highly aggressive. It is likely that the apparent *de novo* conventional high-grade serous carcinoma does develop in a stepwise manner but precursor lesions have not yet been elucidated molecularly or morphologically (Figure 1). Presumably, this is because of rapid transit from inception as a microscopic carcinoma to a clinically diagnosed neoplasm. This is supported by

Table 2. Precursors and Molecular Genetic Alterations of Type II Tumors of the Ovary

Type II tumors*	Precursors	Known molecular genetic alterations
High-grade serous carcinoma	Not yet identified	<i>p53</i> mutations (50–80%) Amplification and overexpression of <i>HER2/neu</i> gene (10%–20%) and <i>AKT2</i> gene (12%–18%) Inactivation of <i>p16</i> gene (10%–17%)
Undifferentiated carcinoma	Not yet identified	Not yet identified
Malignant mixed mesodermal tumor (carcinosarcomas)	Not yet identified	<i>p53</i> mutations (> 90%)

*Type II tumors can contain neoplastic cells with clear cytoplasm and have sometimes been classified as "clear cell carcinoma."

Table 3. Summary of Clinicopathological Features of the Prototypic Type I and Type II Tumors: Low-Grade and High-Grade Serous Carcinoma, Respectively

	Frequency	Histologic features	Precursor lesions	Clinical behavior [†]	Response to chemotherapy
Low grade	~25% of serous carcinomas*	Micropapillary architecture; low-grade nuclei; low mitotic index	Serous cystadenoma Serous atypical proliferative (borderline) tumor	Indolent; slow progression 5-year survival ~55% [‡]	Poor
High grade	~75% of serous carcinomas*	Solid nests and masses; high-grade nuclei; high mitotic index	Not known; probably from ovarian surface epithelium or inclusion cysts (<i>de novo</i>)	Aggressive; rapid progression; 5-year survival ~30%	Good, although recurrence is common

*Based on a survey at the Johns Hopkins Hospital. Most patients will eventually die from the disease after a protracted clinical course.

[†]Advanced stage tumors.

[‡]See Sehdev et al.¹³

the significantly higher Ki-67 nuclear labeling (proliferation) index in conventional high-grade serous carcinomas compared to low-grade serous carcinomas (unpublished data).¹⁹

This dualistic model is the first step in an attempt to elucidate the molecular pathogenesis of ovarian carcinoma, but should not be construed as implying that other pathways of tumorigenesis do not exist. For example, it is not certain whether there are other subsets of type II carcinomas. Molecular profiling and epidemiological studies will be important to determine whether there are distinct subsets of type II tumors. Also it is not clear whether some low-grade serous carcinomas (type I) progress to high-grade serous carcinomas (type II). We have observed serous carcinomas with high-grade nuclei and abundant mitotic activity that display a micropapillary architecture, simulating invasive MPSC (low-grade serous carcinoma). We thought that these high-grade tumors may have arisen from invasive MPSCs (low-grade serous carcinoma) but like conventional high-grade tumors without a micropapillary architecture these tumors did not harbor *KRAS* mutations, indicating that they are not derived from invasive MPSCs (low-grade serous carcinomas) (see below).²⁰ These data are preliminary and do not rule out the possibility that some low-grade serous carcinomas progress to high-grade carcinomas but the findings do support the view that ovarian serous carcinomas can be graded into low- and high-grade based on nuclear rather than architectural features. Preliminary clinicopathological studies of other type I carcinomas (mucinous, endometrioid, and clear cell carcinomas) have demonstrated that some are moderately and even poorly differentiated, suggesting that some type I carcinomas can evolve from low- to high-grade neoplasms.

Molecular Evidence Supporting the Dualistic Model

Serous carcinoma is the most common type of ovarian carcinoma and therefore low-grade and high-grade serous carcinomas serve as the prototypes of type I and type II carcinomas, respectively (Table 3). Accordingly, the molecular genetic data that are being advanced in support of the dualistic model are derived mainly from studies of serous carcinoma.

There are several distinctive molecular changes that distinguish low-grade and high-grade serous carcinomas (Table 4). Among them, the most significant molecular genetic alterations are mutations in *BRAF* and *KRAS* oncogenes. The *RAS*, *RAF*, *MEK*, *ERK*, and *MAP* cascade is important for the transmission of growth signals into the nucleus.²¹ Oncogenic mutations in *BRAF* and *KRAS* result in constitutive activation of this pathway and contribute to neoplastic transformation. Recent studies have demonstrated that *KRAS* mutations at codons 12 and 13 occur in 35% of low-grade serous carcinomas (invasive MPSCs) and 33% of borderline tumors (atypical proliferative tumor and noninvasive MPSC) but not in high-grade serous carcinomas.^{5,20} Similarly, *BRAF* mutations at codon 599 occur in 30% of low-grade serous carcinomas and 28% of borderline tumors but not in high-grade serous carcinomas.²⁰ Mutations in *BRAF* and *KRAS*, therefore, were found in 65% of low-grade invasive serous carcinomas and in 61% of atypical proliferative tumors and noninvasive MPSCs, their putative precursors, but neither of the genes was mutated in high-grade serous carcinomas. It is of interest that *BRAF* mutations were found only in tumors with wild-type *KRAS*.²⁰ The mutually

Table 4. Summary of Molecular Features of Prototypic Type I and Type II Tumors: Low-Grade and High-Grade Serous Carcinoma, Respectively

	<i>KRAS</i> mutations	<i>BRAF</i> mutations	<i>BRAF</i> or <i>KRAS</i> mutations	<i>TP53</i> mutations	HLA-G expression	Proliferation (Ki-67) index
Low grade	35%	30%	65%	0	0	~10–15%
High grade	0	0	0	50%–80%	61%	>50%

exclusive nature of *BRAF* mutations at codon 599 and *KRAS* mutations at codons 12 and 13 in ovarian carcinoma is consistent with similar findings in melanoma and colorectal carcinoma^{22,23} and lends support for the view that *BRAF* and *KRAS* mutations have an equivalent effect on tumorigenesis. Mutations of *BRAF* and *KRAS* seem to occur very early in the development of low-grade serous carcinoma as evidenced by the detection of these mutations in small atypical proliferative serous tumors but not in serous cystadenomas.²⁴ These data provide cogent evidence that the development of conventional high-grade serous carcinomas involves molecular mechanisms not related to mutations in *BRAF* and *RAS*.

In contrast to low-grade serous carcinoma in which mutations in *p53* are rare, mutations in *p53* are common in high-grade serous carcinomas. Most studies have shown that ~50 to 80% of advanced stage, presumably high-grade, serous carcinomas have mutant *p53*.²⁵⁻²⁹ It has also been reported that mutant *p53* is present in 37% of stage I and II presumably high-grade serous carcinomas.³⁰ In a study of very early microscopic stage I serous carcinomas in ovaries removed prophylactically from women who were BRCA heterozygotes, overexpression of *p53* and mutation of *p53* were found in all early invasive high-grade serous carcinomas as well as in the adjacent dysplastic surface epithelium.³¹ It is likely that inherited mutations in BRCA genes predispose the ovarian surface epithelium and inclusion cysts to neoplastic transformation through an increase in genetic instability. Although sporadic ovarian carcinomas were not analyzed in this study, the clinical and pathological features of BRCA-linked ovarian carcinomas and their sporadic counterparts are indistinguishable, suggesting that their histogenesis may be similar. Thus, although the findings are preliminary, they suggest that conventional high-grade serous carcinoma, in its very earliest stage resembles advanced stage serous carcinoma at a molecular as well as at a morphological level. Similar to high-grade serous carcinoma, malignant mixed mesodermal tumors (carcinosarcomas) also demonstrate *p53* mutations in almost all cases analyzed.³²⁻³⁴ It has been reported that the same *p53* mutations occur in the epithelial and the mesenchymal components.³² Moreover, the fact that pure carcinomatous areas are often associated with sarcomatous components suggests a common derivation of both the epithelial and the mesenchymal components in these neoplasms.³⁵ The finding that metastases from these tumors nearly always are composed exclusively of carcinoma has led investigators to suggest that malignant mixed mesodermal tumors are metaplastic carcinomas.

In addition to *p53* mutations, conventional serous carcinomas that are presumably high-grade demonstrate amplification/overexpression of HER-2/neu tyrosine kinase gene in 20 to 67%³⁶ and AKT2 serine/threonine kinase gene in 12 to 18% of samples analyzed.^{37,38} In contrast, amplification of both genes is rare in borderline tumors. Inactivation of the *p16* gene because of promoter methylation, mutation, or homozygous deletion occurs in a variety of human cancers including conventional ovarian serous carcinoma that presumably are high grade.³⁹ Because these are molecular genetic studies in which the

tumors were described simply as "serous carcinomas," we have referred to them as "presumably high-grade" because the vast majority of serous carcinomas are high grade.

Besides molecular genetic alterations, both low-grade and high-grade serous carcinomas are characterized by distinct gene expression profiles. For example, transcriptome-wide gene expression profiling has demonstrated that human leukocyte antigen-G (HLA-G) and apolipoprotein E (apoE) are overexpressed in most high-grade serous carcinomas but rarely in low-grade serous carcinomas. HLA-G immunoreactivity, ranging from focal to diffuse, was detected in 45 of 74 (61%) high-grade ovarian serous carcinomas but in none of the 18 low-grade serous carcinomas or 26 serous borderline tumors (atypical proliferative tumors and noninvasive MPSCs) that were studied.⁴⁰ A similar correlation of HLA-G expression with behavior has been observed in large cell carcinoma.⁴¹ A possible mechanism that explains the association of HLA-G expression with prognosis is that HLA-G seems to facilitate tumor cell evasion of the immune system by protecting malignant cells from lysis by natural killer cells.⁴²

Recently, apoE expression has been detected in ovarian tumors. Besides the well-known role of apoE in cholesterol transport and in the pathogenesis of atherosclerosis and Alzheimer's disease, apoE may play a novel role in the development of human cancer. In ovarian carcinomas, expression of apoE is primarily confined to type II high-grade serous carcinoma because apoE immunoreactivity has been detected in 66% of high-grade but only 12% of low-grade serous carcinomas. In contrast, apoE immunoreactivity was not detected in normal ovarian surface epithelium, serous cystadenomas, serous borderline tumors, and other type I tumors (Chen, unpublished data). Inhibition of apoE expression *in vitro* induces cell-cycle arrest and apoptosis in apoE-expressing ovarian cancer cells, suggesting that apoE expression is important for their growth and survival.

The genes that are specifically expressed in other types of ovarian carcinomas remain primarily unknown. Recently, hepatocyte nuclear factor-1 β and glutathione peroxidase 3 have been reported as molecular markers for ovarian clear cell carcinoma because both genes are highly expressed in ovarian clear cell carcinomas but rarely in other ovarian carcinomas.^{43,44}

Finally, allelic imbalance (calculated as the number of SNP markers with allelic imbalance/total SNP markers examined) has been assessed in atypical proliferative tumors, noninvasive MPSCs, and low-grade serous carcinoma (invasive MPSC).⁵ A progressive increase in the degree of allelic imbalance of chromosomes 1p, 5q, 8p, 18q, 22q, and Xp was noted when comparing atypical proliferative tumors with noninvasive and low-grade serous carcinomas (invasive MPSCs). In particular, allelic imbalance of chromosome 5q was more frequently observed in noninvasive MPSCs compared with atypical proliferative tumors and allelic imbalance of chromosome 1p was more frequently found in low-grade serous carcinoma (invasive MPSC) compared with noninvasive MPSCs. The allelic imbalance patterns in atypical prolif-

erative tumors were also found in noninvasive MPSCs containing adjacent atypical proliferative tumor components, further supporting the view that atypical proliferative tumors are the precursors of MPSCs. In contrast, all high-grade serous carcinomas including the very earliest tumors (less than 8 mm confined to one ovary) showed high levels of allelic imbalance. As allelic imbalance reflects chromosomal instability, the above findings suggest a step-wise increase in chromosomal instability in the progression to low-grade serous carcinoma in contrast to a high level of chromosomal instability in high-grade serous carcinoma even in their earliest stage of development.

The stepwise progression of borderline tumors (atypical proliferative tumor and noninvasive MPSC) to low-grade serous carcinoma (invasive MPSC) closely approximates the adenoma-carcinoma sequence in colorectal carcinoma and the progression of the other type I carcinomas, specifically mucinous and endometrioid carcinoma. In mucinous carcinoma for example, morphological transitions from cystadenoma to an atypical proliferative tumor (borderline tumor), to intraepithelial carcinoma and invasive carcinoma have been recognized for some time and an increasing frequency of *KRAS* mutations at codons 12 and 13 has been described in cystadenomas, borderline tumors, and mucinous carcinomas, respectively.^{8,45-48} In addition, using microdissection, the same *KRAS* mutation has been detected in mucinous carcinoma and in the adjacent mucinous cystadenoma and borderline tumor.⁴⁵ Likewise, in endometrioid carcinomas, mutation of β -catenin has been reported in approximately one-third of cases^{49,50} and mutation of *PTEN* in 20%, rising to 46% in those tumors with 10q23 loss of heterozygosity.⁵¹ These mutations are generally detected in well-differentiated, stage I tumors with a good prognosis, suggesting that inactivation of these genes is an early event. Moreover, similar molecular genetic alterations including loss of heterozygosity at 10q23 and mutations in *PTEN* have been reported in endometriosis, atypical endometriosis, and ovarian endometrioid carcinoma in the same specimen.⁵¹⁻⁵⁶ The molecular genetic findings together with the morphological data showing a frequent association of endometriosis with endometrioid adenofibromas, atypical proliferative (borderline) tumors, adjacent to invasive well-differentiated endometrioid carcinoma provide evidence of step-wise tumor progression in the development of endometrioid carcinoma. Clear cell carcinoma is also frequently associated with endometriosis, clear cell adenofibromas, and clear cell atypical proliferative (borderline) tumors but molecular evidence for the stepwise progression model is lacking because molecular markers specific to clear cell neoplasms have only recently been identified.^{43,44} Transforming growth factor- β receptor type II has been found to be mutated in the kinase domain in two of three clear cell carcinomas but rarely in other histological types of ovarian carcinomas.⁵⁷ Microsatellite instability is present in endometrioid and clear cell carcinoma but is only rarely detected in serous and mucinous tumors.^{58,59} These findings provide further evidence of the close relationship of endometrioid and clear cell carcinoma

and point to a common precursor lesion for these two neoplasms.

Conclusion

Based on morphological and molecular genetic analyses of a large series of ovarian tumors, we have proposed a tumor progression model for ovarian carcinoma. In this model, ovarian tumors are divided into two broad categories designated type I and type II. These designations refer to pathways of tumorigenesis and are not specific histopathological terms. Type I tumors include low-grade serous carcinoma, mucinous carcinoma, endometrioid carcinoma, malignant Brenner tumors, and clear cell carcinoma. Type II tumors are composed of what are currently classified as moderately and poorly differentiated serous carcinoma (high-grade serous carcinoma), malignant mixed mesodermal tumors (carcinosarcomas), and undifferentiated carcinoma. Some of the latter may contain cells with clear cytoplasm and have therefore been classified erroneously as clear cell carcinomas. The tumorigenic pathway for type I tumors resembles the adenoma-carcinoma sequence in colorectal cancer and is characterized by clearly recognized precursor lesions, namely, cystadenoma, atypical proliferative tumor, and noninvasive carcinoma. The latter two noninvasive tumors have traditionally been combined into one category designated "borderline." Type I tumors evolve slowly and are associated with distinct molecular changes that are rarely found in type II tumors such as mutations in *BRAF* and *KRAS* for serous tumors, *KRAS* mutations for mucinous tumors, and β -catenin and *PTEN* mutations for endometrioid tumors. In contrast, type II tumors evolve rapidly, arising directly from the surface epithelium or inclusion cysts and metastasize early in their course. There are very limited data on the molecular alterations associated with type II tumors except frequent mutations of p53 in high-grade serous carcinomas and malignant mixed mesodermal tumors (carcinosarcomas). This model reconciles the inconsistency in the current classification of ovarian tumors that regards borderline tumors as a distinct entity unrelated to invasive carcinoma and provides a morphological and molecular genetic framework for future studies aimed at elucidating the pathogenesis of ovarian cancer. Unraveling the complex molecular genetic pathways involved in ovarian carcinogenesis will require correlated morphological and molecular genetic studies. Identification and characterization of the panoply of molecular changes associated with ovarian carcinogenesis will facilitate development of diagnostic tests for early detection of ovarian cancer and for the development of novel therapies aimed at blocking key growth-signaling pathways.

Acknowledgments

We thank the members of gynecological pathology division at Johns Hopkins Medical Institutions for their review of this manuscript.

References

1. Kinzler KW, Vogelstein B: The Genetic Basis of Human Cancer. Toronto, McGraw-Hill, 1998
2. Seidman JD, Russell P, Kurman RJ: Surface epithelial tumors of the ovary. Blaustein's Pathology of the Female Genital Tract. Edited by RJ Kurman. New York, Springer Verlag, 2002, pp 791-904
3. Scully RE: International Histological Classification of Tumors: Histological Typing of Ovarian Tumors. Geneva, World Health Organization, 1999
4. Scully RE: World Health Organization International Histological Classification of Tumors. New York, Springer, 1999
5. Singer G, Kurman RJ, Chang H-W, Cho SKR, Shih I-M: Diverse tumorigenic pathways in ovarian serous carcinoma. *Am J Pathol* 2002, 160:1223-1228
6. Ortiz BH, Ailawadi M, Colitti C, Muto MG, Deavers M, Silva EG, Berkowitz RS, Mok SC, Gershenson DM: Second primary or recurrence? Comparative patterns of p53 and K-ras mutations suggest that serous borderline ovarian tumors and subsequent serous carcinomas are unrelated tumors. *Cancer Res* 2001, 61:7264-7267
7. Bell DA, Scully RE: Early de novo ovarian carcinoma. A study of fourteen cases. *Cancer* 1994, 73:1859-1864
8. Caduff RF, Svoboda-Newman SM, Ferguson AW, Johnston CM, Frank TS: Comparison of mutations of Ki-RAS and p53 immunoreactivity in borderline and malignant epithelial ovarian tumors. *Am J Surg Pathol* 1999, 23:323-328
9. Dubeau L: Ovarian cancer. The Metabolic and Molecular Bases of Inherited Disease. Edited by CR Scriver, AL Beaudet, WS Sly, D Valle, B Childs, KW Kinzler, B Vogelstein. Toronto, McGraw-Hill, 2001, pp 1091-1096
10. Burks RT, Sherman ME, Kurman RJ: Micropapillary serous carcinoma of the ovary. A distinctive low-grade carcinoma related to serous borderline tumors. *Am J Surg Pathol* 1996, 20:1319-1330
11. Riopel MA, Ronnett BM, Kurman RJ: Evaluation of diagnostic criteria and behavior of ovarian intestinal-type mucinous tumors: atypical proliferative (borderline) tumors and intraepithelial, microinvasive, invasive, and metastatic carcinomas. *Am J Surg Pathol* 1999, 23:617-635
12. Seidman JD, Kurman RJ: Subclassification of serous borderline tumors of the ovary into benign and malignant types. A clinicopathologic study of 65 advanced stage cases. *Am J Surg Pathol* 1996, 20:1331-1345
13. Sehdev AES, Sehdev PS, Kurman RJ: Noninvasive and invasive micropapillary serous carcinoma of the ovary: a clinicopathologic analysis of 135 cases. *Am J Surg Pathol* 2003, 27:725-736
14. Okuda T, Otsuka J, Sekizawa A, Saito H, Makino R, Kushima M, Farina A, Yuzuru K, Okai T: p53 mutations and overexpression affect prognosis of ovarian endometrioid cancer but not clear cell cancer. *Gynecol Oncol* 2003, 88:318-325
15. Modesitt SC, Tortolero-Luna G, Robinson JB, Gershenson D, Wolf JK: Ovarian and extraovarian endometriosis-associated cancer. *Obstet Gynecol* 2002, 100:788-795
16. Horiuchi A, Itoh K, Shimizu M, Nakai I, Yamazaki T, Kimura K, Suzuki A, Shiozawa I, Ueda N, Konishi I: Toward understanding the natural history of ovarian carcinoma development: a clinicopathological approach. *Gynecol Oncol* 2003, 88:309-317
17. Masuda A, Takeda A, Fukami H, Yamada C, Matsuyama M: Characteristics of cell lines established from a mixed mesodermal tumor of the human ovary. Carcinomatous cells are changeable to sarcomatous cells. *Cancer* 1987, 60:1697-2703
18. Moritani S, Moriya T, Kushima R, Sugihara H, Harada M, Hattori T: Ovarian carcinoma recurring as carcinosarcoma. *Pathol Int* 2001, 51:380-384
19. Garzetti GG, Ciavattini A, Goteri G, De Nicolis M, Stramazotti D, Lucarini G, Biagini G: Ki67 antigen immunostaining (MIB 1 monoclonal antibody) in serous ovarian tumors: index of proliferative activity with prognostic significance. *Gynecol Oncol* 1995, 56:169-174
20. Singer G, Oldt III R, Cohen Y, Wang BG, Sidransky D, Kurman RJ, Shih I-M: Mutations in BRAF and KRAS characterize the development of low-grade ovarian serous carcinoma. *J Natl Cancer Inst* 2003, 95:484-486
21. Peyssonnaud C, Eychene A: The Raf/MEK/ERK pathway: new concepts of activation. *Biol Cell* 2001, 93:53-62
22. Davies H, Bignell GR, Cox C, Stephens P, Edkins S, Clegg S, Teague J, Woffendin H, Garnett MJ, Bottomley W, Davis N, Dicks E, Ewing R, Floyd Y, Gray K, Hall S, Hawes R, Hughes J, Kosmidou V, Menzies A, Mould C, Parker A, Stevens C, Watt S, Hooper S, Wilson R, Jayatilake H, Gusterson BA, Cooper C, Shipley J, Hargrave D, Pritchard-Jones K, Maitland N, Chenevix-Trench G, Riggins GJ, Bigner DD, Palmieri G, Cossu A, Flanagan A, Nicholson A, Ho JW, Leung SY, Yuen ST, Weber BL, Seigler HF, Darrow TL, Paterson H, Marais R, Marshall CJ, Wooster R, Stratton MR, Futreal PA: Mutations of the BRAF gene in human cancer. *Nature* 2002, 417:949-954
23. Rajagopalan H, Bardelli A, Lengauer C, Kinzler KW, Vogelstein B, Velculescu VE: Tumorigenesis: RAF/RAS oncogenes and mismatch-repair status. *Nature* 2002, 418:934
24. Cheng EJ, Kurman RJ, Wang M, Oldt III R, Berman DM, Shih I-M: Molecular genetic analysis of ovarian serous cystadenomas. *Lab Invest* 2004, in press
25. Chan W-Y, Cheung K-K, Schorge JO, Huang L-W, Welch WR, Bell DA, Berkowitz RS, Mok SC: Bcl-2 and p53 protein expression, apoptosis, and p53 mutation in human epithelial ovarian cancers. *Am J Pathol* 2000, 156:409-417
26. Kohler MF, Marks JR, Wiseman RW, Jacobs IJ, Davidoff AM, Clarke-Pearson DL, Soper JT, Bast Jr RC, Berchuck A: Spectrum of mutation and frequency of allelic deletion of the p53 gene in ovarian cancer. *J Natl Cancer Inst* 1993, 85:1513-1519
27. Kupryjanczyk J, Thor AD, Beauchamp R, Merritt V, Edgerton SM, Bell DA, Yandell DW: p53 gene mutations and protein accumulation in human ovarian cancer. *Proc Natl Acad Sci USA* 1993, 90:4961-4965
28. Berchuck A, Carney M: Human ovarian cancer of the surface epithelium. *Biochem Pharmacol* 1997, 54:541-544
29. Wen WH, Reles A, Runnebaum IB, Sullivan-Halley J, Bernstein L, Jones LA, Felix JC, Kreienberg R, el-Naggar A, Press MF: p53 mutations and expression in ovarian cancers: correlation with overall survival. *Int J Gynecol Pathol* 1999, 18:29-41
30. Shelling AN, Cooke I, Ganesan TS: The genetic analysis of ovarian cancer. *Br J Cancer* 1995, 72:521-527
31. Pothuri B, Leitao M, Barakat R, Akram M, Bogomolny F, Olvera N, Lin O: Genetic analysis of ovarian carcinoma histogenesis. *Gynecol Oncol* 2001, 80:Abstract (Society of Gynecologic Oncologists 32nd Annual Meeting)
32. Gallardo A, Matias-Guiu X, Lagarda H, Catusas L, Bussaglia E, Gras E, Suarez D, Prat J: Malignant mullerian mixed tumor arising from ovarian serous carcinoma: a clinicopathologic and molecular study of two cases. *Int J Gynecol Pathol* 2002, 21:268-272
33. Kounelis S, Jones MW, Papadaki H, Bakker A, Swalsky P, Finkelstein SD: Carcinosarcomas (malignant mixed mullerian tumors) of the female genital tract: comparative molecular analysis of epithelial and mesenchymal components. *Hum Pathol* 1998, 29:82-87
34. Abeln EC, Smit VT, Wessels JW, de Leeuw WJ, Cornelisse CJ, Fleuren GJ: Molecular genetic evidence for the conversion hypothesis of the origin of malignant mixed mullerian tumours. *J Pathol* 1997, 183:424-431
35. Sreenan JJ, Hart WR: Carcinosarcomas of the female genital tract. A pathologic study of 29 metastatic tumors: further evidence for the dominant role of the epithelial component and the conversion theory of histogenesis. *Am J Surg Pathol* 1995, 19:666-674
36. Ross JS, Yang F, Kallakury BV, Sheehan CE, Ambros RA, Muraca PJ: HER-2/neu oncogene amplification by fluorescence in situ hybridization in epithelial tumors of the ovary. *Am J Clin Pathol* 1999, 111:311-316
37. Cheng JQ, Godwin AK, Bellacosa A, Taguchi T, Franke TF, Hamilton TC, Tschlis PN, Testa JR: AKT2, a putative oncogene encoding a member of a subfamily of protein-serine/threonine kinases, is amplified in human ovarian carcinomas. *Proc Natl Acad Sci USA* 1992, 89:9267-9271
38. Bellacosa A, de Feo D, Godwin AK, Bell DW, Cheng JQ, Altomare DA, Wan M, Dubeau L, Scambia G, Masciullo V: Molecular alterations of the AKT2 oncogene in ovarian and breast carcinomas. *Int J Cancer* 1995, 64:280-285
39. Rocco JW, Sidransky D: p16(MTS-1/CDKN2/INK4a) in cancer progression. *Exp Cell Res* 2001, 264:42-55
40. Singer G, Rebmann V, Y-C C, Liu H-T, Ali SZ, Reinsberg J, McMaster M, Pfeiffer K, Chan DW, Wardelmann E, Grosse-Wilde H, Kurman RJ, Shih I-M: HLA-G is a potential tumor marker in malignant ascites. *Clin Cancer Res* 2003, 9:4460-4464
41. Urosevic M, Kurrer MO, Kamarashev J, Mueller B, Weder W, Burg G,

- Stahel RA, Dummer R, Trojan A: Human leukocyte antigen G up-regulation in lung cancer associates with high-grade histology, human leukocyte antigen class I loss and interleukin-10 production. *Am J Pathol* 2001, 159:817-824
42. Urosevic M, Willers J, Mueller B, Kempf W, Burg G, Dummer R: HLA-G protein up-regulation in primary cutaneous lymphomas is associated with interleukin-10 expression in large cell T-cell lymphomas and indolent B-cell lymphomas. *Blood* 2002, 99:609-617
 43. Tsuchiya A, Sakamoto M, Yasuda J, Chuma M, Ohta T, Ohki M, Yasugi T, Taketani Y, Hirohashi S: Expression profiling in ovarian clear cell carcinoma: identification of hepatocyte nuclear factor-1beta as a molecular marker and a possible molecular target for therapy of ovarian clear cell carcinoma. *Am J Pathol* 2003, 163:2503-2512
 44. Hough CD, Sherman-Baust CA, Pizer ES, Montz FJ, Im DD, Rosen-shein NB, Cho KR, Riggins GJ, Morin PJ: Large-scale serial analysis of gene expression reveals genes differentially expressed in ovarian cancer. *Cancer Res* 2000, 60:6281-6287
 45. Mok SC, Bell DA, Knapp RC, Fishbaugh PM, Welch WR, Muto MG, Berkowitz RS, Tsao SW: Mutation of K-ras protooncogene in human ovarian epithelial tumors of borderline malignancy. *Cancer Res* 1993, 53:1489-1492
 46. Ichikawa Y, Nishida M, Suzuki H: Mutation of KRAS protooncogene is associated with histological subtypes in human mucinous ovarian tumors. *Cancer Res* 1994, 54:33-35
 47. Enomoto T, Weghorst CM, Inoue M, Tanizawa O, Rice JM: K-ras activation occurs frequently in mucinous adenocarcinomas and rarely in other common epithelial tumors of the human ovary. *Am J Pathol* 1991, 139:777-785
 48. Gemignani ML, Schlaerth AC, Bogomolny F, Barakat R, Lin O, Soslow R, Venkatraman E, Boyd J: Role of KRAS and BRAF gene mutations in mucinous ovarian carcinoma. *Gynecol Oncol* 2003, 90:378-381
 49. Wu R, Zhai Y, Fearon ER, Cho KR: Diverse mechanisms of beta-catenin deregulation in ovarian endometrioid adenocarcinomas. *Cancer Res* 2001, 61:8247-8255
 50. Moreno-Bueno G, Gamallo C, Perez-Gallego L, deMora JC, Suarez A, Palacios J: Beta-catenin expression pattern, beta-catenin gene mutations, and microsatellite instability in endometrioid ovarian carcinomas and synchronous endometrial carcinomas. *Diagn Mol Pathol* 2001, 10:116-122
 51. Obata K, Morland SJ, Watson RH, Hitchcock A, Chenevix-Trench G, Thomas EJ, Campbell IG: Frequent PTEN/MMAC mutations in endometrioid but not serous or mucinous epithelial ovarian tumors. *Cancer Res* 1998, 58:2095-2097
 52. Sato N, Tsunoda H, Nishida M, Morishita Y, Takimoto Y, Kubo T, Noguchi M: Loss of heterozygosity on 10q23.3 and mutation of the tumor suppressor gene PTEN in benign endometrial cyst of the ovary: possible sequence progression from benign endometrial cyst to endometrioid carcinoma and clear cell carcinoma of the ovary. *Cancer Res* 2000, 60:7052-7056
 53. Saito M, Okamoto A, Kohno T, Takakura S, Shinozaki H, Isonishi S, Yasuhara T, Yoshimura T, Ohtake Y, Ochiai K, Yokota J, Tanaka T: Allelic imbalance and mutations of the PTEN gene in ovarian cancer. *Int J Cancer* 2000, 85:160-165
 54. Thomas EJ, Campbell IG: Molecular genetic defects in endometriosis. *Gynecol Obstet Invest* 2000, 50:44-50
 55. Obata K, Hoshiai H: Common genetic changes between endometriosis and ovarian cancer. *Gynecol Obstet Invest* 2000, 50:39-43
 56. Bischoff FZ, Simpson JL: Heritability and molecular genetic studies of endometriosis. *Hum Reprod Update* 2000, 6:37-44
 57. Francis-Thickpenny KM, Richardson DM, van Ee CC, Love DV, Winship IM, Baguley BC, Chenevix-Trench G, Shelling AN: Analysis of the TGF-beta functional pathway in epithelial ovarian carcinoma. *Br J Cancer* 2001, 85:687-691
 58. Fujita M, Enomoto T, Yoshino K, Nomura T, Buzard GS, Inoue M, Okudaira Y: Microsatellite instability and alterations in the hMSH2 gene in human ovarian cancer. *Int J Cancer* 1995, 64:361-366
 59. Gras E, Catusus L, Arguelles R, Moreno-Bueno G, Palacios J, Gamallo C, Matias-Guiu X, Prat J: Microsatellite instability, MLH1 promoter hypermethylation, and frameshift mutations at coding mononucleotide repeat microsatellites in ovarian tumors. *Cancer* 2001, 92:2829-2836
 60. Singer G, Shih Ie M, Truskinovsky A, Umudum H, Kurman RJ: Mutational analysis of K-ras segregates ovarian serous carcinomas into two types: invasive MPSC (low-grade tumor) and conventional serous carcinoma (high-grade tumor). *Int J Gynecol Pathol* 2003, 22:37-41

(In press, Cancer Res, 2004)

Mutations of BRAF and KRAS Precede the Development of Ovarian Serous Borderline Tumors

Chung-Liang Ho, Robert J. Kurman, Reiko Dehari, Tian-Li Wang, Ie-Ming Shih

Affiliations of authors: C-L Ho, R.J. Kurman, R. Dehari, I-M Shih (Department of Pathology), R.J. Kurman, T-L Wang, I-M Shih (Departments of Oncology and Gynecology and Obstetrics), Johns Hopkins Medical Institutions, Baltimore, USA

Correspondence to: Ie-Ming Shih, M.D., Ph.D. The Johns Hopkins Medical Institutions, 1503 E. Jefferson Street, Room B-315, Baltimore, MD 21231, USA (e-mail: ishih@jhmi.edu; Phone: 410-502-7774; Fax: 410-502-7943).

Molecular genetic changes that are associated with the initiating stage of tumor development are important in tumorigenesis. Ovarian serous borderline tumors (SBTs), putative precursors of low-grade serous carcinomas, are among the few human neoplasms with a high frequency of activating mutations in BRAF and KRAS genes. However, it remains unclear as to how these mutations contribute to tumor progression. To address this issue, we compared the mutational status of BRAF and KRAS in both SBTs and the adjacent epithelium from cystadenomas, the presumed precursor of SBTs. We found that 3 of 8 SBTs contained mutant BRAF and 4 SBTs contained mutant KRAS. All specimens with mutant BRAF harbored wild type KRAS and vice versa. Thus, 7 (88%) of 8 SBTs contained either BRAF or KRAS mutations. The same mutations detected in SBTs were also identified in the cystadenoma epithelium adjacent to the SBTs in 6 (86%) of 7 informative cases. As compared to SBTs, the cystadenoma epithelium, like ovarian surface epithelium, lacks cytological atypia. Our findings provide cogent evidence that mutations of BRAF and KRAS occur in the epithelium of cystadenomas adjacent to SBTs and strongly suggest that they are very early events in tumorigenesis, preceding the development of SBT.

INTRODCUTION

It has been shown that tumors result from an accumulation of genetic alterations that result in uncontrolled cellular proliferation. Identification of the alterations that occur early in tumor development is critical to understanding carcinogenesis and can provide insight into potential markers for early detection (1, 2). Ovarian cancer is one of the most lethal neoplasms in women and serous carcinoma is the most common type (3) but the molecular events that underlie the development of ovarian serous carcinoma are largely unknown. Recent studies have shown that ovarian serous carcinoma develops along two distinct pathways and we have proposed a model of ovarian carcinogenesis that reflects this concept (4-6). In one pathway, invasive low-grade serous carcinoma develops from a non-invasive (or *in situ*) tumor which has traditionally been termed "serous borderline tumor (SBT)" (7). The progression of SBT to invasive low-grade carcinoma mimics the adenoma-carcinoma sequence in colorectal carcinoma (2). Detailed analysis of SBTs demonstrates that SBTs consist of two tumors at different stages of tumor progression, a benign tumor termed "atypical proliferative serous tumor" and an intraepithelial low-grade (non-invasive micropapillary serous) carcinoma, the immediate precursor of invasive low-grade serous carcinoma (4, 6). SBTs are frequently associated with serous cystadenomas which develop from ovarian surface epithelium through a hyperplastic process (8). Like ovarian surface epithelium, the epithelial cells of a cystadenoma do not show cytological atypia and their proliferation index is extremely low (8). In the second pathway, high-grade serous carcinoma develops from ovarian surface epithelium or from surface inclusion cysts (9) but precursor lesions have not been well characterized. Accordingly, this process has been described as "de novo" (4).

Molecular genetic analysis has shown that SBTs and invasive low-grade serous carcinomas are characterized by mutations of BRAF and KRAS in 61%-68% of cases (5, 6, 10, 11) but p53 mutations are rare (11-13). In contrast, high-grade serous carcinomas frequently contain p53 mutations (> 50%) but rarely BRAF and KRAS mutations (5, 6, 12-16). These studies analyzed advanced stage tumors in which putative precursor lesions may have been obliterated by the tumor. In this study, we confined our analysis to small SBTs and associated cystadenomas in order to delineate the early molecular genetic events in their pathogenesis. Specifically, we compared the mutational status of BRAF and KRAS in SBTs and the adjacent non-transformed epithelium of serous cystadenomas.

MATERIALS AND METHODS

A total of eight small SBTs (corresponding to what has been classified as atypical proliferative tumor) and the associated cystadenomas were collected. The acquisition of tumor samples was approved by the Johns Hopkins institutional review board. The SBTs ranged from 8 to 20 mm (average 16 mm) in greatest dimension and associated cystadenomas ranged from 5 to 8 cm (average 6.8 cm). The SBTs occupied 5-15% of the total surface area of the cystadenomas. Only a small number of cases were studied because although cystadenomas and SBTs are not uncommon, cystadenomas containing synchronous small SBTs are relatively rare. Microscopically, the SBTs contained a hierarchical branching papillae lined by epithelial cells with mild to moderate cellular atypia (Fig. 1). The epithelium of the SBTs merged abruptly with the cystadenoma epithelium which was composed of a single layer of flat to columnar cells without atypia (Fig.1). The epithelium from the SBTs and adjacent cystadenoma was collected separately using the Palm laser capture microdissection microscope (Zeiss). Genomic DNA was prepared using the PicoPure DAN extraction kit (Arcturus, Mountain View, CA). Polymerase chain reaction (PCR) was then performed followed by nucleotide sequencing using an ABI 3100 sequencer (ABI, Foster City, CA). Exon 1 of KRAS and exon 15 of BRAF were both sequenced as each exon harbors almost all the mutations in both genes (5, 6, 10, 17). The primers for PCR and sequencing were as follows. For BRAF: 5'-tgcttgctctgataggaaaatga-3' (forward), 5'-ccacaaaatggatccagacaac-3' (reverse) and 5'-gaaaatgagatctactgttttcctta-3' (sequencing) and for KRAS: 5'-taaggcctgctgaaaatgactg-3' (forward), 5'-tggtcctgcaccagtaatatgc-3' (reverse) and 5'-ctgcaccagtaatatgcatataaaac-3' (sequencing). The sequences were analyzed using the Lasergene program (DNASTAR, Madison, WI).

RESULTS

The results of the mutational status correlated with the SBT or cystadenoma component of the tumors are shown in Table 1. We found that four SBTs (cases 1, 4, 5 and 8) contained activating KRAS mutations at codon 12 (three mutations of GGT to GAT and one mutation of GGT to GTT) and three SBTs (cases 3, 5 and 6) had BRAF mutations at codon 599 (all of T1796A mutation). As in our previous report (5), the presence of KRAS and BRAF mutations was mutually exclusive. Thus, 7 (88%) of 8 SBTs had either a BRAF or a KRAS mutation. Case 2 contained wild type KRAS and BRAF. Analysis of the mutational status in the epithelium from the cystadenomas adjacent to the SBTs revealed that both the cystadenoma and SBT components contained identical mutations in 6 of 7 informative cases. Representative sequence analyses are shown in Fig. 2. The frequent mutations of KRAS and BRAF in small SBTs are consistent with previous reports showing mutations in either BRAF or KRAS in 66%-68% of large SBTs (5, 10). The higher frequency of mutations (88%) in the current report is probably due to the use of purer tumor cell samples obtained by laser capture microdissection or may have resulted from the small sample size in the present analysis.

DISCUSSION

The findings in this study provide important insights into the molecular pathogenesis of low-grade ovarian serous tumors (Fig. 3). Since we only analyzed a single time point in the sequence of cystadenoma to SBTs, we can only infer that the findings truly describe the events in early tumor progression. However, the coexistence of a cystadenoma with a SBT strongly suggests that the latter arises from the former (Fig. 3). Accordingly, the presence of identical mutations in the cystadenoma epithelium which displayed no evidence of cytologic atypia strongly suggests that mutations of BRAF and KRAS occur before the development of a SBT and indicates that cystadenomas are the precursors of SBTs. Our results support the view that mutations of BRAF and KRAS (or NRAS) are early events associated with tumor initiation as occurs in melanoma (18) and colorectal carcinoma (19).

We have recently studied 30 consecutive pure cystadenomas without SBTs and demonstrated an absence of BRAF and KRAS mutations in all of them (8). The frequency of mutations in BRAF and KRAS in cystadenomas associated with SBTs was significantly higher than those without SBTs ($p < 0.001$, Fisher's exact test) (Table 2). This finding together with the fact that SBTs are relatively uncommon as compared to cystadenomas (20-24) suggests that only a small proportion of serous cystadenomas are neoplastic with the potential to progress to SBTs. Finally, our findings suggest a "gatekeeper" role of BRAF and KRAS genes in the development of low-grade serous carcinomas (25). This is supported by the observation that activating mutations in these genes are oncogenic in experimental cell culture systems (17, 26, 27) probably through a constitutive activation of mitogen activated protein kinase (28, 29). Future experiments will determine whether mutations of BRAF and KRAS are sufficient to initiate the development of SBTs or additional genetic "hits" are required in tumorigenesis. Because mutations of BRAF and KRAS in serous cystadenomas may predispose to the development of SBTs, detection of BRAF and KRAS mutations could facilitate the differentiation of cystadenomas with a high risk of progression from the vast majority of cystadenomas that lack BRAF or KRAS mutations and have a very low risk of progression. Development of molecular assays (30, 31) that can detect such mutations (in cyst fluid, for example) could play an important role in the management of patients with ovarian cystadenomas, particularly young women who would prefer fertility-sparing treatment.

Acknowledgements

Supported by a research grant OC010017 from the US Department of Defense. We gratefully acknowledge the technical support of the Oncology Imaging Core at the Johns Hopkins Medical Institutions for the photomicrographs and the laser capture microdissection.

REFERENCES:

1. Kinzler KW and Vogelstein B. Colorectal Tumors. In: B. Vogelstein and K. W. Kinzler (eds.), *The Genetic Basis of Human Cancer*. New York: McGraw-Hill; 1998. p.565-87.
2. Kinzler KW and Vogelstein B. Landscaping the cancer terrain. *Science* 1998; 280(5366): 1036-7.
3. Seidman JD, Horkayne-Szakaly I, Haiba M, et al. The histologic type and stage distribution of ovarian carcinomas of surface epithelial origin. *Int J Gynecol Pathol* 2004; 23(1): 41-4.
4. Shih I-M and Kurman RJ Ovarian tumorigenesis- a proposed model based on morphological and molecular genetic analysis. *Am J Pathol* 2004; 164(5): 1511-8.
5. Singer G, Oldt R, 3rd, Cohen Y, et al. Mutations in BRAF and KRAS characterize the development of low-grade ovarian serous carcinoma. *J Natl Cancer Inst* 2003; 95(6): 484-6.
6. Singer G, Kurman RJ, Chang H-W, et al. Diverse tumorigenic pathways in ovarian serous carcinoma. *Am J Pathol* 2002; 160:1223-8.
7. Burks RT, Sherman ME, and Kurman RJ Micropapillary serous carcinoma of the ovary. A distinctive low-grade carcinoma related to serous borderline tumors. *Am J Surg Pathol* 1996; 20(11): 1319-30.
8. Cheng EJ, Kurman RJ, Wang M, et al. Molecular genetic analysis of ovarian serous cystadenomas. *Lab Invest* 2004; 84:778-84.
9. Yang DH, Smith ER, Cohen C, et al. Molecular events associated with dysplastic morphologic transformation and initiation of ovarian tumorigenicity. *Cancer* 2002; 94(9): 2380-92.
10. Sieben NLG, Macropoulos P, Roemen G, et al. In ovarian neoplasms, BRAF, but not KRAS, mutations are restricted to low-grade serous tumors. *J Pathol* 2004; 202:336-40.
11. Cuatrecasas M, Erill N, Musulen E, et al. K-ras mutations in nonmucinous ovarian epithelial tumors: a molecular analysis and clinicopathologic study of 144 patients. *Cancer* 1998; 82(6): 1088-95.
12. Zheng J, Benedict WF, Xu HJ, et al. Genetic disparity between morphologically benign cysts contiguous to ovarian carcinomas and solitary cystadenomas [see comments]. *J Natl Cancer Inst* 1995; 87(15): 1146-53.
13. Teneriello MG, Ebina M, Linnoila RI, et al. p53 and Ki-ras gene mutations in epithelial ovarian neoplasms. *Cancer Res* 1993; 53(13): 3103-8.
14. Leitao MM, Soslow RA, Baergen RN, et al. Mutation and expression of the TP53 gene in early stage epithelial ovarian carcinoma. *Gynecol Oncol* 2004; 93(2): 301-6.
15. Kappes S, Milde-Langosch K, Kressin P, et al. p53 mutations in ovarian tumors, detected by temperature-gradient gel electrophoresis, direct sequencing and immunohistochemistry. *Int J Cancer* 1995; 64(1): 52-9.
16. Singer G, Stohr R, Dehari R, et al. Patterns of p53 mutations separate ovarian serous borderline tumors, low and high-grade carcinomas and provide support for a new model of ovarian carcinogenesis. *Am J Surg Pathol*, in press.
17. Davies H, Bignell GR, Cox C, et al. Mutations of the BRAF gene in human cancer. *Nature* 2002; 417(6892): 949-54.

18. Pollock PM, Harper UL, Hansen KS, et al. High frequency of BRAF mutations in nevi. *Nat Genet* 2003; 33(1): 19-20.
19. Chan TL, Zhao W, Leung SY, et al. BRAF and KRAS mutations in colorectal hyperplastic polyps and serrated adenomas. *Cancer Res* 2003; 63(16): 4878-81.
20. Mink PJ, Sherman ME, and Devesa SS Incidence patterns of invasive and borderline ovarian tumors among white women and black women in the United States. Results from the SEER Program, 1978-1998. *Cancer* 2002; 95(11): 2380-9.
21. Conway C, Zalud I, Dilena M, et al. Simple cyst in the postmenopausal patient: detection and management. *J Ultrasound Med* 1998; 17(6): 369-72; quiz 73-4.
22. Oyelese Y, Kueck AS, Barter JF, et al. Asymptomatic postmenopausal simple ovarian cyst. *Obstet Gynecol Surv* 2002; 57(12): 803-9.
23. Christensen JT, Boldsen JL, and Westergaard JG Functional ovarian cysts in premenopausal and gynecologically healthy women. *Contraception* 2002; 66(3): 153-7.
24. Seidman JD, Russell P, and Kurman RJ Surface epithelial tumors of the ovary. In: R. J. Kurman (ed.), *Blaustein's Pathology of the Female Genital Tract*. New York: Springer Verlag; 5th edition, 2002. p.791-904.
25. Kinzler KW and Vogelstein B Cancer-susceptibility genes: Gatekeepers and caretakers [news; comment]. *Nature* 1997; 386(6627): 761, 3.
26. Peyssonnaud C and Eychene A The Raf/MEK/ERK pathway: new concepts of activation. *Biol Cell* 2001; 93(1-2): 53-62.
27. Malumbres M and Barbacid M RAS oncogenes: the first 30 years. *Nat Rev Cancer* 2003; 3:459-65.
28. Allen LF, Sebolt-Leopold J, and Meyer MB CI-1040 (PD184352), a targeted signal transduction inhibitor of MEK (MAPKK). *Semin Oncol* 2003; 30(5 Suppl 16): 105-16.
29. Satyamoorthy K, Li G, Gerrero MR, et al. Constitutive mitogen-activated protein kinase activation in melanoma is mediated by both BRAF mutations and autocrine growth factor stimulation. *Cancer Res* 2003; 63(4): 756-9.
30. Vogelstein B and Kinzler KW Digital PCR. *Proc Natl Acad Sci U S A* 1999; 96(16): 9236-41.
31. Dressman D, Yan H, Traverso G, et al. Transforming single DNA molecules into fluorescent magnetic particles for detection and enumeration of genetic variations. *PNAS* 2003; 100(15): 8817-22.

Table 1. Mutational status of KRAS and BRAF genes in eight small serous borderline tumors and associated cystadenomas.

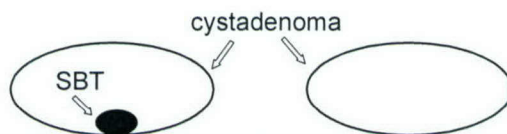
Gene		case1	case 2	case 3	case 4	case 5	case 6	case 7	case 8
KRAS	SBT	G35A* G12D#	WT	WT	G35T G12V	G35A G12D	WT	WT	G35A G12D
	Cyst	G35A G12D	WT	WT	WT	G35A G12D	WT	WT	G35A G12D
BRAF	SBT	WT	WT	T1796A V599E	WT	WT	T1796A V599E	T1796A V599E	WT
	Cyst	WT	WT	T1796A V599E	WT	WT	T1796A V599E	T1796A V599E	WT

Abbreviations: SBT: serous borderline tumor; WT: wild type

*Alteration in nucleotide sequence

Alteration in amino acid sequence

Table 2. Frequency of mutations in BRAF and KRAS in cystadenomas with associated serous borderline tumor and pure cystadenomas



	Cystadenoma associated with SBT	Pure cystadenoma
Mutations in BRAF or KRAS	6	0
Wild type in BRAF and KRAS	2	30
Total cases	8	30

APST: atypical proliferative serous tumor
 SBT: serous borderline tumor

FIGURE LEGEND

Fig. 1

A: Small serous borderline tumor and associated serous cystadenoma (case E). The tumor measures 0.8 cm in greatest dimension and is composed of hierarchical branching papillae lined by cells with mild to moderate atypia (left inset). The adjacent cystadenoma epithelium is composed of a single layer of epithelium without cytologic atypia (right inset). B: Epithelial cells lining the cystadenoma (between arrows) were isolated using laser capture microdissection with minimal contamination from the underlying stromal cells.

Fig. 2

Chromatograms of nucleotide sequences of BRAF and KRAS in two representative cases. Left panel (case A) shows a point mutation in the KRAS gene in both serous borderline tumor (SBT) and the adjacent cystadenoma (cyst) of the same specimen. Right panel (case F) shows a point mutation in the BRAF gene in both the serous borderline tumor and the corresponding cystadenoma.

Fig. 3

Schematic representation of tumor progression in low-grade serous carcinoma. Mutations of BRAF and KRAS occur in a small proportion of cystadenomas which may contribute to the development of a serous borderline tumor (SBT). Some serous borderline tumors progress further to intraepithelial and then to invasive low-grade serous carcinoma.

Molecular genetic analysis of ovarian serous cystadenomas

Eric J Cheng¹, Robert J Kurman^{1,2}, Menglin Wang¹, Robert Oldt III¹, Brant G Wang¹, David M Berman¹ and Ie-Ming Shih^{1,2}

¹Department of Pathology and ²Department of Gynecology and Obstetrics, The Johns Hopkins University School of Medicine, Baltimore, MD, USA

Ovarian serous cystadenomas are common ovarian lesions that may be precursors of serous borderline tumors, which can in turn progress to low-grade serous carcinomas. It has been shown that low-grade serous carcinoma and serous borderline tumors are characterized by frequent mutations in *BRAF* or *KRAS* genes, but the mutational status of these genes in serous cystadenomas and the clonal nature of serous cystadenomas have not been fully investigated. We isolated cyst-lining epithelium from 30 consecutive serous cystadenomas, and analyzed their *BRAF* and *KRAS* mutational status. Wild-type sequences of *BRAF* and *KRAS* were detected in all specimens. Using the human androgen receptor gene as a polymorphic marker, we also examined the clonal status of epithelial cells in all of the serous cystadenomas. Four of 29 (14%) informative specimens were monoclonal based on the methylation pattern. These monoclonal cystadenomas were significantly ($P < 0.01$) larger in size (> 8 cm) than the nonclonal cystadenomas. These data indicate that serous cystadenomas do not contain mutations in either *BRAF* or *KRAS* genes and that most serous cystadenomas are polyclonal. Accordingly, it appears that serous cystadenomas develop as a hyperplastic expansion from epithelial inclusions with a clonal/neoplastic transformation occurring in a subset of them.

Laboratory Investigation (2004) 84, 778–784, advance online publication, 12 April 2004; doi:10.1038/labinvest.3700103

Keywords: BRAF; clonality; HUMARA; inactivation; KRAS; serous cystadenomas; X-chromosome

Ovarian carcinoma is believed to arise either from the surface epithelium covering the ovary, benign epithelial inclusions or cystic tumors termed 'cystadenomas'. The World Health Organization classification divides ovarian surface epithelial tumors into three groups: benign cystadenomas, invasive carcinomas and an intermediate group designated 'borderline' tumors.^{1,2} Ovarian cystadenomas are further subclassified according to the cell type into serous cystadenomas, mucinous cystadenomas and endometriomas.^{3–7} Cystadenomas occur in 5–15% of postmenopausal women in the general population.^{8,9} Serous cystadenomas are the most common followed by mucinous cystadenomas and endometriomas.¹⁰ Previous studies have demonstrated that mucinous cystadenomas^{11,12} and endometriomas¹³ are clonal and therefore are benign neoplasms, but similar studies of serous cystadenomas have not been performed to our knowledge.

Based on our previous morphological and molecular studies, we have proposed that serous borderline tumors (atypical proliferative tumors and noninvasive micropapillary serous carcinomas) can progress to low-grade serous carcinomas (invasive micropapillary serous carcinomas).^{14,15} These low-grade serous carcinomas and borderline tumors exhibit frequent *BRAF* or *KRAS* mutations but rare p53 mutations.^{6,14,16} In contrast, high-grade serous carcinomas have wild-type *KRAS* and *BRAF* but frequent p53 mutations even when they are small and confined to the ovary.^{17,18} It has therefore been proposed that high-grade serous carcinomas in contrast to low-grade (invasive micropapillary) serous carcinomas develop directly from epithelial inclusions or ovarian surface epithelium, so-called, 'de novo' development.^{14,19} In order to elucidate the mechanisms of serous carcinogenesis, specifically the molecular genetic alterations in early tumorigenesis, we undertook a study of serous cystadenomas aimed at assessing whether mutations of *BRAF* and *KRAS*, which are common in serous borderline tumors and low-grade serous carcinomas are present in serous cystadenomas.^{6,19–21} In addition, we determined the clonality of serous cystadenomas by analyzing the patterns of X-chromosome

Correspondence: Dr I-M Shih, MD, PhD, 418 N Bond St., B-315, Baltimore, MD 21231, USA.
E-mail: ishih@jhmi.edu, URL: <http://pathology2.jhu.edu/shihlab/index.cfm>

Received 9 January 2004; revised 28 February 2004; accepted 29 February 2004; published online 12 April 2004

inactivation of the X-linked androgen receptor (HUMARA) gene. For molecular genetic analyses, we have applied a new method to isolate pure and abundant cyst-lining epithelial cells from fresh serous cystadenomas. Finally, we compared the proliferative and apoptotic activity of the epithelium of the cystadenomas to that of ovarian surface epithelium and serous borderline tumors.

Materials and methods

Epithelial Cell Isolation from Serous Cystadenomas

A total of 30 consecutive ovarian serous cystadenomas were collected from women undergoing oophorectomy at the Johns Hopkins Hospital, Baltimore, Maryland. One serous borderline tumor was also included as a control. The study protocol was approved by the local institutional review board. Frozen sections of the cystadenomas were performed to confirm the diagnosis before harvesting the epithelial cells from at least half of the sample. For multilocular cystadenomas, the largest one was used in the assays. In order to obtain abundant and pure cyst-lining epithelial cells for multiple molecular genetic analyses, we employed a method to enrich the epithelial cells by combining chemical or mechanical separation and immunosorting. After washing in phosphate buffer saline

(PBS) 3 times, the cyst-lining was incubated in 0.05% trypsin and 0.53 mM EDTA (Invitrogen, Grand Island, NY, USA) at 37°C for 10 min, then mechanically separated from the cyst wall by agitating the cyst fragments and/or gentle scraping using a rubber cell scraper (Sarstedt, Newton, NC, USA). The epithelial cell fragments were collected and washed in PBS (Figure 1). The epithelial cells were enriched by Epi-CAM-conjugated Dynal Beads (Dynal, Hamburg, Germany) that specifically bound epithelial cells. The procedures were detailed in the vendor's instructions. The purity of isolated epithelial cells was assessed by immunostaining for the expression of cytokeratin 8 (an epithelial marker), using the antibody CAM5.2 (Becton Dickinson, San Jose, CA)²² on the isolated cells after short-term culture in 24-well plates. The isotype-matched MN-4 antibody that reacted with Mel-CAM (CD146) was also used as a negative control.²³ The immunofluorescence staining and nuclear counterstaining were detailed in the previous report.²⁴

Mutational Analysis

Nucleotide sequencing was used to analyze the mutational status of *BRAF* and *KRAS*. The primers that were used to amplify exon 15 of *BRAF* and exon 1 of *KRAS* containing codons 12 and 13 and the PCR protocols have been previously described.^{14,25,26}

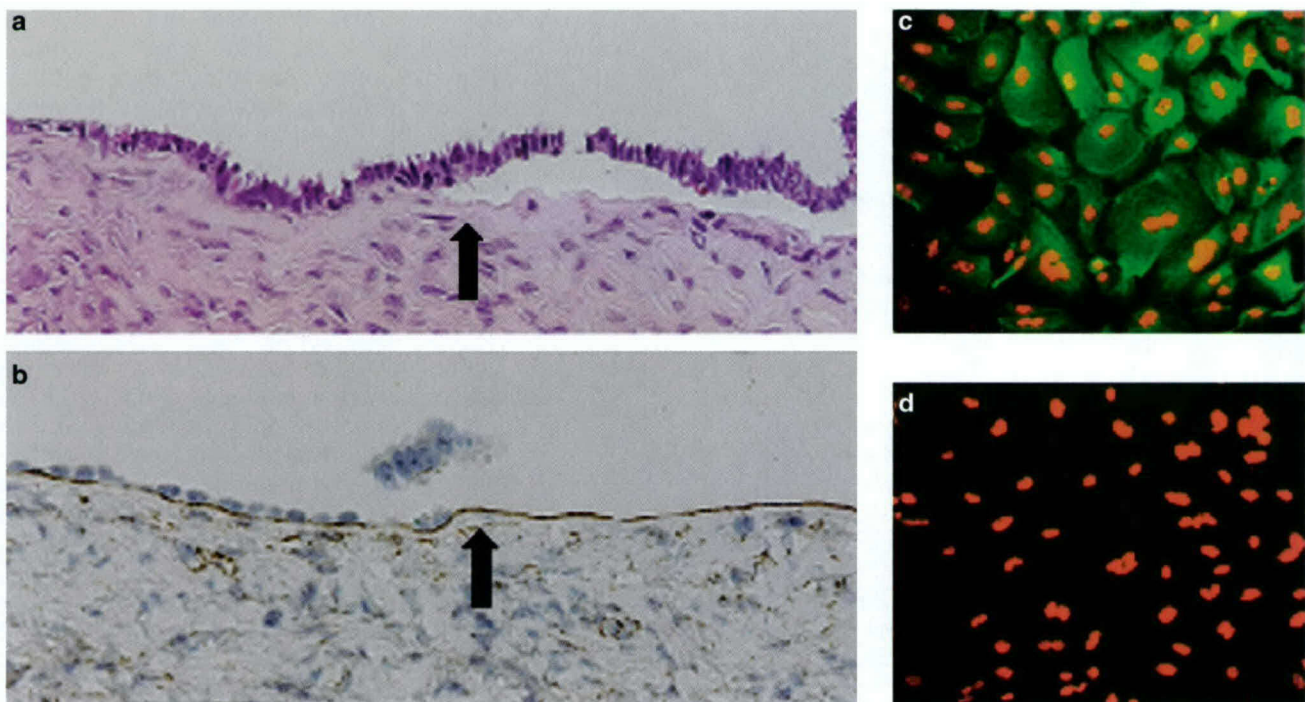


Figure 1 Isolation of cyst-lining epithelium. (a) The lining epithelium was gently scraped from the cyst wall to the right of the arrow; the epithelium to the left of the arrow was undisturbed (hematoxylin and eosin stain). (b): Immunostains for collagen IV demonstrate the basement membrane. The epithelium is present to the left of the arrow and absent to the right of the arrow that has been harvested. (c) Immunostaining for CK8 antibody shows green fluorescence in the cytoplasm of isolated epithelial cells in all the cells. Nuclei are counterstained red. (d) Immunostaining for CD146 antibody as a negative control. There is no green fluorescence present.

PCR products were purified using a MiniElute™ PCR purification kit (Qiagen, Valencia, CA, USA). Nucleotide sequencing was performed using fluorescent labeled Applied Biosystems Big Dye terminators and an Applied Biosystems 377 automated sequencer (Applied Biosystems, Foster City, CA, USA). Analysis of the 1796T/A status in *BRAF* was also performed using a PCR-based restriction fragment length polymorphism (RFLP) technique as previously described.^{27,28} For this method, the *BRAF* PCR product of exon 15 containing the relevant nucleotide at position 1796 was digested with TspR1 (New England BioLabs, Beverly, MA, USA) at 65°C for 3 h. The samples were electrophoresed on a 10% polyacrylamide gel.

Clonality Assay

The clonal status of the cystadenomas was evaluated by analyzing the patterns of X-chromosome inactivation in exon 1 of the X-linked androgen receptor gene (HUMARA), which contains a highly polymorphic trinucleotide repeat.^{29,30} The QiaQuick PCR purification kit (Qiagen, Valencia, CA, USA) was used to isolate genomic DNA from the purified cyst epithelial cells from all the 30 specimens. In addition, a serous borderline tumor served as a positive control. Predigestion of DNA (2 µg) with 20 U of methylation-sensitive restriction endonuclease *HhaI* or *HpaII* (New England BioLabs, Beverly, MA, USA) resulted in selective PCR amplification from the methylated (uncleaved) allele. For PCR, 3 µl of the enzyme digest was mixed with primers and all essential PCR reagents as previously reported.³⁰ The PCR product was separated in 6% polyacrylamide gels and visualized by ethidium bromide.

Assessment of Proliferation and Apoptotic Activity

The proliferative and apoptotic activity of the cyst-lining epithelial cells was assessed by immunohistochemistry using the MIB1 antibody to detect Ki-67^{31,32} and the M30 antibody³³ to detect the cytokeratin epitope after apoptosis, respectively. The immunohistochemistry methodology has been previously described.³⁴ Paraffin sections from 10 normal ovaries, 50 serous cystadenomas and 15 serous borderline tumors were stained with the MIB1 and the M30 antibody. At least 4000 epithelial cells were randomly selected from different regions and analyzed using the Spotlight morphometric program under a Nikon inverted light microscope (Image System, Columbia, MD, USA). The Ki-67 and M30 labeling index was expressed as the percentage of Ki-67 or M30 labeled epithelial cells from among the total number of epithelial cells counted. Two-sided Student's *t*-test was used to compare the difference in the Ki-67 and M30 labeling index between the serous cystadenomas, normal surface ovarian epithelium and serous borderline tumors.

Results

The 30 serous cystadenomas ranged from 1.2 to 10 cm in greatest dimension with a median of 5 cm (Table 1). Of the 30 cystadenomas, 26 were unilocular and the remaining four cystadenomas were multilocular (specimen no. 15, 17, 21 and 29). The epithelial cells lining the cystadenomas ranged from flattened to columnar (Figure 1). The latter cells frequently contained cilia (serous differentiation) at least in focal areas. The nuclei were bland and none displayed cytologic atypia (so-called dysplasia). Immunostaining revealed that more than 98% of the cells isolated from cystadenomas were positive for cytokeratin 8, confirming the purity of the epithelial cells isolated by our technique (Figure 1). Mutational analysis with direct nucleotide sequencing demonstrated that none of the samples harbored mutations in either *BRAF* (exon 15) or *KRAS* (exon 1) gene. As a control, the epithelial cells isolated from a serous borderline tumor revealed a missense mutation at the codon 12 of *KRAS* (GGT to GAT). The presence of wild-type *BRAF* gene in all of the serous cystadenomas was confirmed using a restriction fragment length polymorphism assay that detects rare mutations at codon 599 of *BRAF*.^{27,28}

The lack of mutations in *BRAF* and *KRAS* raises the possibility that serous cystadenomas may not be clonal. Therefore, we determined the clonality of all serous cystadenomas by analyzing patterns of X-chromosome inactivation of the X-linked androgen receptor (HUMARA). All the samples except one were heterozygous and therefore informative for clonal analysis (Table 1). The positive control specimen, a serous borderline tumor, demonstrated a monoclonal composition, as one of the alleles was absent after enzyme digestion. Based on HUMARA assay, we found that only four of the 29 (14%) of the serous cystadenomas showed a clonal pattern (Figure 2 and Table 1). The clonal serous cystadenomas tended to be larger in size (>8 cm) than the polyclonal serous cystadenomas ($P < 0.01$; two-tailed *t*-test).

The Ki-67 labeled epithelial cells were scattered randomly, not clustered, as single positive cells in the serous cystadenoma with a frequency of $0.84 \pm 0.33\%$. This proliferative index was significantly higher than the $0.10 \pm 0.028\%$ in normal ovarian surface epithelium ($P < 0.001$) and significantly lower than the $8.15 \pm 2.80\%$ in serous borderline tumors ($P < 0.001$) (Figure 3). The apoptotic index as determined by the M30 immunoreactivity was extremely low ($< 0.01\%$) in serous cystadenomas, as well as in ovarian surface epithelium and serous borderline tumors. There was no statistically significant difference in Ki-67 or M30 labeling index ($P > 0.1$) between clonal and polyclonal cystadenomas nor did the size of the cystadenomas correlate with the Ki-67 or M30 labeling index (data not shown).

The time for a serous cystadenomas to double in diameter was calculated by assuming that the

Table 1 *BRAF* and *KRAS* mutation and clonality assays in serous cystadenomas

Sample		<i>BRAF</i> mutational status	<i>KRAS</i> mutational status	Clonality assay
ID	Size (cm)			
1	1.2 ^a	Wild type	Wild type	Polyclonal
2	2	Wild type	Wild type	Polyclonal
3	2.5	Wild type	Wild type	Polyclonal
4	3	Wild type	Wild type	Polyclonal
5	3.5	Wild type	Wild type	Polyclonal
6	3.5	Wild type	Wild type	Polyclonal
7	3.8	Wild type	Wild type	Polyclonal
8	4	Wild type	Wild type	Polyclonal
9	4	Wild type	Wild type	Polyclonal
10	4.3	Wild type	Wild type	Polyclonal
11	4.5	Wild type	Wild type	Polyclonal
12	4.5	Wild type	Wild type	Polyclonal
13	5	Wild type	Wild type	Polyclonal
14	5	Wild type	Wild type	Polyclonal
15	5	Wild type	Wild type	Polyclonal
16	5	Wild type	Wild type	Polyclonal
17	5.2	Wild type	Wild type	Polyclonal
18	5.5	Wild type	Wild type	Polyclonal
19	5.8	Wild type	Wild type	Polyclonal
20	6.5	Wild type	Wild type	Polyclonal
21	8	Wild type	Wild type	Polyclonal
22	8	Wild type	Wild type	Polyclonal
23	8.3	Wild type	Wild type	NA
24	8.5	Wild type	Wild type	Clonal
25	9	Wild type	Wild type	Polyclonal
26	9	Wild type	Wild type	Clonal
27	9.2	Wild type	Wild type	Clonal
28	9.8	Wild type	Wild type	Polyclonal
29	10	Wild type	Wild type	Polyclonal
30	10	Wild type	Wild type	Clonal
SBT	12.6	Mutated ^b	Wild type	Clonal

SBT: serous borderline tumor; NA: homozygous to the polymorphic markers of the HUMARA allele.

^aThe greatest dimension of the cystadenoma.

^bMutation occurs at the codon 12 of *KRAS* (GGT to GAT).

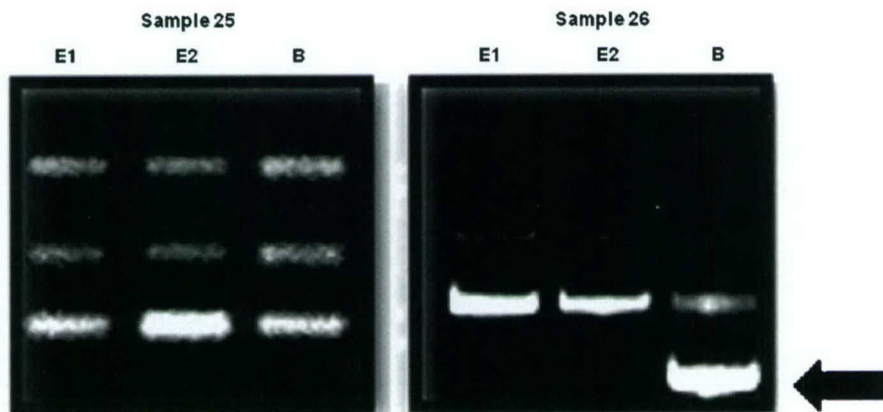


Figure 2 Clonality assay with the polymorphic markers of the HUMARA gene. Representative cystadenoma samples (25 and 26) are shown. Sample 25 retains all the bands in *Hpa*II (E1) and *Hha*I (E2) predigested samples as compared to the control with buffer only (B). In contrast, sample 26 shows an absence of the shorter band (arrow) in enzyme-digested samples, indicating a homogenous methylation pattern, that is, monoclonality, in this sample.

cystadenomas are spheres with a diameter of A cm and that the epithelium evenly lined the inner surface of the cyst. The total number of epithelial cells in a cyst (N_A) was equal to the total inner

surface area of a cyst ($A^2\pi$)/the (en face) area of an individual epithelial cell which was $12 \times 12 \mu\text{m}$ based on morphometric measurements. For a cyst with a diameter of A cm to enlarge to a diameter

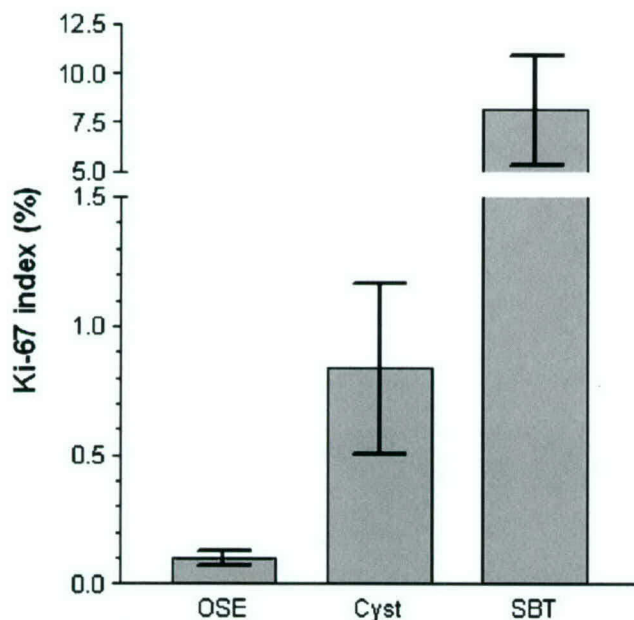


Figure 3 Proliferative activity in ovarian surface epithelium (OSE), serous cystadenomas and serous borderline tumors (SBT) as determined by the Ki-67 labeling index. Serous cystadenomas have a significantly higher Ki-67 labeling index than ovarian surface epithelium ($P < 0.001$) but a lower index than serous borderline tumors ($P < 0.001$).

of 2A cm, a four fold increase in cell number is required since $N_{2A}/N_A = 4A^2\pi/144\mu\text{m}^2/A^2\pi/144\mu\text{m}^2 = 4$. Given the net proliferation index (Ki-67 index–M30 index) of 0.84% and a presumable cell doubling time of t hours in cyst-lining epithelial cells, it was estimated that it would take $200/0.84 \times t$ hours for a cyst with an original cell number of N_A to increase to $4 N_A$ (N_{2A}). The cell doubling time, t , depends on the cell type and the microenvironment, and generally is between 48 and 96 h. Therefore, given $t = 72$ h, the estimated time for a serous cyst to double in size was $200/0.84 \times 72 \text{ h} = 17.143 \text{ h} = 714$ days or 23.8 months.

Discussion

Clonality and mutations are the molecular signatures of the vast majority of neoplasms.³⁵ Accordingly, our data demonstrating an absence of *BRAF* and *KRAS* mutations in all of the serous cystadenomas in this analysis and an absence of clonality in the vast majority of them provide cogent evidence that most so-called 'serous cystadenomas' are not neoplasms. This conclusion is supported by other studies showing a diploid chromosomal content³⁶ and lack of p53 mutations in serous cystadenomas.⁶ The Ki-67 immunohistochemical findings in the present study indicating that the epithelial cells of these cystadenomas do proliferate, albeit at a very low rate, suggest that the development of a non-

clonal serous cyst is a hyperplastic process. The mechanism underlying increased proliferative activity in the cyst-lining epithelium as compared to the ovarian surface epithelium is unknown, but it may be related to the sustained hydrostatic pressure that has been shown to induce cellular proliferation.^{37–39} The mildly increased proliferation index could explain why serous cystadenomas can reach a size as large as 10 cm. Based on our estimates, the time for a cyst to double in size (diameter) is approximately 2 years. Therefore, it may take 16 years for a small inclusion cyst of 300 μm in diameter to enlarge to a 10 cm cyst. It should be noted that the doubling time of a cyst is based on estimation and in fact it depends on several factors, especially the cell cycle transit time of proliferating cyst-lining epithelium, which is difficult to measure *in vivo*. It is apparent that not all serous inclusion cysts will progress to large cysts and further studies are required to investigate the growth kinetics of cysts and molecular mechanisms underlying their development. The present study demonstrates that ovarian serous cystadenomas do not contain mutations in either *BRAF* or *KRAS* genes and that most are polyclonal. In previous studies, we reported that low-grade serous carcinomas develop in a stepwise fashion from serous borderline tumors.^{14,15} Although the molecular events that lead to the development of serous borderline tumors are not known, our findings suggest that activating mutations in *BRAF* or *KRAS* may play an important role as both mutations are found in over 60% of serous borderline tumors and in low-grade serous carcinomas.²⁷ This view is supported by the observation that activating mutations in these genes are oncogenic in experimental cell culture systems.^{25,40,41} Accordingly, the clonal nature of only a small proportion of serous cystadenomas and the absence of *KRAS* or *BRAF* mutations in them suggests that mutations in these genes may be a key early event in the transformation of clonal serous cystadenomas to serous borderline tumors.

Although the findings in this report indicate that 86% of ovarian serous cystadenomas are polyclonal and non-neoplastic, this may be an overestimate as monoclonality may have been undetected in some cases for several reasons. First, for the genetic analysis, we pooled the bulk of the cyst-lining epithelium from each specimen to avoid the bias introduced by the X-inactivation patch size in the assessment of clonality.⁴² It is possible that clonal proliferation occurs only focally in some cystadenomas and that the molecular changes in these foci occur in the absence of morphologic alterations that are not detected microscopically. Second, our results do not exclude the possibility that multiple independent clonal events occur in a cyst, which would then result in the erroneous impression of polyclonality. Third, since the monoclonal cystadenomas tended to be large and the number of large cystadenomas (>8 cm) that were analyzed in this study was relatively small, it is possible that the

proportion of monoclonal serous cystadenomas would have been higher if a greater number of large cystadenomas were analyzed. Finally, very small inclusion cysts (<1 cm) were not analyzed in this study because they are too small and by definition do not qualify as cystadenomas.⁴³

In conclusion, the data in this report demonstrate that mutations in *BRAF* and *KRAS* that characterize serous borderline tumors and low-grade serous carcinomas are absent in serous cystadenomas. In fact, only 14% of serous cystadenomas are clonal, suggesting that serous cystadenomas develop as a hyperplastic expansion of ovarian surface epithelial inclusions. We speculate that a small proportion of these cystadenomas become clonal and that mutations of *KRAS* or *BRAF* in some of these clonal cystadenomas lead to the development of serous borderline tumors, which are the precursors of low-grade serous carcinoma. These findings have important implications for understanding the pathogenesis of ovarian serous carcinoma, and for the screening and treatment of ovarian cancer.

Acknowledgement

This work was supported by the research Grant OC010017 from the US Department of Defense.

References

- 1 Serov SF, Scully RE, Sobin LH. International Histological Classification and Staging of Tumors, Histologic Typing of Ovarian Tumors. World Health Organization: Geneva, 1973.
- 2 Scully RE. World Health Organization International Histological Classification of Tumours, 2 edn. Springer: New York, NY, 1999.
- 3 Feeley KM, Wells M. Precursor lesions of ovarian epithelial malignancy. *Histopathology* 2001;38:87–95.
- 4 Scully RE. Pathology of ovarian cancer precursors. *J Cell Biochem* 1995;23(Suppl):208–218.
- 5 Scully RE. Early *de novo* ovarian cancer and cancer developing in benign ovarian lesions. *Int J Gynaecol Obstet* 1995;49(Suppl):S9–S15.
- 6 Zheng J, Benedict WF, Xu HJ, *et al*. Genetic disparity between morphologically benign cysts contiguous to ovarian carcinomas and solitary cystadenomas [see comments]. *J Natl Cancer Inst* 1995;87:1146–1153.
- 7 Hutson R, Ramsdale J, Wells M. p53 protein expression in putative precursor lesions of epithelial ovarian cancer. *Histopathology* 1995;27:367–371.
- 8 Oyelese Y, Kueck AS, Barter JF, *et al*. Asymptomatic postmenopausal simple ovarian cyst. *Obstet Gynecol Surv* 2002;57:803–809.
- 9 Christensen JT, Boldsen JL, Westergaard JG. Functional ovarian cysts in premenopausal and gynecologically healthy women. *Contraception* 2002;66:153–157.
- 10 Seidman JD, Russell P, Kurman RJ. Surface epithelial tumors of the ovary. In: Kurman RJ (ed). *Blaustein's Pathology of the Female Genital Tract*, 5th edn. Springer-Verlag: New York, 2002, pp 791–904.

- 11 van der Bijl AE, Fleuren GJ, Kenter GG, *et al*. Unique combination of an ovarian gonadoblastoma, dysgerminoma, and mucinous cystadenoma in a patient with Turner's syndrome: a cytogenetic and molecular analysis. *Int J Gynecol Pathol* 1994;13:267–272.
- 12 Cuatrecasas M, Villanueva A, Matias-Guiu X, *et al*. K-ras mutations in mucinous ovarian tumors: a clinicopathologic and molecular study of 95 cases. *Cancer* 1997;79:1581–1586.
- 13 Jimbo H, Hitomi Y, Yoshikawa H, *et al*. Evidence for monoclonal expansion of epithelial cells in ovarian endometrial cysts. *Am J Pathol* 1997;150:1173–1178.
- 14 Singer G, Kurman RJ, Chang H-W, *et al*. Diverse tumorigenic pathways in ovarian serous carcinoma. *Am J Pathol* 2002;160:1223–1228.
- 15 Sehdev AES, Sehdev PS, Kurman RJ. Noninvasive and invasive micropapillary serous carcinoma of the ovary: a clinicopathologic analysis of 135 cases. *Am J Surg Pathol* 2003;27:725–736.
- 16 Deligdisch L. Ovarian dysplasia: a review. *Int J Gynecol Cancer* 1997;7:89–94.
- 17 Shelling AN, Cooke I, Ganesan TS. The genetic analysis of ovarian cancer. *Br J Cancer* 1995;72:521–527.
- 18 Pothuri B, Leitao M, Barakat R, *et al*. Genetic analysis of ovarian carcinoma histogenesis. *Gynecol Oncol* 2001;80:277.
- 19 Teneriello MG, Ebina M, Linnoila RI, *et al*. p53 and K-ras gene mutations in epithelial ovarian neoplasms. *Cancer Res* 1993;53:3103–3108.
- 20 Cuatrecasas M, Erill N, Musulen E, *et al*. K-ras mutations in nonmucinous ovarian epithelial tumors: a molecular analysis and clinicopathologic study of 144 patients. *Cancer* 1998;82:1088–1095.
- 21 Kappes S, Milde-Langosch K, Kressin P, *et al*. p53 mutations in ovarian tumors, detected by temperature-gradient gel electrophoresis, direct sequencing and immunohistochemistry. *Int J Cancer* 1995;64:52–59.
- 22 Moll R, Franke WW, Schiller DL, *et al*. The catalog of human cytokeratins: patterns of expression in normal epithelia, tumors and cultured cells. *Cell* 1982;31:11–24.
- 23 Shih IM, Nesbit M, Herlyn M, *et al*. A new Mel-CAM (CD146)-specific monoclonal antibody, MN-4, on paraffin-embedded tissue. *Mod Pathol* 1998;11:1098–1106.
- 24 Shih IM, Yu J, He TC, *et al*. The beta-catenin binding domain of adenomatous polyposis coli is sufficient for tumor suppression. *Cancer Res* 2000;60:1671–1676.
- 25 Davies H, Bignell GR, Cox C, *et al*. Mutations of the *BRAF* gene in human cancer. *Nature* 2002;417:949–954.
- 26 Vogelstein B, Kinzler KW. Digital PCR. *Proc Natl Acad Sci USA* 1999;96:9236–9241.
- 27 Singer G, Oldt III R, Cohen Y, *et al*. Mutations in *BRAF* and *KRAS* characterize the development of low-grade ovarian serous carcinoma. *J Natl Cancer Inst* 2003;95:484–486.
- 28 Cohen Y, Zhao XM, Mambo E, *et al*. *BRAF* mutation occurs in a majority of papillary thyroid carcinoma. *J Natl Cancer Inst* 2003;95:625–627.
- 29 Enomoto T, Fujita M, Inoue M, *et al*. Analysis of clonality by amplification of short tandem repeats. Carcinomas of the female reproductive tract. *Diagn Mol Pathol* 1994;3:292–297.

- 30 Allen RC, Zoghbi HY, Moseley AB, *et al*. Methylation of *HpaII* and *HhaI* sites near the polymorphic CAG repeat in the human androgen-receptor gene correlates with X chromosome inactivation. *Am J Hum Genet* 1992;51:1229–1239.
- 31 Gerdes J, Schwab U, Lemke H, *et al*. Production of a mouse monoclonal antibody reactive with a human nuclear antigen associated with cell proliferation. *Int J Cancer* 1983;31:13–20.
- 32 Gerdes J, Lemke H, Baisch H, *et al*. Cell cycle analysis of a cell proliferation-associated human nuclear antigen defined by the monoclonal antibody Ki-67. *J Immunol* 1984;133:1710–1715.
- 33 Leers M, Kolgen W, Bjorklund V, *et al*. Immunocytochemical detection and localization of a cytokeratin 18 epitope exposed during early apoptosis. *J Pathol* 1999;5:567–572.
- 34 Shih IM, Kurman RJ. Ki-67 labeling index in the differential diagnosis of exaggerated placental site, placental site trophoblastic tumor, and choriocarcinoma: a double immunohistochemical staining technique using Ki-67 and Mel-CAM antibodies. *Hum Pathol* 1998;29:27–33.
- 35 Vogelstein B, Kinzler KW. *The Genetic Basis of Human Cancer*. McGraw-Hill Health Professions Division: New York, 1998.
- 36 Kotylo PK, Michael H, Fineberg N, *et al*. Flow cytometric analysis of DNA content and RAS P21 oncoprotein expression in ovarian neoplasms. *Int J Gynecol Pathol* 1992;11:30–37.
- 37 Acevedo AD, Bowser SS, Gerritsen ME, *et al*. Morphological and proliferative responses of endothelial cells to hydrostatic pressure: role of fibroblast growth factor. *J Cell Physiol* 1993;157:603–614.
- 38 Haberstroh KM, Kaefer M, Retik AB, *et al*. The effects of sustained hydrostatic pressure on select bladder smooth muscle cell functions. *J Urol* 1999;162: 2114–2118.
- 39 Hirokawa M, Miura S, Kishikawa H, *et al*. Loading of mechanical pressure activates mitogen-activated protein kinase and early immediate gene in intestinal epithelial cells. *Dig Dis Sci* 2001;46:1993–2003.
- 40 Peyssonnaud C, Eychene A. The Raf/MEK/ERK pathway: new concepts of activation. *Biol Cell* 2001;93: 53–62.
- 41 Malumbres M, Barbacid M. RAS oncogenes: the first 30 years. *Nat Rev Cancer* 2003;3:459–465.
- 42 Novelli M, Cossu A, Oukrif D, *et al*. X-inactivation patch size in human female tissue confounds the assessment of tumor clonality. *Proc Natl Acad Sci USA* 2003;27:27.
- 43 Scully RE, Young RH, Clement PB. Surface epithelial-stromal tumours and serous tumors. In: Rosai J (ed). *Tumors of the Ovary, Maldeveloped Gonads, Fallopian Tube, and Broad Ligament*, Third series edn. Armed Forces Institute of Pathology: Washington, DC, 1998, pp 51–79.

HLA-G Is a Potential Tumor Marker in Malignant Ascites

Gad Singer, Vera Rebmann, Yu-Chi Chen,
Hsu-Tai Liu, Syed Z. Ali, Jochen Reinsberg,
Michael T. McMaster, Kerstin Pfeiffer,
Daniel W. Chan, Eva Wardelmann,
Hans Grosse-Wilde, Chih-Chien Cheng,
Robert J. Kurman, and Ie-Ming Shih¹

Department of Pathology [G. S., Y.-C. C., S. Z. A., D. W. C., C.-C. C., R. J. K., I.-M. S.], and Department of Epidemiology [H.-T. L.], Johns Hopkins University Medical Institutions, Baltimore Maryland 21231; Department of Immunology, University Hospital of Essen, Essen, Germany [V. R., H. G.-W.]; Departments of Gynecology and Obstetrics [J. R., K. P.], and Department of Pathology [E. W.], University of Bonn, Bonn, Germany; and Department of Stomatology, University of California, San Francisco, California [M. T. M.]

ABSTRACT

Purpose: Molecular approaches as supplements to cytological examination of malignant ascites may play an important role in the clinical management of cancer patients. HLA-G is a potential tumor-associated marker and that one of its isoforms, HLA-G5, produces a secretory protein. This study is to assess the clinical utility of secreted HLA-G levels in differential diagnosis of malignant ascites.

Experimental Design: We used ELISA to assess whether secretory HLA-G (sHLA-G) could serve as a marker of malignant ascites in ovarian and breast carcinomas, which represent the most common malignant tumors causing ascites in women.

Results: On the basis of immunohistochemistry, 45 (61%) of 74 ovarian serous carcinomas and 22 (25%) invasive ductal carcinomas of the breast demonstrated HLA-G immunoreactivity ranging from 2 to 100% of the tumor cells. HLA-G staining was not detected in a wide variety of normal tissues, including ovarian surface epithelium and normal breast tissue. Reverse transcription-PCR demonstrated the presence of HLA-G5 isoform in all of the tumor samples expressing HLA-G. ELISA was performed to measure the sHLA-G in 42 malignant and 18 benign ascites

supernatants. sHLA-G levels were significantly higher in malignant ascites than in benign controls ($P < 0.001$). We found that the area under the receiver-operating characteristic curve for sHLA-G was 0.95 for malignant versus benign ascites specimens. At 100% specificity, the highest sensitivity to detect malignant ascites was 78% (95% confidence interval, 68–88%) at a cutoff of 13 ng/ml.

Conclusions: Our findings suggest that measurement of sHLA-G is a useful molecular adjunct to cytology in the differential diagnosis of malignant versus benign ascites.

INTRODUCTION

Ascites is commonly associated with a variety of infectious diseases, inflammatory disorders, and cardiac, liver, and renal diseases as well as benign and malignant neoplasms (1–3). Cytological examination of ascites is performed in an effort to diagnose malignant tumors, but the sensitivity of cytology has been estimated to be 60% at best (4). The low sensitivity may be because of small numbers of tumor cells in the ascites or the presence of a large amount of leukocytes, mesothelial cells, and blood that can obscure the malignant cells. For example, inflammation that is often associated with a malignant ascites can result in reactive changes in mesothelial cells that make their morphological distinction from carcinoma cells extremely difficult (4). Thus, a molecular test that is able to distinguish malignant from benign ascites could have great diagnostic utility.

HLA-G is a nonclassical MHC class I antigen that interacts with natural killer cells (5). HLA-G expression has not been detected in normal tissues except in trophoblast in placentas from early gestation (6–8). In contrast, HLA-G expression has been detected in several human cancers including melanoma, renal cell carcinoma, breast carcinoma, and large cell carcinoma of the lung (9–14). HLA-G expression in cancer cells has been shown to be important for the escape of immunosurveillance by host T-lymphocytes and natural killer cells (6, 9–11, 15, 16). Recently, an HLA-G-specific ELISA was developed to measure sHLA-G, a product of an HLA-G5 isoform (17–19). Because HLA-G is not detected in normal adult tissues but is expressed by some carcinomas, we hypothesized that the detection of sHLA-G² using the newly developed ELISA might be useful in the detection of cancer in ascites. In this study, we tested this hypothesis by assessing the expression pattern of HLA-G in women with ovarian serous carcinomas and invasive ductal carcinomas of the breast because these are the most common malignant tumors in women that produce ascites. We measured sHLA-G in peritoneal fluid supernatant to evaluate its potential as a marker for malignant ascites.

Received 2/24/03; revised 5/20/03; accepted 5/21/03.

The costs of publication of this article were defrayed in part by the payment of page charges. This article must therefore be hereby marked *advertisement* in accordance with 18 U.S.C. Section 1734 solely to indicate this fact.

This work was supported in part by the United States Department of Defense OC 010017 Grant, the Richard TeLinde Research Fund from The Johns Hopkins University (JHU) School of Medicine, the JHU-American Cancer Society, and the Swiss National Science Foundation (to G. S.).

¹ To whom requests for reprints should be addressed, at The Johns Hopkins Medical Institutions, 418 North Bond Street, Room B-315, Baltimore, MD 21231. Phone: (410) 502-774; Fax: (410) 502-7943; E-mail: ishih@jhmi.edu.

² The abbreviations used are: sHLA-G, secretory or soluble HLA-G; CI, confidence interval; RT-PCR, reverse transcription-PCR; ROC, receiver operating characteristic (curve).

MATERIALS AND METHODS

Tissue Samples and Ascites Specimens. The acquisition of paraffin tissues and ascites specimens was approved by the local Institutional Review Boards. A total of 180 formalin-fixed, paraffin-embedded tissue samples including 74 ovarian serous carcinomas, 88 breast invasive ductal carcinomas, 8 normal ovaries, and 10 benign breast tissues were retrieved from the surgical pathology files. Peritoneal fluid specimens (3–5 ml) were obtained from the Cytopathology Division of the University of Bonn, Bonn, Germany, and from the Johns Hopkins Medical Institutions; they included 41 cytology-confirmed malignant ascites samples (24 ovarian serous carcinomas and 17 breast carcinomas) and 19 cytology-negative benign specimens in which the patients did not have concurrent malignant diseases. There was a cytology-false-negative specimen that was initially diagnosed by cytopathologists as benign, but the patients had stage III ovarian cancer, and the ascites sample contained ovarian serous carcinoma cells in culture (20). Thus, this sample was later classified into the ovarian cancer group in this study. The ascites samples were centrifuged at $2000 \times g$ for 5 min within 6 h after collection. The supernatant and cell pellets were aliquoted and frozen until use. All of the specimens were obtained from female adult patients.

Immunohistochemistry and Western Blot Analysis.

Expression of HLA-G was studied in surgical specimens using immunohistochemistry and Western blot analysis. Paraffin sections were used for immunohistochemistry with an HLA-G-specific monoclonal antibody, 4H84 (1:600), which reacted to the denatured HLA-G heavy chain (6), followed by the avidin-biotin peroxidase method (8, 15). The frequency of positive cells was estimated by randomly counting more than 500 tumor cells from three different high-power fields ($\times 40$). Western blot analysis was performed using the 4H84 antibody (1:1000) on five ovarian serous carcinomas that showed positive HLA-G immunostaining, two specimens of epithelium isolated from ovarian serous cystadenomas, one primary culture from normal ovarian surface, one sample of normal ovarian tissue, and one sample of isolated peripheral leukocytes. Similar amounts of total protein from each lysate were loaded and separated on 12% Tris-Glycine-SDS polyacrylamide gels (Novex, San Diego, CA) and electroblotted to Millipore Immobilon-P polyvinylidene difluoride membranes. Western blots were developed by chemiluminescence (Pierce, Rockford, IL).

RT-PCR. RT-PCR was performed to validate the HLA-G expression and to determine the isoforms expressed in a panel of 11 ovarian and 5 breast carcinomas using the protocol described previously (21). The assay was not performed in samples that stained negative for the HLA-G antibody. The primer sequences for all of the HLA-G isoforms were: 5'-ggaagaggagacacggaaca-3' and 5'-gcagctccagtgactacagc-3'. The primer sequences for HLA-G5-specific primers were: 5'-accgacctgttaaaggtctt-3' and 5'-caatgtggctgaacaaggagag-3'. Total RNA was purified and cDNA was synthesized using standard protocols. Briefly, frozen tissues were minced and placed in the TRIzol reagent (Invitrogen, Carlsbad, CA). Total RNA was isolated, and contaminating genomic DNA was removed using the DNA-free kit (Ambion, Austin, TX). cDNA was prepared using oligo(dT) primers and was diluted for PCR.

H&E-stained sections were prepared from a portion of the frozen tumors and were reviewed by a surgical pathologist (I-M. S.) to confirm the diagnosis. The PCR products were separated by 2% agarose gels.

ELISA. sHLA-G was measured using ELISA, which has been described previously by us (18, 19). Briefly, soluble HLA-A, B, C, E molecules (sHLA-I) were selectively depleted from samples using immunomagnetic beads (Dynabeads M280; Dynal, Hamburg, Germany) coupled with the monoclonal antibody TP25.99. The remaining sHLA-G molecules were measured in an ELISA format using monoclonal antibody W6/32 [0.2 $\mu\text{g/ml}$ in PBS (pH 7.2)] as the capture reagent. After the blocking of free binding sites with BSA in PBS (2%), diluted samples (1:2) were added and incubated for 1 h at room temperature. Unbound antigens were removed by intensive washing with PBS-Tween (0.05%). Bound sHLA-G heavy chains were detected by the sequential addition of pox-labeled antihuman $\beta 2$ -microglobulin antiserum (Dakopatts, Hamburg, Germany), and substrate [0.075% H_2O_2 , 0.1% ortho-phenylenediamine in 0.035 M citrate buffer (pH 5.0)]. The absorbance was measured at 490 nm (BIO-TEK Instruments, Winooski, VT). The intra- and interassay variations were 3.5 and 13.1%, respectively. The sensitivity of the assay in detecting sHLA-G was 3 ng/ml. ELISA was performed in a blinded fashion.

Statistical Analysis. The feasibility of using sHLA-G levels as a diagnostic tool for detecting malignant *versus* benign ascites was assessed using the ROC curve analysis. A ROC curve is a graphic presentation of the sensitivity against the false-positive rate (1-specificity), and the areas under the ROC curves were measured to evaluate test performance at different thresholds of a diagnostic measure. The χ^2 test (one-sided) of the medians was used to analyze the difference in sHLA-G levels in malignant *versus* benign ascites samples. The CIs were estimated for the sensitivity of the HLA-G ELISA.

RESULTS

Expression of HLA-G in Ovarian and Breast Cancer

Tissues. Immunohistochemical analysis of ovarian and breast carcinomas revealed HLA-G immunoreactivity in 45 (61%) of 74 high-grade ovarian serous carcinomas and in 22 (25%) of 88 invasive ductal carcinomas of the breast (Fig. 1). The positive tumor cells showed a discrete membranous staining pattern, and the proportion of positive cells varied from 2 to 100% in any given specimen. HLA-G staining was not detected in low-grade ovarian serous carcinomas and normal tissues including ovarian surface epithelium, mammary ducts, and lobules. We also assessed HLA-G immunoreactivity in benign ovarian and breast lesions. HLA-G expression was not detected in 8 ovarian serous cystadenomas, 12 ovarian borderline tumors (atypical proliferative serous tumors and noninvasive micropapillary serous carcinomas), nor 10 intraductal hyperplasias of the breast. Only rare HLA-G-positive tumor cells were identified in 2 of 10 intraductal carcinomas of the breast. The specificity of HLA-G immunostaining was confirmed by Western blot analysis and RT-PCR as shown in Fig. 2. A 39 kDa band corresponding to the HLA-G protein was identified in five ovarian serous carcinomas but not in two ovarian cystadenomas, ovarian surface epithelium, and stroma. RT-PCR was performed in ovarian

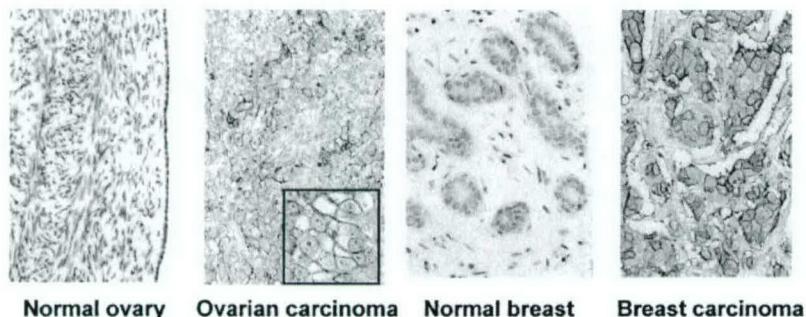


Fig. 1 HLA-G expression based on immunohistochemistry in ovarian serous carcinomas and breast ductal carcinomas. HLA-G immunoreactivity is predominantly localized in the cell membrane of tumor cells (*inset*) in ovarian serous carcinoma and breast ductal carcinoma. There is no detectable HLA-G immunoreactivity in ovarian surface epithelium of normal ovary and normal breast tissue. The stromal cells and inflammatory cells are negative.

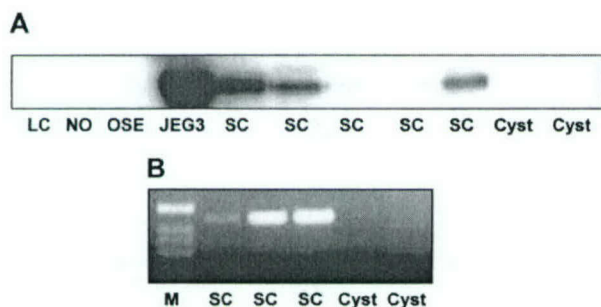


Fig. 2 Western blot analysis. *A*, a 39 kDa band corresponding to HLA-G protein is demonstrated in all five of the ovarian serous carcinomas (SC) and the positive control, JEG3 choriocarcinoma cell line, but not in peripheral leukocytes (LC), normal ovarian stromal tissue (NO), ovarian surface epithelium (OSE), and cyst epithelium (Cyst) from two ovarian serous cystadenomas. *B*, RT-PCR. HLA-G5 PCR products were present in three ovarian cancer tissues that express HLA-G using immunohistochemistry but not in two ovarian serous cysts that fail to show HLA-G immunostaining. *M*, 1-Kb DNA marker.

serous carcinomas and invasive ductal carcinomas of the breast using primers that amplified all HLA-G isoforms. The PCR products were isolated by electrophoresis to reveal a predominance of the HLA-G1 and G5 isoforms. HLA-G5 RNA transcript, a secretory isoform, was specifically amplified using the HLA-G5-specific primers in all five of the representative ovarian serous carcinomas and in the two invasive ductal carcinomas of breast that expressed HLA-G (Fig. 2). This finding prompted us to assess whether sHLA-G could be detected in peritoneal fluid samples in ovarian and breast cancer patients.

Measurement of sHLA-G in Ascites Specimens. sHLA-G levels were measured in the supernatant of ascites from 60 samples using ELISA. All but one malignant ascites supernatant contained detectable sHLA-G, including one specimen that had been missed on cytology (20). In contrast, 7 of 18 benign specimens contained detectable but low levels of sHLA-G. As shown in Fig. 3, the levels of sHLA-G were significantly higher in malignant as compared with benign ascites ($P < 0.001$). Among 11 benign ascites specimens with undetectable sHLA-G, 2 were obtained from patients with ovarian serous cystadenomas that could be confused with ovarian cancer on clinical examination. The remaining seven benign samples with detectable sHLA-G were from patients with non-neoplastic diseases including liver, cardiac, and renal diseases.

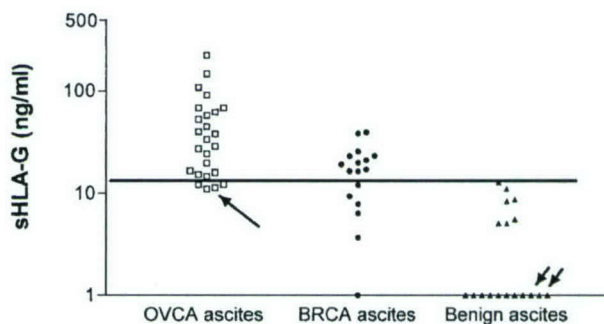


Fig. 3 Scatter plot showing sHLA-G concentrations in a total of 60 ascites samples as determined by ELISA. All of the 25 ovarian cancer (OVCA) patients (□) and 16 of 17 breast cancer (BRCA) patients (●) have detectable HLA-G levels. *Long arrow*, the patient with malignant ascites but with a negative cytology. In contrast, 7 of 18 benign ascitic fluid samples in the age-matched control group (▲) has a detectable but low HLA-G level. *Short arrows*, the two patients with ovarian cystadenomas. As compared with benign group, the levels of sHLA-G are significantly higher in ovarian ($P < 0.001$) and breast cancer groups ($P < 0.001$). *Solid line*, an arbitrary cutoff (13 ng/ml) to give 100% specificity in diagnosing malignant ascites.

ROC curves were used to evaluate the performance of sHLA-G in detecting ovarian and breast cancer in ascites using multiple cutoff values. The area under the ROC curve was 0.95 in assessing sHLA-G levels as the diagnostic tool to detect ovarian and breast cancer. More specifically, the areas under the ROC curve were 0.99 and 0.90 for ovarian cancer *versus* benign samples and breast cancer *versus* benign samples, respectively (Fig. 4). Given 100% specificity, the highest sensitivity achieved to detect cancer was 78% (95% CI, 68–88%) at a cutoff of 13 ng/ml. The sensitivity to diagnose ovarian cancer and breast cancer was 84% (95% CI, 70–98%) and 65% (95% CI, 42–87%), respectively, at this arbitrary cutoff. With a specificity of 94.4%, the sensitivity was 100% (95% CI, 100%) and 71% (95% CI, 49–93%) for ovarian cancer and breast cancer, respectively.

Correlation of HLA-G expression in tissue or ascites cell pellets and the sHLA-G level in ascites supernatants was performed in 31 patients as the corresponding surgical specimens or cell pellets were available for analysis. In 21 malignant ascites samples with detectable sHLA-G, HLA-G expression was demonstrated in 12 tissue specimens and ascites cell pellets by immunohistochemistry or Western blot analysis (data not

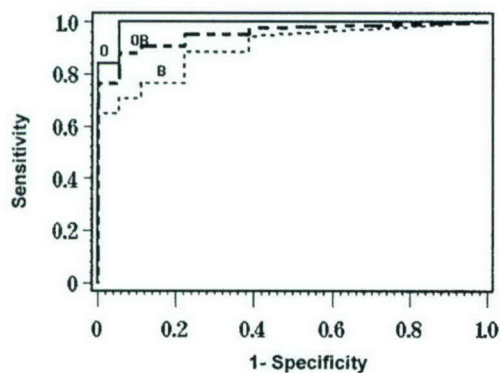


Fig. 4 ROC curve analysis based on 60 samples to assess the performance of sHLA-G levels in diagnosing malignant ascites. The area under the ROC curve assessing sHLA-G levels as the diagnostic tool to detect ovarian and breast cancer is 0.95. Specifically, the areas under the ROC curve are 0.99 and 0.90 for ovarian cancer *versus* benign samples and breast cancer *versus* benign samples, respectively. O: ovarian cancer; B, breast cancer; OB, ovarian and breast cancer.

shown). In 10 benign ascites samples (5 with detectable sHLA-G), there was no HLA-G expression detectable in ascites cell pellets using Western blot analysis.

DISCUSSION

The results of this study provide evidence that HLA-G is expressed in ovarian and breast carcinomas and that measurement of sHLA-G using ELISA is a highly sensitive technique to diagnose malignant ascites. Ninety-eight % of specimens with malignant cells, identified by cytology, had detectable sHLA-G levels. In addition, sHLA-G was detected in one specimen that was ultimately shown to be a false-negative case by cytological examination. The areas under the ROC curve were 0.99 and 0.90 for ovarian cancer *versus* benign samples and breast cancer *versus* benign samples, respectively. The better performance of sHLA-G in detecting ovarian cancer as compared with breast cancer is consistent with our immunohistochemical findings that ovarian cancers express HLA-G more frequently than breast cancers.

How does HLA-G compare with other soluble tumor-associated markers in diagnosing malignant ascites? Several protein markers have been studied including CA125 (22), tissue polypeptide-specific antigen, soluble interleukin-2 receptor α (23), soluble aminopeptidase N/CD13 (24), α -fetoprotein (25), carcinoembryonic antigen, CA 19-9, CA 15-3 (25), and several cytokines (26), but none are specific enough for cancer diagnosis because a variety of normal tissues, benign tumors, and nonneoplastic diseases also express these markers (24, 27-28). Using a cutoff value to achieve >90% specificity in detecting malignant ascites, the sensitivity of these markers was generally very low and, therefore, unacceptable for clinical application. In contrast, HLA-G has very limited tissue distribution because only a subpopulation of trophoblast (intermediate trophoblast) is known to express this molecule (7, 8) suggesting that sHLA-G would be more specific for cancer diagnosis. The findings in this study confirm this impression because the HLA-G ELISA

achieved a sensitivity of 78% and a specificity of 100% for diagnosing malignant ascites at a cutoff of 13 ng/ml.

The finding that almost all of the malignant ascites samples contained detectable sHLA-G contrasted with the lower rate of HLA-G expression in the tumors based on immunohistochemistry, because 61% of ovarian and only 25% of breast cancer tissue specimens were positive. In addition, some malignant ascites supernatants contained elevated sHLA-G levels, whereas HLA-G immunoreactivity was not detected in the corresponding tissue specimens and cell pellets from ascites by immunohistochemistry. This discordant finding can be explained by the fact that HLA-G is only focally expressed in most tumors and, therefore, may be undetected in representative tissue specimens selected for immunostaining or immunoblotting. It is likely that carcinoma cells in ascitic fluid secrete sHLA-G, resulting in high sHLA-G levels in ascites. If only a few tumor cells are present in the peritoneal fluid they may not be detected by cytology. Although these are our favorite explanations, other possibilities, albeit unlikely, should be also pointed out. For example, sHLA-G is expressed by other tissues in response to malignant diseases. The low level of sHLA-G in benign ascites may be attributable to nonspecific binding (background noise) of the antibody used in the ELISA. Alternatively, there may be unknown tissue resources that express sHLA-G and contribute to the low level of sHLA-G in ascites samples.

In summary, HLA-G is a tumor-associated molecule that is expressed by ovarian serous carcinoma and ductal carcinomas of the breast, the most common malignant tumors that produce ascites in women. Malignant ascites specimens contained much higher levels of sHLA-G than the benign ascites specimens. The detection of sHLA-G in ascitic fluid may provide a novel molecular approach to supplement cytological examination in the evaluation of ascites. It should be noted that the sensitivity of sHLA-G ELISA to diagnose malignant ascites may not be as high as shown in this study because the threshold to distinguish benign and malignant ascites could be higher than 13 ng/ml after a larger number of benign samples are analyzed. In order for this new marker to have clinical utility, several issues must be addressed. Although the sensitivity of sHLA-G ELISA in diagnosing malignant ascites in this study was 78% with 100% specificity, higher sensitivity would be desirable. Sensitivity could be improved by combining the measurement of sHLA-G with other tumor-associated markers (20, 29). It will be necessary to compare the performance of the sHLA-G ELISA and routine cytological examination by testing a large number of cytology-negative but biopsy-positive samples. It will also be important to address how age, menopausal status, histological grade and other clinical parameters affect HLA-G levels in ascites. Lastly, the potential use of sHLA-G in other body fluids such as plasma should be further investigated.

ACKNOWLEDGMENTS

We thank John Lauro at the Johns Hopkins Medical Institutions for his excellent technical support. This study is in memory of Dr. Frederick J. Montz of the Kelly Gynecologic Oncology Service at Johns Hopkins Hospital.

REFERENCES

- Senger, D. R., Galli, S. J., Dvorak, A. M., Perruzzi, C. A., Harvey, V. S., and Dvorak, H. F. Tumor cells secrete a vascular permeability factor that promotes accumulation of ascites fluid. *Science (Wash. DC)*, *219*: 983-985, 1983.
- Nagy, J. A., Herzberg, K. T., Dvorak, J. M., and Dvorak, H. F. Pathogenesis of malignant ascites formation: initiating events that lead to fluid accumulation. *Cancer Res.*, *53*: 2631-2643, 1993.
- Garrison, R. N., Galloway, R. H., and Heuser, L. S. Mechanisms of malignant ascites production. *J. Surg. Res.*, *42*: 126-132, 1987.
- Motherby, H., Nadjari, B., Friegel, P., Kohaus, J., Ramp, U., and Bocking, A. Diagnostic accuracy of ascites cytology. *Diagn. Cytopathol.*, *20*: 350-357, 1999.
- van der Ven, K., Pfeiffer, K., and Skrablin, S. HLA-G polymorphisms and molecule function—questions and more questions—a review. *Placenta*, *21* (Suppl. A): S86-S92, 2000.
- McMaster, M. T., Shorter, S., Kapasi, K., Geraghty, D., Lim, K. H., and Fisher, S. HLA-G isoforms produced by placental cytotrophoblasts and found in amniotic fluid are due to unusual glycosylation. *J. Immunol.*, *160*: 5922-5928, 1998.
- McMaster, M. T., Librach, C. L., Zhou, Y., Lim, K. H., Janatpour, M. J., DeMars, R., Kovats, S., Damsky, C. S., and Fisher, S. J. Human placental HLA-G expression is restricted to differentiated cytotrophoblasts. *J. Immunol.*, *154*: 3771-3778, 1995.
- Singer, G., Kurman, R. J., McMaster, M., and Shih, I-M. HLA-G immunoreactivity is specific for intermediate trophoblast in gestational trophoblastic disease and can serve as a useful marker in differential diagnosis. *Am. J. Surg. Pathol.*, *26*: 914-920, 2002.
- Paul, P., Rouas-Freiss, N., Khalil-Daher, I., Moreau, P., Riteau, B., Le Gal, F. A., Avril, M. F., Dausset, J., and Guillet, J. G. HLA-G expression in melanoma: a way for tumor cells to escape from immunosurveillance. *Proc. Natl. Acad. Sci. USA*, *95*: 4510-4515, 1998.
- Ibrahim, E. C., Guerra, N., Lacombe, M. J., Angevin, E., Chouaib, S., Carosella, E. D., Caignard, A., and Paul, P. Tumor-specific up-regulation of the nonclassical class I HLA-G antigen expression in renal carcinoma. *Cancer Res.*, *61*: 6838-6845, 2001.
- Urosevic, M., Kurrer, M. O., Kamarashev, J., Mueller, B., Weder, W., Burg, G., Stahel, R. A., Dummer, R., and Trojan, A. Human leukocyte antigen G up-regulation in lung cancer associates with high-grade histology, human leukocyte antigen class I loss and interleukin-10 production. *Am. J. Pathol.*, *159*: 817-824, 2001.
- Polakova, K., and Russ, G. Expression of the non-classical HLA-G antigen in tumor cell lines is extremely restricted. *Neoplasma*, *47*: 342-348, 2000.
- Davies, B., Hiby, S., Gardner, L., Loke, Y. W., and King, A. HLA-G expression by tumors. *Am. J. Reprod. Immunol.*, *45*: 103-107, 2001.
- Real, L. M., Cabrera, T., Collado, A., Jimenez, P., Garcia, A., Ruiz-Cabello, F., and Garrido, F. Expression of HLA G in human tumors is not a frequent event. *Int. J. Cancer*, *81*: 512-518, 1999.
- Lefebvre, S., Antoine, M., Uzan, S., McMaster, M., Dausset, J., Carosella, E. D., and Paul, P. Specific activation of the non-classical class I histocompatibility HLA-G antigen and expression of the ILT2 inhibitory receptor in human breast cancer. *J. Pathol.*, *196*: 266-274, 2002.
- Urosevic, M., Willers, J., Mueller, B., Kempf, W., Burg, G., and Dummer, R. HLA-G protein up-regulation in primary cutaneous lymphomas is associated with interleukin-10 expression in large cell T-cell lymphomas and indolent B-cell lymphomas. *Blood*, *99*: 609-617, 2002.
- Paul, P., Cabestre, F. A., Ibrahim, E. C., Lefebvre, S., Khalil-Daher, I., Vazeux, G., Quiles, R. M., Bermond, F., Dausset, J., and Carosella, E. D. Identification of HLA-G7 as a new splice variant of the HLA-G mRNA and expression of soluble HLA-G5, -G6, and -G7 transcripts in human transfected cells. *Hum. Immunol.*, *61*: 1138-1149, 2000.
- Rebmann, V., Pfeiffer, K., Passler, M., Ferrone, S., Maier, S., Weiss, E., and Grosse-Wilde, H. Detection of soluble HLA-G molecules in plasma and amniotic fluid. *Tissue Antigens*, *53*: 14-22, 1999.
- Ugurel, S., Rebmann, V., Ferrone, S., Tilgen, W., Grosse-Wilde, H., and Reinhold, U. Soluble human leukocyte antigen-G serum level is elevated in melanoma patients and is further increased by interferon- α immunotherapy. *Cancer (Phila.)*, *92*: 369-376, 2001.
- Chang, H-W, Ali, S. Z., Cho, S. K. R., Kurman, R. J., and Shih, I-M. Detection of allelic imbalance in ascitic supernatant by Digital SNP analysis. *Clin. Cancer Res.*, *8*: 2580-2585, 2002.
- Morrison, T. B., Weis, J. J., and Wittwer, C. T. Quantification of low-copy transcripts by continuous SYBR Green I monitoring during amplification. *Biotechniques*, *24*: 954-958, 960, 962, 1998.
- Sevinc, A., Sari, R., and Buyukberber, S. Cancer antigen 125: tumor or serosal marker in case of ascites? *Arch. Intern. Med.*, *161*: 2507-2508, 2001.
- Sedlacek, P., Frydecka, I., Gabrys, M., Van Dalen, A., Einarsson, R., and Harlozinska, A. Comparative analysis of CA125, tissue polypeptide specific antigen, and soluble interleukin-2 receptor α levels in sera, cyst, and ascitic fluids from patients with ovarian carcinoma. *Cancer (Phila.)*, *95*: 1886-1893, 2002.
- van Hensbergen, Y., Broxterman, H. J., Hanemaaijer, R., Jorna, A. S., van Lent, N. A., Verheul, H. M. W., Pinedo, H. M., and Hoekman, K. Soluble aminopeptidase N/CD13 in malignant and nonmalignant ascites and intratumoral fluid. *Clin. Cancer Res.*, *8*: 3747-3754, 2002.
- Sari, R., Yildirim, B., Sevinc, A., Bahceci, F., and Hilmioğlu, F. The importance of serum and ascites fluid alpha-fetoprotein, carcinoembryonic antigen, CA 19-9, and CA 15-3 levels in differential diagnosis of ascites etiology. *Hepatogastroenterology*, *48*: 1616-1621, 2001.
- Punnonen, R., Teisala, K., Kuoppala, T., Bennett, B., and Punnonen, J. Cytokine production profiles in the peritoneal fluids of patients with malignant or benign gynecologic tumors. *Cancer (Phila.)*, *83*: 788-796, 1998.
- Shahab, N. Tumor markers in malignant ascites. *Arch. Intern. Med.*, *162*: 949-950, 2002.
- Topalak, O., Saygili, U., Soyuturk, M., Karaca, N., Batur, Y., Uslu, T., and Erten, O. Serum, pleural ascites, and ascites CA-125 levels in ovarian cancer and nonovarian benign and malignant diseases: a comparative study. *Gynecol. Oncol.*, *85*: 108-113, 2002.
- Shih, I-M., Sokoll, L. J., and Chan, D. W. Tumor markers in ovarian cancer. In: E. P. Diamandis, H. A. Fritsche, H. Lilja, D. W. Chan, and M. K. Schwartz (eds.), *Tumor Markers physiology, Pathobiology, Technology and Clinical Applications*, pp. 239-252. Philadelphia: AACR Press, 2002.

**PROJECT 2 – IDENTIFICATION OF AUTOLOGOUS ANTIGENS IN EARLY
STAGE SEROUS CARCINOMA**

Richard Roden, Ph.D.

ABSTRACT:

Our goal is to develop an early detection screening test for serous carcinoma. **Specific aim 1:** Obtain cDNAs of autologous tumor antigens recognized by sera of patients with early stage serous carcinoma, but not controls. **Specific aim 2:** Identify autologous tumor antigens expressed in serous carcinoma but absent from, or a low level in normal tissue. **Progress:** Two novel tumor associated antigens, the General Cell isoform of UNC-45 (GC-UNC-45) and KIAA1529, were identified by matrix-assisted laser desorption ionization time-of-flight analysis. Ectopic over-expression of GC-UNC-45 enhanced the rate of cell proliferation in vitro. Although GC-UNC-45 is present in normal surface epithelium, benign cystadenoma and low-grade serous carcinoma, elevated GC-UNC-45 expression was associated with high grade and advanced stage ovarian serous carcinomas. GC-UNC-45 transcripts were higher in high grade disease than immortalized ovarian surface epithelium. We tested multiplex detection of antibodies to candidate ovarian TAAs and statistical modeling for discrimination of sera of ovarian cancer patients and controls. The best model generated an AUC of 0.86 (0.78-0.90) for discrimination of sera of EOC patients and healthy patients using antibody specific to p53, NY-CO-8 and HOXB7. Inclusion of CA125 level in the model provided an AUC of 0.89 (0.84-0.92), as compared to an AUC of 0.83 (0.81-0.83) using CA125 alone. Serum antibody to p53 and HOXB7 is positively associated with EOC, whereas NY-CO-8-specific antibody shows negative association. Bayesian modeling of key TAA-specific serum antibody responses is complementary to CA125 testing for discrimination of sera from patients with EOC from those of healthy women.

Table of Contents

Cover	1
Abstract	2
Table of Contents	3
Introduction	4
Body	4
Key Research Accomplishments	7
Reportable Outcomes	8
Conclusions	8
References	8
Appendices	
<ul style="list-style-type: none"> • Application of Bayesian modeling of autologous antibody responses against ovarian tumor-associated antigens to cancer detection. Al Erkanli, Douglas D Taylor, Deyrick Dean, Faria Eksir, Daniel Egger, James Geyer, Brad H Nelson, Herbert A Fritsche, and Richard BS Roden. (Submitted to Clinical Cancer research) • Elevated expression of the General Cell UNC-45 isoform associates with high grade invasive ovarian carcinoma. Martina Bazzaro, Taylor Tang, Catherine J Turski, Robert E Bristow, le-Ming Shih, and Richard BS Roden. (Submitted to the American Journal of Pathology) 	

Introduction

The immune system constantly surveys the body for 'non-self' antigens, and generates a response in the appropriate context. A key finding of cancer biology is that cancer patients often generate antibody to neoantigens specifically expressed in their tumor (1). Autologous antibodies have been documented in patients afflicted with a variety of different cancers, (2-4) including ovarian cancer (5). Autologous antibodies generated by cancer patients have been used to screen expression libraries for tumor antigens. This technique, originally described by Sahin *et al* and termed SEREX (serologic analysis of recombinant cDNA expression libraries of human tumors with autologous serum), has been used to obtain tumor antigen cDNA clones. SEREX has been applied to tumors of many organs (6) and antibody specific for antigens identified by SEREX in other cancer types have been demonstrated in ovarian cancer patients (7, 8). Tumor-specific autoantigens that are common among ovarian cancer patients but not recognized by sera of healthy volunteers have been identified by us e.g. HOXA7 and HOXB7, and others e.g. cathepsin D and GRP78 (9). Although expressed, Cathepsin D and GRP78 derived from normal tissue were not recognized by sera from ovarian cancer patients implying that they contain tumor-specific epitopes (9). Detection of these autologous antibody responses to ovarian cancer antigens appears to have prognostic significance (10). SEREX antigens derived from early stage serous carcinoma may represent useful biomarkers for the dissection of molecular pathways of serous carcinoma (Dr Shih, Project 1). SEREX antigens are also potential targets for cancer immunotherapy (11) (Dr Wu, Project 3).

Body

Objective 1: Obtain cDNAs of autologous tumor antigens recognized by sera of patients with early stage serous carcinoma, but not controls.

Task 1.1. Screen sera of patients (n=12) with early stage serous carcinoma by Western blot analysis to identify those patients with high titer autologous tumor-reactive antibody (months 0-2).

Task 1.2. Generate serous carcinoma cDNA expression libraries and immuno-screen with autologous patient (n=3) serum antibody to identify SEREX antigens (months 2-14).

Task 1.3. Sequence SEREX antigen cDNAs identified in screen and analyze sequences using BLAST searches (months 14-15).

Task 1.4 Express SEREX antigens and purify from bacteria (months 15-21).

Task 1.5 Determine the prevalence of serum antibody specific to each SEREX antigen by direct ELISA in a case/control study (months 21-27). (100 ovarian carcinoma patient sera, 102 sera from patients with benign ovarian tumors and 200 control sera will be tested.)

Identification of GC-UNC-45 as an ovarian TAA (results detailed in Bazzaro et al., appended)

To identify ovarian TAAs, we derived a cell line JH514 from tumor excised from an 83 year old woman with metastatic low grade serous carcinoma of the ovary. Western blot analysis with

AE1/AE3 and anti-CK19 confirmed cytokeratin expression by the JH514 cell line (not shown). Autologous serum antibodies were covalently coupled to a protein G-Sepharose minicolumn and used to immunoprecipitate antigens from detergent lysate of the JH514 cell line. Bound antigens were eluted with low pH and analyzed by SDS-PAGE. The serum antibody from this patient immunoprecipitated two antigens of approximately 100kDa and 200kDa. Each band was excised from the gel and subjected to trypsin digestion. The charge/mass ratio for the tryptic peptides of the ~100kDa and ~200kDa antigens was determined by matrix-assisted laser desorption ionization time-of-flight analysis. The prospector website was used to search for proteins with matching peptides. The ~200kDa antigen was identified as KIAA1529 (195kDa). Nothing is known about the KIAA1529 antigen and no significant homologies or domains were identified. The ~100kDa was identified as GC-UNC-45 (SMAP-1 Genbank AB014729) which has a predicted mass of 101kDa. Matched peptides cover 12% of the GC-UNC-45 protein.

Application of Bayesian modeling of autologous antibody responses against ovarian tumor-associated antigens to cancer detection (results detailed in Erkanli et al., appended)

To explore the utility of autologous serum antibody specific to particular TAAs as an additional tool for discrimination of sera from cancer patients and healthy women, we generated recombinant protein from 13 markers previously identified as candidate TAAs and selected 5 presumptive control reagents. Sera from both healthy women and EOC patients were tested in parallel for reactivity to all 18 panel elements. Initially we tested sera of 23 healthy patients from MDACC as controls, and sera from 59 stage III/IV ovarian cancer patients obtained at ULSM and 27 from MDACC as cases, respectively. This set of sera was analyzed for reactivity to microspheres of discrete sizes coated with individual recombinant TAA or control protein. The presence of antibody bound to the beads was detected with PE-labeled anti-human IgG and the fluorescence quantified using a Luminex plate reader. Since 5 presumptive control elements were included in the panel, absolute MFI values without background subtraction were employed.

Our analytical strategy consisted of fitting the logistic regression model in Equation 1 for ULSM cases and MDACC cases and controls. By using $BF \geq 3$ as a selection criterion, we picked the best model and computed multiple sensitivity, specificity, ROC curve and AUC by varying a probability cutoff between 0.01 to 1.00. The AUC was calculated as 0.86 (95% confidence interval 0.78-0.90) for this best fitting model.

We also compared the best model for discrimination of cases and controls with detection of absolute level of CA125 or p53-specific antibody or both. The AUC was calculated as 0.83 (95% confidence interval 0.81-0.83) for the standard CA125 assay alone. Detection of p53 antibody alone was not useful for discrimination of cases and controls in this serum set (AUC of 0.52 with 95% confidence interval 0.20-0.58) and combination of absolute CA125 level and serum reactivity to p53 provided an AUC of 0.81 (95% confidence interval 0.79-0.83).

We tested whether addition of absolute serum level of CA125 as an element of the panel conferred additional predictive value upon re-analysis of the serum set. The posterior distributions of the regression parameters are displayed in Figure 3 and the ROC curve is given in Figure 4 of Erkanli et al. Although there is improvement in terms of the accuracy of the fitted model (AUC with CA125

goes slightly up from 0.86 (95% confidence interval 0.78-0.90) to 0.89 (95% confidence interval 0.84-0.92), the same markers NY-CO-8, HOXB7, and p53 are again selected as most informative along with CA125.

Objective 2: Select autologous tumor antigens expressed in early stage serous carcinoma but absent from, or a low level in normal tissue.

Task 2.1. Generate rat antiserum to SEREX antigens (months 27-29)

Task 2.2. Affinity purify and validate specificity of antibodies (months 29-32).

Task 2.3. Examine the expression pattern of each SEREX antigen by immunohistochemical staining in normal ovary and a spectrum of ovarian tumors (months 32-36). (n>30 each for serous, endometrioid, clear cell, mucinous and undifferentiated carcinoma of a range of stages, and n>30 for serous borderline tumors, serous cystadenoma and normal ovary, giving an approximate total of 250 patient samples tested for each antigen).

GC-UNC-45 over-expression is associated with high grade, advanced stage ovarian serous carcinoma (results detailed in Bazzaro et al., appended)

In order to evaluate GC-UNC-45 expression in ovarian tumors and normal tissue we generated rabbit antisera against KLH coupled to a peptide comprising the final 18 residues of human GC-UNC-45. Peptide binding antibody was affinity purified on a peptide column. The specificity of the affinity purified peptide antibody was analysed by Western blot using 6His-Tagged human GC-UNC-45 purified from E.coli and 293T cells transfected with pEGFP-C1-GC-UNC-45 or pEGFP-C1. The antibody specifically recognized recombinant GC-UNC-45 with either the 6His or GFP tags. We optimized conditions for detection of GC-UNC-45 in paraffin-embedded human tissue using the affinity purified peptide antibody. Immunohistochemical staining suggested a cytoplasmic localization for GC-UNC-45, consistent with our in vitro studies using GFP-GC-UNC-45. A similar immunohistochemical staining pattern was observed using the rabbit antiserum to full length GC-UNC-45.

In order to assess whether GC-UNC-45 is differentially expressed in ovarian serous carcinoma, we performed immunohistochemical staining of tissue microarrays using GC-UNC-45-specific antibody for low grade (14 cases) and high grade (32 cases) serous carcinoma. Staining was scored blind as absent=0, weak=1, intermediate=2, and intense=3. Using this scoring system we observed that high grade serous carcinomas stained more intensely than low grade serous carcinoma (p=0.027). Conversely, staining of normal ovarian surface epithelium (12 cases) and benign serous cystadenoma (n=4) were not significantly different from each other (p=0.29, Figure 5) or from low grade serous carcinoma (p=0.48 and p=0.21 respectively). In contrast, staining of normal ovarian surface epithelium (12 cases) and benign serous cystadenoma (n=4) was significantly weaker than for high grade serous carcinoma (32 cases, p=0.0028 and p=0.0065 respectively). The GC-UNC-45 antibody staining of low stage (stages 1-2) serous carcinoma (18

cases) was also significantly weaker than for high stage (stages 3-4) serous carcinoma (32 cases, $P=0.0021$).

To assess whether the lower expression of GC-UNC-45 in normal surface epithelium is reflected at the transcriptional level, we compared the expression of GC-UNC-45 transcripts relative to the house keeping gene GAPDH using Q-PCR and expressed the ratio in relative units. We noted that 7/15 high grade serous carcinoma expresses GC-UNC-45 mRNA at a >2-fold higher level than an immortalized ovarian surface epithelial cell line, IOSE-29 (a mean of 0.081 ± 0.107 for high grade disease versus 0.025 relative units for IOSE-29). In an attempt to control for culture effects upon GC-UNC-45 mRNA level we compared expression in both the primary low grade serous carcinoma from patient JH514 with and the cell line derived from the same tumor. We observed similar expression levels of GC-UNC-45 mRNA in both the JH514 primary tissue and the cell line (0.044 and 0.050 relative units respectively) both of which are lower than for high grade serous carcinoma (mean of 0.081 relative units).

Effect of GC-UNC-45 over-expression on cell proliferation (results detailed in Bazzaro et al., appended)

Prior studies indicate that skeletal myogenic cell proliferation is retarded when levels of GC-UNC-45 mRNA are reduced. Therefore, we asked whether over-expression of GC-UNC-45 influences proliferation rate. Initially, we compared the proliferation of 293T cells upon transient transfection with pEGFP-C1-GC-UNC-45 or pcDNA3.1-GC-UNC-45 versus vector control. The efficiency of transfection was estimated at 50-70% by fluorescence microscopy. By fluorescence microscopy, GFP alone was present partially in the nucleus and predominantly in cytoplasm, whereas the GFP-GC-UNC45 protein was localized exclusively to the cytoplasm. We further confirmed the expression of GFP-GC-UNC-45 by Western blot using rabbit antiserum to GC-UNC-45 produced as a 6His fusion protein in *E. coli*. Rabbit antiserum to GFP specifically reacted with ~130kDa and ~30kDa proteins in pEGFP-C1-GC-UNC-45 and pEGFP-C1 transfected cells respectively. Upon counting the number of fluorescent cells at 12, 24 and 36h after transfection we noted a significantly greater proliferation rate in cells transfected with pEGFP-C1-GC-UNC-45 as compared to pEGFP-C1 ($p=0.0001$ at both 24h and 36h post transfection). To exclude the possibility that GFP fusion affects the function of GC-UNC-45 or potential toxic effects of GFP expression, we transiently transfected 293T cells with pEGFP-C1 and pcDNA3.1 (vector control) or with pEGFP-C1 and pcDNA3.1-GC-UNC-45 and the proliferation rate was followed by counting the number of fluorescent cells 12, 24 and 36 hours post-transfection. Again, there was an increase in cell proliferation in 293T cells transfected with pcDNA3.1-GC-UNC-45 versus pcDNA3.1 vector control, noticeable from 24 hours after transfection ($p=0.0001$). Similar results were obtained in HeLa cells (not shown) and Western blot analysis using antisera to full-length human GC-UNC-45 confirmed GC-UNC-45 over expression after transfection with pcDNA3.1-GC-UNC-45 (not shown).

Key Research Accomplishments

- Identification of 2 new tumor associated antigens for serous carcinoma using immunoprecipitation and MALDI-TOF
- Demonstration that elevated expression of the General Cell UNC-45 isoform associates with high grade invasive ovarian carcinoma

- Application of Bayesian modeling of autologous antibody responses against ovarian tumor-associated antigens to cancer detection

Reportable Outcomes

- Application of Bayesian modeling of autologous antibody responses against ovarian tumor-associated antigens to cancer detection. Al Erkanli, Douglas D Taylor, Deyrick Dean, Faria Eksir, Daniel Egger, James Geyer, Brad H Nelson, Herbert A Fritsche, and Richard BS Roden. (Submitted to Clinical Cancer research)
- Elevated expression of the General Cell UNC-45 isoform associates with high grade invasive ovarian carcinoma. Martina Bazzaro, Taylor Tang, Catherine J Turski, Robert E Bristow, le-Ming Shih, and Richard BS Roden. (Submitted to the American Journal of Pathology)

Conclusions

We have built upon the progress of our first year of funding, and have demonstrated that all of the tasks in our Statement of Work are feasible. We have developed a methodology for the identification of ovarian cancer-associated antigens that is complementary to SEREX. While we are generating the cDNA expression library for SEREX screening, we have used this alternate immunoprecipitation and mass spectrometry-based approach to identify two new ovarian cancer associated antigens. Almost nothing is known about the function of either antigen. For one of these new antigens, GC UNC-45, we have demonstrated its ability to increase the rate of cell proliferation. We have also shown that GC UNC-45 expression is elevated in high grade as compared to low grade ovarian carcinoma, and advanced relative to local ovarian carcinoma. Furthermore, we have built upon our previous work in which HOXB7 was identified by SEREX as an ovarian cancer antigen. We have used Bayesian modeling of autologous antibody responses against ovarian tumor-associated antigens to compile a panel of markers CA125, HOXB7, p53 and NY-CO-8 useful in detection of ovarian cancer. Notably our data suggest that serum antibody to NY-CO-8 may be associated with reduced incidence of ovarian cancer and we are exploring this phenomenon further.

References

1. L. J. Old, Y. T. Chen, *J Exp Med* 187, 1163-7 (1998).
2. U. Sahin *et al.*, *Proc Natl Acad Sci U S A* 92, 11810-3 (1995).
3. N. Brass *et al.*, *Hum Mol Genet* 6, 33-9 (1997).
4. M. J. Scanlan *et al.*, *Int J Cancer* 76, 652-8 (1998).
5. J. R. Dawson, P. M. Lutz, H. Shau, *Am J Reprod Immunol* 3, 12-7 (1983).
6. U. Sahin, O. Tureci, M. Pfreundschuh, *Curr Opin Immunol* 9, 709-16 (1997).
7. O. Tureci *et al.*, *Cancer Res* 56, 4766-72 (1996).
8. E. Stockert *et al.*, *J Exp Med* 187, 1349-54 (1998).
9. S. R. Chinni *et al.*, *Clin Cancer Res* 3, 1557-64 (1997).
10. S. R. Chinni, C. Gercel-Taylor, G. E. Conner, D. D. Taylor, *Cancer Immunol Immunother* 46, 48-54 (1998).
11. E. Jager *et al.*, *J Exp Med* 191, 625-30 (2000).

Application of Bayesian modeling of autologous antibody responses against ovarian tumor-associated antigens to cancer detection

Al Erkanli, Douglas D Taylor, Deyrick Dean, Faria Eksir, Daniel Egger, James Geyer, Brad H Nelson, Herbert A Fritsche, and Richard BS Roden¹

[A. E.] Department of Biostatistics and Bioinformatics, Duke University Medical Center, Durham, North Carolina 27701, USA; [D. D. T.] Departments of Obstetrics & Gynecology and Radiation Oncology, University of Louisville School of Medicine, Louisville, Kentucky 40202, USA; [D. D., F. E., D. E., J. G.] Amplistar Inc, Winston-Salem, NC; [B. H. N.] Deeley Research Centre, British Columbia Cancer Agency, Victoria, British Columbia, Canada; [H. A. F.] University of Texas M. D. Anderson Cancer Center, Houston, Texas 77030-4009, USA; [R. B. S. R.] Department of Pathology, Johns Hopkins School of Medicine, Baltimore, MD 21205.

¹ Corresponding author: (Tel: 410 502 5161; Fax: 443 287 4295; email: roden@jhmi.edu)

ABSTRACT

Purpose: Biomarkers for early detection of epithelial ovarian cancer (EOC) are urgently needed. Patients can generate a humoral response to tumor-associated antigens (TAAs). Therefore we tested multiplex detection of antibodies to candidate ovarian TAAs and statistical modeling for discrimination of sera of ovarian cancer patients and controls. Methods: Specific binding of antibody from sera of women with EOC or healthy controls to candidate TAA-coated microspheres was assayed in parallel. A Bayesian model/variable selection approach using Markov Chain Monte Carlo computations was applied to these data, together with standard serum CA125 measurement to determine the best predictive model. The selected model was subjected to area under the receiver-operator curve (AUC) analysis. Results: The best model generated an AUC of 0.86 (0.78-0.90) for discrimination of sera of EOC patients and healthy patients using antibody specific to p53, NY-CO-8 and HOXB7. Inclusion of CA125 level in the model provided an AUC of 0.89 (0.84-0.92), as compared to an AUC of 0.83 (0.81-0.83) using CA125 alone. Conclusion: Serum antibody to p53 and HOXB7 is positively associated with EOC, whereas NY-CO-8-specific antibody shows negative association. Bayesian modeling of key TAA-specific serum antibody responses is complementary to CA125 testing for discrimination of sera from patients with EOC from those of healthy women.

[206 WORDS]

INTRODUCTION

Conventional treatment has limited efficacy against advanced stage epithelial ovarian cancer (EOC) whereas >80% patients with early stage disease survive five years after diagnosis. However, since there is no diagnostic tool for reliable screening and detection of pre-malignant or localized ovarian cancer, 70% of patients with ovarian cancer have advanced disease upon initial diagnosis (1).

Measurement of serum CA125 levels was approved as a prognostic indicator to monitor disease recurrence (2). Approximately 1% of normal healthy donors have serum CA125 levels greater than 35U/ml. Elevated levels of CA125 are detected >90% of sera of disseminated ovarian cancer cases (stages II-IV), but only 50% of patients with stage I disease (2). Thus the CA125 assay is inappropriate as a 'stand alone' population screen for early stage ovarian cancer, although its positive predictive value can be improved by combination with other screening tools e.g serial measurements, trans vaginal sonography or combinations with other markers and statistical modeling.

The immune system constantly surveys the body for 'non-self' antigens, and generates a response in the appropriate context. Significantly, cancer patients often mount a humoral response to autologous tumor-associated antigens (TAAs) (3). Autologous antibodies have been documented in patients afflicted with a variety of different cancers, including melanoma, breast, head and neck, colon, lung, renal cancer (4-6). Ovarian tumor-reactive antibodies have been detected in patient serum and ascites (7) and their antigens identified by SEREX (8, 9) or mass spectrometry of immunoprecipitates (10).

The relationship between carcinogenesis and most TAAs identified by SEREX is unclear. However autologous antibodies specific for such regulators of cell growth as mutant p53, ras, c-myc, c-myb, and Her-2/neu have been demonstrated in cancer patients (11). Several studies indicate that autologous antibodies specific for TAAs are prevalent in cancer patients but absent from controls, and therefore have potential as serum biomarkers (12). Perhaps the autoantigen best studied in ovarian cancer patients is p53 (13). In stage I/II ovarian disease 22% of patients had p53 antibody, 31% in stage III and 50% in stage IV (14). Although there was no association of p53 antibody with clinical stage, tumor histologic type or overall patient survival (15, 16), detection of autologous antibody to some ovarian cancer antigens appears to have prognostic significance (17).

While many other TAAs have been identified (<http://www.licr.org/SEREX.html>), the percentage of ovarian cancer patients with reactivity to individual TAAs is generally low. Therefore a panel of such markers and a statistically rigorous approach to marker selection are required to develop a clinically applicable diagnostic test. Herein we describe the application of multiplex detection of autologous antibodies to ovarian TAA and the Bayesian model/variable selection

approach using Markov Chain Monte Carlo (MCMC) computations to determine the best predictive model. MCMC variable selection is a model-based approach with a specified statistical model that puts no distributional restriction on the predictors (markers). It compares favorably to the existing statistical approaches such as recursive partitioning (29, 34, 35) by providing a better assessment of uncertainty through Bayesian learning. A unique feature of our methods is easy incorporation of previously described markers in a natural way into existing models. Thus our application of multiplex detection of autologous antibodies to ovarian TAA and Bayesian model selection for detection of EOC complements the CA125 test and implicates p53, HOXB7 and NY-CO-8 in the biology of EOC.

METHODS

Samples

Sera were collected as part of informed consent protocols approved by the local Institutional Review Boards and the study was approved by the Johns Hopkins University Institutional Review Board. Blood samples were allowed to clot at room temperature and were then centrifuged at 400g to remove clot and cells. Clarified sera were stored at -70°C. A set of 59 sera was obtained at the University of Louisville School of Medicine (ULSM), Louisville, KY from women with stage III/IV ovarian cancer. A second set of sera was obtained at the University of Texas MD Anderson Cancer Center (MDACC), Houston TX. This set were obtained from women with breast cancer (n=18), colon cancer (n=6), lung cancer (n=10), stage III/IV ovarian cancer (n=27), and healthy women (n=23).

Preparation of recombinant TAA

TAAAs were cloned from polymerase chain reaction products into the prokaryotic expression vector pBADgIII (InVitrogen, Carlsbad, CA, USA). ABC7 (AF133659), HOXA7 (AF032095) (9), HOXB7 (NM_004502) (8) and NY-ESO-1 (U87459) (18), Ubiquilin-1 (NM_013438), ZFP161 (Y12726), FLJ21522 (AK025175) (19), Calmodulin (InVitrogen, Cat. #: V450-01) and p53 (X02469) (13) were amplified from published constructs, whereas EPS8R3 (NM_024526), NY-CO-8 (AF039690), NY-CO-16 (AF039694) (6) were amplified directly from commercial cDNA libraries. Constructs were validated using Automated Laser Fluorescent Sequencing. Bacterial cultures were grown in Terrific broth supplemented with 1%(v/v) glycerol and 100 µg/ml ampicillin at 37°C to mid-log phase ($OD_{650} \sim 0.6-0.7$) and induced with 0.02%(w/v) L-(+)-arabinose for 2-3h. Induction was performed at 30°C with 0.002%(w/v) L-(+)-arabinose for HOXA7 and HOXB7. Cell pellets from 1l cultures were solubilized by sonication in 20ml of 8M urea, 3.7ml of 10% (w/v) sodium N-lauroyl-sarcosinate and brought to 50ml with 20 mM TrisHCl pH8.0/ 0.2 M NaCl/ 10% (v/v) glycerol and 0.1% (w/v) sodium N-lauroyl-sarcosinate. After centrifugation at 12,000g for 30min at 4°C, the supernatant was loaded onto an Ni-NTA Superflow (Qiagen) column. The column was washed with a step gradient of 10mM, 20mM, 50mM, 100mM and finally 0.5 M imidazole in 20 mM TrisHCl pH8.0/ 0.2 M NaCl/ 10% (v/v) glycerol

and 0.1% (v/v) Triton X-100. The purity and size of the purified proteins was determined by staining SDS-PAGE gels for total protein (Sypro Ruby) and performing Western blotting on duplicate gels for (His)₆ labeled antigen using horseradish peroxidase-labeled anti-(His)₆ and chemiluminescent substrate.

Coupling to microspheres and Luminex analysis

Monoclonal antibody to (His)₆ was coupled to eleven distinct sets of LabMAP carboxylated microspheres (Luminex Corporation, Austin, TX) which were then individually bound overnight at 4°C with 30µg of each purified (his)₆-tagged recombinant TAA. Similarly, a further six distinct sets of LabMAP carboxylated microspheres were directly coupled to 25µg of purified Hsp27, Hsp70, and Hsp90 (Stressgen, Victoria, BC, Canada) (20-22), or as controls, Glutathione-S-transferase (GST), 5µg/ml of anti-human IgG (Sigma Chemical Company, St Louis, MO), or 50µg/ml human IgG. Equivalent counts of each set of protein-coupled microspheres were mixed to a concentration of 5000 per set per 50µl well in PBS containing 10% normal mouse serum (Jackson Laboratories, West Grove, PA). The beads were shaken with 50µl of patient serum diluted 1:25 in a 96 well filter-bottom microtiter plate for 1h in the dark at ambient temperature. The beads were washed three times with 100µl of buffer by filtration, and then shaken in 100µl/well of R-Phycoerythrin (PE)-conjugated donkey anti-human IgG diluted 1:200 in PBS/BSA for 45min in the dark. After three washes, the beads were resuspended in 100µl/well of PBS/BSA and their mean fluorescence intensity assayed on a Luminex 100 plate reader. The median fluorescence intensity (MFI) of 100 of each set of microspheres was determined for each well.

Statistical analyses

A Bayesian Model/Variable Selection approach using a Markov Chain Monte Carlo (23) computations was implemented in the WinBugs (24) programming environment. A full description of the model selection and details of our Bayesian Computations using Gibbs Sampling are provided in supplemental materials. The MCMC variable (here the 13 markers and 5 controls) selection approach is a stochastic search algorithm that effectively visits all $2^{18} = 216,144$ different models obtained from including/excluding any of the markers or controls in a logistic regression for the probability of ovarian cancer. For numerical stability, we transformed the measured MFI levels of the markers and controls to logarithmic scale. Our approach adjusts for the associations amongst the 13 markers, and effects of the 5 controls. Given the limited number of cases and controls, we focused on an additive model assuming no interactions among the markers, controls, and between markers and controls. A priori, each specific marker or control is assumed to be equally likely to be included/excluded (i.e., with probability of 0.5) in the model. This corresponds to an equally likely prior probability of $1/2^{18}$ for each possible configuration in the model space. The inclusion probability for a specific marker or control is then updated by their posterior probability using all the available information about the other markers and controls, conditional on the observed ovarian cancer status. Although, in principle, one can compute the posterior probability of each of the 2^{18} models

using the Bayesian analysis, a simpler alternative is to use the Bayes factor (BF) (25), defined as the posterior and prior odds ratio, to select relevant markers or controls for future analyses. For a specific marker or control, larger values of BF provide evidence in favor of inclusion, while smaller values support exclusion from the model. Usually, a value between 1 and 3 is considered weak, between 3 and 10 as substantial, between 10 and 100 as strong, and greater than 100 as very strong (26).

Model Description

Let d_j denote a binary indicator variable for the j -th marker or control in the logit, for $i = 1, 2, \dots, n$ and $j = 1, 2, \dots, J$,

$$\text{logit}(p_i) = \log\left(\frac{p_i}{1-p_i}\right) = a + \sum_{j=1}^J d_j b_j X_{ij}, \quad (1)$$

where $d_j = 0/1$ indicates the exclusion/inclusion of the j -th variable, p_i is the probability that the i -th subject has ovarian cancer, X_{ij} is the value of the j -th variable (a marker or a control) for the i -th patient, and b_j is the regression coefficient measuring the strength of the association between X_{ij} and p_j in the log-odds ratio scale, for n patients, and J variables; here $J=18$, and $n = 123$ (23 controls, and 100 cases in the training data set). A priori, before seeing the cancer status and all the relevant marker/control information, $\Pr(d_j = 1) = \Pr(d_j = 0) = 0.5$. Using the specific a Gibbs sampling (23) algorithm, we can compute the posterior probability of inclusion probability $\Pr(d_j = 1|Data)$ and the BF for the j -th variable (marker or control) as

$$\begin{aligned} BF_j &= \frac{\Pr(d_j = 1|Data) \Pr(d_j = 0)}{\Pr(d_j = 0|Data) \Pr(d_j = 1)} \\ &= \frac{\Pr(d_j = 1|Data)}{\Pr(d_j = 0|Data)} \end{aligned} \quad (2)$$

since $\Pr(d_j = 1) = \Pr(d_j = 0) = 0.5$ a priori. Here $Data$ is the vector that consists of all the diagnostic and marker/control information available for n patients and J variables. The uncertainty about the marginal posterior probability of inclusion $\Pr(d_j = 1|Data)$ is automatically adjusted, as a result of Bayesian updating, for the other markers/controls present in the model.

Our analytical strategy consists of fitting logistic regression model in Equation 1 for ULSM cases and MDACC cases and controls, and cross-validate the best model against the GOG cases and ULSM controls which consists of $n = 44$

patients. By using $BF \geq 3$ as a selection criterion, we picked the best combination of antigens and controls and computed multiple sensitivity, specificity, ROC curve and AUC by varying a probability cutoff between 0.01 to 1.00. As an additional data analysis, we also compared the best model with those obtained using p53 and CA125.

Bayesian Computations using Gibbs Sampling

Using the logistic model described in Equation 1, the joint posterior density for all the unknown quantities is obtained using Bayes theorem as, up to a constant of proportionality,

$$f(\boldsymbol{\psi}, d | \text{Data}) \propto L(\boldsymbol{\psi}, d) f(\boldsymbol{\psi}, d) = \left[\prod_{i=1}^n p_i^{Y_i} (1 - p_i)^{1 - Y_i} \right] f(\boldsymbol{\psi}, d), \quad (3)$$

where $\boldsymbol{\psi} = (a, b)$ is the $J+1$ -dimensional parameter vector, $L(\boldsymbol{\psi}, d)$ denotes the likelihood function, and $f(\boldsymbol{\psi}, d)$ is the joint prior density for $\boldsymbol{\psi}$ and model indicators $d = (d_1, \dots, d_J)$, respectively. The probability of ovarian cancer for each patient, $p_i = \Pr(Y_i = 1 | \boldsymbol{\psi}, d, \{X_{ij}\})$, is described as, by inverting the logit in Equation 1.

$$p_i = \frac{\exp(a + \sum_j d_j b_j X_{ij})}{1 + \exp(a + \sum_j d_j b_j X_{ij})}, \quad (4)$$

where $Y_i = 1$, if the i -th subject has ovarian cancer, and $Y_i = 0$, otherwise, and as in (1), X_{ij} denotes the value of the j -th marker for the i -th patient, for $i = 1, 2, \dots, n$, and $j = 1, 2, \dots, J$. We assume that the components of $\boldsymbol{\psi}$ and d are independently distributed with uninformative normal priors for the intercept a , and regression parameters (slopes) $b = (b_1, \dots, b_J)$ described as

$$a \sim N(0, \infty), \quad (5)$$

$$b_j \stackrel{\text{ind}}{\sim} N(0, \infty), j = 1, \dots, J$$

where ∞ denotes a large variance, e.g., 10,000, but can be fine tuned for specific applications to achieve numerical stability, and to guarantee posterior propriety, i.e., posterior densities of a and b are proper. Under these "vague" priors, the Bayesian analysis is directly comparable to classical Maximum Likelihood Estimation method.

The prior distributions of the indicator variables are as described before, i.e., components of d are independently distributed as Bernoulli (0.5), corresponding to the belief that each marker or control is equally likely to be


included or excluded in the model, prior to seeing the data. If there is prior information or belief that, some of the markers are more likely to be included in the model, than one can adjust these probabilities to accommodate such information, i.e., change 0.5 to 0.9 (say) for at least one marker. More detailed examples of Bayesian variable selection can be found in (42-45).

The independent Bernoulli(0.5) priors results in a joint 2^{-J} uniform prior for all $d \in \{0,1\}^J$. Although conceptually simple, the evaluation of the posterior density in Equation 3 is computationally intractable, as it does not lend itself to a closed analytical form. Consequently, a numerical method is needed to compute Equation 3 and the other related quantities of interest such as the marginal posterior distributions of a and $b = (b_1, \dots, b_J)$.

We used a Markov Chain Monte Carlo (MCMC) approach based on a Gibbs sampler that is similar to those described in (42, 44, 45). The usual Gibbs sampler (23) when the indicators are fixed a priori in the model space $\{0,1\}^J$, e.g., $d_j = 1$ for all $j=1, \dots, J$, simulates successively from the full conditional posterior densities

$$f(a|\dots) \propto L(\boldsymbol{\psi}, d) f(a) \quad (6)$$

$$f(b_j|\dots) \propto L(\mathbf{Q}, d) f(b_j), j=1, \dots, J \quad (7)$$

where we write ... to denote conditioning on all the other parameters and the cancer status $Data = (Y_1, \dots, Y_n)$. Starting from an initial vector (for fixed d) a^0, b_1^0, \dots, b_J^0 , the Gibbs sampler simulates first a new a^1 using Equation 6 by conditioning on $Data$ and b_1^0, \dots, b_J^0 . Next, it simulates a new b_j^1 using Equation 7 for the j -th coefficient by conditioning on $a^1, b_1^0, \dots, b_{j-1}^0, b_{j+1}^0, \dots, b_J^0$ and so forth until all the parameters have been simulated. This iterative process continues using  in Equations 6 and 7 to generate a new sequence of a and b and so forth. After a sufficiently large number of R , (e.g., $R = 10,000$) simulations, we have a Markov Chain $\{a^r, b_1^r, \dots, b_J^r\}_{r=1}^R$ that, under suitable regularity conditions, as $R \rightarrow \infty$, resembles the parameter values generated from the true joint posterior distribution $f(\boldsymbol{\psi} | Data)$. Accordingly, point and interval estimates for any quantity of interest can be obtained by using simple tools such as arithmetic averages to any desired degree of accuracy. In practice, to ensure that simulated MC has established stability, an initial part of R is used for a burn-in period and multiple starting points may be used for better mixing, see for example (25). The conditional densities in Equations 6 and 7 are not available in closed analytical form, however, they are log-concave and hence the adaptive rejection sampling (ARS) (46) can be used for simulations. An alternative method is Metropolis-Hastings (MH) algorithm (25). In this application we used WinBugs program, Version 1.4, (24) which uses both ARS and MH methods. It is recommended that

an initial number of iterations to be used for burn-in and remaining for assessing convergence. Also, one may start with multiple initial points to make sure that the resulting MC sequence is well mixing.

An advantage of the Gibbs sampling is that it can be generalized to run simultaneously on the model space $\{0,1\}^J$. By augmenting the parameter space with the model space, a Gibbs sampler can be set-up to simulate successively from the full conditional posterior distributions $f(\psi|Data,d)$ and $f(d|Data,\psi)$. For generating ψ , we use Equations 6 and 7 as before, by conditioning on d . The only difference is that we now simulate from a modified version of Equation 7 for generating regression coefficients $b = (b_1, \dots, b_J)$:

$$f(b_j|\dots) \propto \begin{cases} L(\psi, d_j = 1, d_{-j})f(b_j|d_j = 1) & \text{if } d_j = 1 \\ f(b_j|d_j = 0) & \text{if } d_j = 0, \end{cases} \quad (8)$$

where, because of a priori independence between the parameters, $f(b_j|d_j) = f(b_j)$. The vector d_{-j} in the likelihood indicates values of all d s except d_j . In other words, the prior distribution of b_j is updated only when the j -th marker/control is active, $d_j = 1$. When $d_j = 0$, the conditional posterior density for b is the same as its prior. For that reason, the normal prior in Equation 5 should be chosen carefully to insure convergence. We used several normal priors, $N(0,1)$, $N(0,10)$ and $N(0,100)$, without having any convergence problems. An alternative parameterization is achieved by the transformation $\theta_j = d_j b_j$, which effectively results in a two-component finite mixture prior with a point mass at zero (when $d_j = 0$) with probability of 0.5, and a normal distribution $N(0, \sigma_j^2)$ (when $d_j = 1$) with probability 0.5. In our application, we used $\theta_j = d_j b_j$ for simplicity.

Simulation of the indicators is trivial as the full conditional posterior for each of them is a Bernoulli(q_j), where

$$q_j = L(\psi, d_j = 1, d_{-j}) / [L(\psi, d_j = 1, d_{-j}) + L(\psi, d_j = 0, d_{-j})]. \quad (9)$$

To obtain the model probability for a particular configuration of markers and controls, one can, in principle, compute its posterior probability by counting the frequency of the simulated events that support it, using the MCMC samples such generated. However, this can be computationally very demanding due to memory limitations and computer speed. An alternative approach is to use the marginal Bayes factors as we have illustrated in equation Equation 2 above.

RESULTS

To explore the utility of autologous serum antibody specific to particular TAAs as an additional tool for discrimination of sera from cancer patients and healthy women, we generated recombinant protein from 13 markers previously identified as candidate TAAs and selected 5 presumptive control reagents. Sera from both healthy women and EOC patients were tested in parallel for reactivity to all 18 panel elements. Initially we tested sera of 23 healthy patients from MDACC as controls, and sera from 59 stage III/IV ovarian cancer patients obtained at ULSM and 27 from MDACC as cases, respectively. This set of sera was analyzed for reactivity to microspheres of discrete sizes coated with individual recombinant TAA or control protein. The presence of antibody bound to the beads was detected with PE-labeled anti-human IgG and the fluorescence quantified using a Luminex plate reader. Since 5 presumptive control elements were included in the panel, absolute MFI values without background subtraction were employed.

Our analytical strategy consisted of fitting the logistic regression model in Equation 1 for ULSM cases and MDACC cases and controls. By using $BF \geq 3$ as a selection criterion, we picked the best model and computed multiple sensitivity, specificity, ROC curve and AUC by varying a probability cutoff between 0.01 to 1.00 (Table 1, Figures 1 and 2). The AUC was calculated as 0.86 (95% confidence interval 0.78-0.90) for this best fitting model (Table 1).

We also compared the best model for discrimination of cases and controls with detection of absolute level of CA125 or p53-specific antibody or both. The AUC was calculated as 0.83 (95% confidence interval 0.81-0.83) for the standard CA125 assay alone. Detection of p53 antibody alone was not useful for discrimination of cases and controls in this serum set (AUC of 0.52 with 95% confidence interval 0.20-0.58) and combination of absolute CA125 level and serum reactivity to p53 provided an AUC of 0.81 (95% confidence interval 0.79-0.83).

We tested whether addition of absolute serum level of CA125 as an element of the panel conferred additional predictive value upon re-analysis of the serum set (Table 2). The posterior distributions of the regression parameters are displayed in Figure 3 and the ROC curve is given in Figure 4. Although there is improvement in terms of the accuracy of the fitted model (AUC with CA125 goes slightly up from 0.86 (95% confidence interval 0.78-0.90) to 0.89 (95% confidence interval 0.84-0.92), the same markers NY-CO-8, HOXB7, and p53 are again selected as most informative along with CA125.

DISCUSSION

Our study examines the applicability of multiplex detection of autologous antibody to TAAs as a diagnostic tool for cancer. The detection of autologous antibody to this 3 member panel of TAAs, in addition to CA125, shows merit as an approach for ovarian cancer detection. However, much larger studies are

required to assess its sensitivity at the high specificity required for screening healthy women. In particular it warrants further examination in high-risk populations such as female first-degree relatives of ovarian cancer patients or women carrying mutations that predispose toward cancer. The application of longitudinal screening may also significantly increase the positive predictive value of the test (27, 28). Sera collected over four time points from individual patients with ovarian (n=5) or breast (n=5) cancer were analyzed for the stability of TAA reactivity. The reactivities were generally stable over several years despite therapy indicating that this approach is not useful to monitor therapy (not shown).

Our modeling of TAA-specific antibody discriminates poorly the patients with ovarian cancer from those with cancer of other organ sites (not shown). This reflects the use of p53 as a diagnostic marker and its importance in cancers in addition to ovarian cancer (13). However, other investigators have made progress to this end (29, 30). Three of the seven TAAs tested proved useful in detecting particular cancer types (29, 30). Over 2000 TAAs have been entered into the SEREX database (<http://www.licr.org/SEREX.html>). Several other approaches have also been used to identify candidate TAAs including mass spectrometric analysis of immunoprecipitates (10) and screening of phage display libraries (31, 32). Inclusion of other TAAs using similar, highly multiplexed approaches (33), in large case/control studies may provide better discrimination between cancer types.

Here we describe the application of Bayesian model/variable selection approach using Markov Chain Monte Carlo computations, implemented in the freely available WinBUGS program, to determine the best predictive model. The MCMC variable selection is a model-based approach with a specified statistical model on the cases and controls (in our case Binomial distribution with logistic link) but puts no distributional restriction on the predictors (markers). It compares favorably to the existing statistical approaches such as recursive partitioning (29, 34, 35) by providing a better assessment of uncertainty through Bayesian learning. A unique feature of our methods is easy incorporation in a natural way into existing models of prior information obtained from earlier clinical studies or scientist's experience.

Pattern recognition analysis of proteomic profiles has been used to discriminate sera of ovarian cancer patients from those of healthy women, but the biological underpinning of these patterns is as yet unclear (36). By contrast the significance of the TAAs p53 and HOXB7 in cancer biology has been studied extensively for ovarian and other cancers (8, 37-40). A partial cDNA sequence NY-CO-8 was initially identified as a colon cancer antigen. The full length gene was recently cloned and its product, CCCAP, shown to associate with centrosomes (41). Subsequent analysis of the serologic reactivity to NY-CO-8 suggests that it is a naturally occurring autoantigen (33). The presence of NY-CO-8-reactive antibody in healthy controls may account for its negative

association with ovarian cancer in our study. This possible protective effect warrants further investigation.

ACKNOWLEDGEMENTS

Under a licensing agreement between Amplistar, Inc. and the Johns Hopkins University, R. B. S. R. is entitled to a share of royalty received by the University on sales of products related to the research described in this article. The terms of this arrangement are being managed by the Johns Hopkins University in accordance with its conflict of interest policies. R. B. S. R. is funded by the Department of Defense grant OC010017.

REFERENCES

1. Rosenthal, A. and Jacobs, I. Ovarian cancer screening. *Semin Oncol*, 25: 315-325, 1998.
2. Jacobs, I. and Bast, R. C., Jr. The CA 125 tumour-associated antigen: a review of the literature. *Hum Reprod*, 4: 1-12, 1989.
3. Old, L. J. and Chen, Y. T. New paths in human cancer serology. *J Exp Med*, 187: 1163-1167, 1998.
4. Sahin, U., Tureci, O., Schmitt, H., Cochlovius, B., Johannes, T., Schmits, R., Stenner, F., Luo, G., Schober, I., and Pfreundschuh, M. Human neoplasms elicit multiple specific immune responses in the autologous host. *Proc Natl Acad Sci U S A*, 92: 11810-11813, 1995.
5. Brass, N., Heckel, D., Sahin, U., Pfreundschuh, M., Sybrecht, G. W., and Meese, E. Translation initiation factor eIF-4gamma is encoded by an amplified gene and induces an immune response in squamous cell lung carcinoma. *Hum Mol Genet*, 6: 33-39, 1997.
6. Scanlan, M. J., Chen, Y. T., Williamson, B., Gure, A. O., Stockert, E., Gordan, J. D., Tureci, O., Sahin, U., Pfreundschuh, M., and Old, L. J. Characterization of human colon cancer antigens recognized by autologous antibodies. *Int J Cancer*, 76: 652-658, 1998.
7. Dawson, J. R., Lutz, P. M., and Shau, H. The humoral response to gynecologic malignancies and its role in the regulation of tumor growth: a review. *Am J Reprod Immunol*, 3: 12-17, 1983.
8. Naora, H., Yang, Y. Q., Montz, F. J., Seidman, J. D., Kurman, R. J., and Roden, R. B. A serologically identified tumor antigen encoded by a homeobox gene promotes growth of ovarian epithelial cells. *Proc Natl Acad Sci U S A*, 98: 4060-4065., 2001.
9. Naora, H., Montz, F. J., Chai, C. Y., and Roden, R. B. Aberrant expression of homeobox gene HOXA7 is associated with mullerian-like differentiation of epithelial ovarian tumors and the generation of a specific autologous antibody response. *Proc Natl Acad Sci U S A*, 98: 15209-15214, 2001.
10. Chinni, S. R., Falchetto, R., Gercel-Taylor, C., Shabanowitz, J., Hunt, D. F., and Taylor, D. D. Humoral immune responses to cathepsin D and

- glucose-regulated protein 78 in ovarian cancer patients. *Clin Cancer Res*, 3: 1557-1564, 1997.
11. Canevari, S., Pupa, S. M., and Menard, S. 1975-1995 revised anti-cancer serological response: biological significance and clinical implications. *Ann Oncol*, 7: 227-232, 1996.
 12. Stockert, E., Jager, E., Chen, Y. T., Scanlan, M. J., Gout, I., Karbach, J., Arand, M., Knuth, A., and Old, L. J. A survey of the humoral immune response of cancer patients to a panel of human tumor antigens [see comments]. *J Exp Med*, 187: 1349-1354, 1998.
 13. Soussi, T. p53 Antibodies in the sera of patients with various types of cancer: a review. *Cancer Res*, 60: 1777-1788, 2000.
 14. Gadducci, A., Ferdeghini, M., Buttitta, F., Fanucchi, A., Annicchiarico, C., Prontera, C., Bevilacqua, G., and Genazzani, A. R. Preoperative serum antibodies against the p53 protein in patients with ovarian and endometrial cancer. *Anticancer Res*, 16: 3519-3523, 1996.
 15. Angelopoulou, K., Rosen, B., Stratis, M., Yu, H., Solomou, M., and Diamandis, E. P. Circulating antibodies against p53 protein in patients with ovarian carcinoma. Correlation with clinicopathologic features and survival. *Cancer*, 78: 2146-2152, 1996.
 16. Gadducci, A., Ferdeghini, M., Buttitta, F., Cosio, S., Fanucchi, A., Annicchiarico, C., Galletti, O., Bevilacqua, G., and Genazzani, A. R. Assessment of the prognostic relevance of serum anti-p53 antibodies in epithelial ovarian cancer. *Gynecol Oncol*, 72: 76-81, 1999.
 17. Chinni, S. R., Gercel-Taylor, C., Conner, G. E., and Taylor, D. D. Cathepsin D antigenic epitopes identified by the humoral responses of ovarian cancer patients. *Cancer Immunol Immunother*, 46: 48-54, 1998.
 18. Chen, Y. T., Scanlan, M. J., Sahin, U., Tureci, O., Gure, A. O., Tsang, S., Williamson, B., Stockert, E., Pfreundschuh, M., and Old, L. J. A testicular antigen aberrantly expressed in human cancers detected by autologous antibody screening. *Proc Natl Acad Sci U S A*, 94: 1914-1918, 1997.
 19. Stone, B., Schummer, M., Paley, P. J., Thompson, L., Stewart, J., Ford, M., Crawford, M., Urban, N., O'Briant, K., and Nelson, B. H. Serologic analysis of ovarian tumor antigens reveals a bias toward antigens encoded on 17q. *Int J Cancer*, 104: 73-84, 2003.
 20. Castelli, M., Cianfriglia, F., Manieri, A., Palma, L., Pezzuto, R. W., Falasca, G., and Delpino, A. Anti-p53 and anti-heat shock proteins antibodies in patients with malignant or pre-malignant lesions of the oral cavity. *Anticancer Res*, 21: 753-758, 2001.
 21. Kaur, J., Srivastava, A., and Ralhan, R. Serum p53 antibodies in patients with oral lesions: correlation with p53/HSP70 complexes. *Int J Cancer*, 74: 609-613, 1997.
 22. Luo, L. Y., Herrera, I., Soosaipillai, A., and Diamandis, E. P. Identification of heat shock protein 90 and other proteins as tumour antigens by serological screening of an ovarian carcinoma expression library. *Br J Cancer*, 87: 339-343, 2002.

23. Gelfand, A. E. and Smith, A. F. M. Sampling based approaches to calculation marginal densities. *Journal of the American Statistical Association*, 85: 398-340, 1990.
24. Spiegelhalter, D., Thomas, A., Best, N., and Lunn, D. WinBUGS User Manual Version 1.4. Cambridge, UK: MRC Biostatistics Unit, 2003.
25. Carlin, B. P. and Louis, T. A. Bayes and Empirical Bayes Methods for data analysis. London: Chapman and Hall, 1996.
26. Kass, R. E. and Raftery, A. E. Bayes factors. *Journal of the American Statistical Association*, 90: 773-795, 1995.
27. McIntosh, M. W., Urban, N., and Karlan, B. Generating longitudinal screening algorithms using novel biomarkers for disease. *Cancer Epidemiol Biomarkers Prev*, 11: 159-166, 2002.
28. McIntosh, M. W. and Urban, N. A parametric empirical Bayes method for cancer screening using longitudinal observations of a biomarker. *Biostatistics*, 4: 27-40, 2003.
29. Koziol, J. A., Zhang, J. Y., Casiano, C. A., Peng, X. X., Shi, F. D., Feng, A. C., Chan, E. K., and Tan, E. M. Recursive partitioning as an approach to selection of immune markers for tumor diagnosis. *Clin Cancer Res*, 9: 5120-5126, 2003.
30. Zhang, J. Y., Casiano, C. A., Peng, X. X., Koziol, J. A., Chan, E. K., and Tan, E. M. Enhancement of antibody detection in cancer using panel of recombinant tumor-associated antigens. *Cancer Epidemiol Biomarkers Prev*, 12: 136-143, 2003.
31. Mintz, P. J., Kim, J., Do, K. A., Wang, X., Zinner, R. G., Cristofanilli, M., Arap, M. A., Hong, W. K., Troncoso, P., Logothetis, C. J., Pasqualini, R., and Arap, W. Fingerprinting the circulating repertoire of antibodies from cancer patients. *Nat Biotechnol*, 21: 57-63, 2003.
32. Fossa, A., Alsoe, L., Cramer, R., Funderud, S., Gaudernack, G., and Smeland, E. B. Serological cloning of cancer/testis antigens expressed in prostate cancer using cDNA phage surface display. *Cancer Immunol Immunother*, 53: 431-438, 2004.
33. Scanlan, M. J., Welt, S., Gordon, C. M., Chen, Y. T., Gure, A. O., Stockert, E., Jungbluth, A. A., Ritter, G., Jager, D., Jager, E., Knuth, A., and Old, L. J. Cancer-related serological recognition of human colon cancer: identification of potential diagnostic and immunotherapeutic targets. *Cancer Res*, 62: 4041-4047, 2002.
34. Breiman, L., Friedman, J. H., Olshen, R. A., and Stone, C. J. Classification and Regression Trees. Monterey, CA: Wadsworth, 1984.
35. Zhang, H. and Singer, B. Recursive Partitioning in the Health Sciences. New York: Springer, 1999.
36. Petricoin, E. F., Ardekani, A. M., Hitt, B. A., Levine, P. J., Fusaro, V. A., Steinberg, S. M., Mills, G. B., Simone, C., Fishman, D. A., Kohn, E. C., and Liotta, L. A. Use of proteomic patterns in serum to identify ovarian cancer. *Lancet*, 359: 572-577, 2002.

37. Shih le, M. and Kurman, R. J. Ovarian tumorigenesis: a proposed model based on morphological and molecular genetic analysis. *Am J Pathol*, *164*: 1511-1518, 2004.
38. Care, A., Silvani, A., Meccia, E., Mattia, G., Stoppacciaro, A., Parmiani, G., Peschle, C., and Colombo, M. P. HOXB7 constitutively activates basic fibroblast growth factor in melanomas. *Mol Cell Biol*, *16*: 4842-4851, 1996.
39. Care, A., Silvani, A., Meccia, E., Mattia, G., Peschle, C., and Colombo, M. P. Transduction of the SkBr3 breast carcinoma cell line with the HOXB7 gene induces bFGF expression, increases cell proliferation and reduces growth factor dependence. *Oncogene*, *16*: 3285-3289, 1998.
40. Care, A., Valtieri, M., Mattia, G., Meccia, E., Masella, B., Luchetti, L., Felicetti, F., Colombo, M. P., and Peschle, C. Enforced expression of HOXB7 promotes hematopoietic stem cell proliferation and myeloid-restricted progenitor differentiation. *Oncogene*, *18*: 1993-2001, 1999.
41. Kenedy, A. A., Cohen, K. J., Loveys, D. A., Kato, G. J., and Dang, C. V. Identification and characterization of the novel centrosome-associated protein CCCAP. *Gene*, *303*: 35-46, 2003.
42. George, E. I. and McCulloch, R. Variable selection via Gibbs sampling. *Journal of the American Statistical Association*, *88*: 881-889, 1993.
43. Carlin, B. P. and Chib, S. Bayesian model choice via Markov Chain Monte Carlo Methods. *Journal of the Royal Statistical Society. Series B.*, *57*: 473-484, 1995.
44. Kuo, L. and Mallick, B. K. Variable selection for regression models. *Sanhkya (Series B)*, *60*: 65-81, 1998.
45. Erkanli, A., Soyer, R., and Angold, A. Bayesian analyses of longitudinal binary data using Markov regression models of unknown order. *Statistics in Medicine*, *20*: 755-770, 2001.
46. Gilks, W. R. and Wild, P. Adaptive rejection sampling for Gibbs sampling. *Applied Statistics*, *41*: 337-348, 1992.

Table 1. Modeling of serum responses to the 18 element panel in cases and controls. Identification of the best fitting model for discrimination between sera of 23 healthy patients from MDACC as controls, versus sera from 59 stage III/IV ovarian cancer patients obtained at ULSM and 27 from MDACC as cases using the 18 element panel. The table shows the posterior estimates (mean and standard deviations) of $\Pr(d_j = 1|Data)$, the regression coefficients $\{\theta_j = d_j b_j\}$, and the Bayes Factors for 13 markers and 5 controls using the data set of ULSM cases, and MDACC cases and controls. The regression coefficients θ_j are assumed to be statistically independent, and each have a two-component mixture prior distribution with a point mass at zero (when $d_j = 0$) with probability of 0.5, and a normal distribution $N(0, \sigma_j^2)$ (when $d_j = 1$) with probability 0.5.

Table 1.

Marker	$\Pr(d_j = 1 Data)$	θ_j	BF_j
FLJ21522	0.49 (0.50)		
NY-CO-8	0.98 (0.15)	-1.49 (0.62)	49
NY-CO-16	0.45 (0.49)		
ABC7	0.65 (0.48)		
α HslgG	0.42 (0.49)		
Calmodulin	0.42 (0.49)		
HOXB7	0.92 (0.27)	1.42 (0.76)	11.5
Hsp70	0.57 (0.49)		
Hsp90	0.49 (0.50)		
HslgG	0.43 (0.49)		
No Antigen	0.60 (0.49)		
NY-ESO-1	0.48 (0.50)		
p53	0.96 (0.20)	1.21 (0.58)	24
Ubiquilin-1	0.61 (0.49)		
ZFP161	0.28 (0.45)		
Vector	0.40 (0.49)		
HOXA7	0.42 (0.49)		
Hsp27	0.42 (0.49)		
	Post. Mean	95% CI interval for AUC	
	(Std D.)		
AUC	0.86 (0.03)	0.78	0.90

Table 2. Modeling of the serum responses to the 18 element panel and CA125 level in cases and controls. Identification of the best fitting model for discrimination between sera of 23 healthy patients from MDACC as controls, versus sera from 59 stage III/IV ovarian cancer patients obtained at ULSM and 27 from MDACC as cases using the 18 element panel and absolute CA125 level. Statistical analysis was performed as described for Table 1.

Marker	$Pr(d_j = 1 Data)$	θ_j	BF_j
FLJ21522	0.37 (0.48)		
NY-CO-8	0.90 (0.31)	-1.18 (0.67)	9
NY-CO-16	0.44 (0.50)		
ABC7	0.53 (0.50)		
α HsIgG	0.35 (0.48)		
Calmodulin	0.42 (0.49)		
HOXB7	0.87 (0.33)	1.17 (0.73)	6.7
Hsp70	0.33 (0.47)		
Hsp90	0.41 (0.49)		
HsIgG	0.36 (0.48)		
No Antigen	0.52 (0.50)		
NY-ESO-1	0.41 (0.50)		
p53	0.76 (0.43)	0.73 (0.62)	3.2
Ubiquilin-1	0.52 (0.50)		
ZFP161	0.49 (0.50)		
Vector	0.41 (0.50)		
HOXA7	0.43 (0.49)		
Hsp27	0.37 (0.48)		
CA125	0.99 (0.07)	0.90 (0.37)	99
	Post. Mean (Std D.)	95% CI interval for AUC	
AUC	0.89 (0.03)	0.84	0.92

FIGURE LEGENDS

Figure 1. Posterior distributions of $\{\theta_j\}$ in the variable selection algorithm for data of Table 1.

Figure 2. Posterior estimate of ROC curve for markers NY-CO-8, HOXB7 and p53 with 95% Credible Interval for cut off values ranging from 0.01 and 1.00 for data of Table 1.

Figure 3. Posterior distributions of $\{\theta_j\}$ for all 18 candidate markers plus CA125 levels (marked as [19] above) in the variable selection algorithm for data of Table 2.

Figure 4. Posterior estimate of ROC curve for training set using NY-CO-8, HOXB7, p53, and CA125 with 95% Credible Interval for cut off values ranging from 0.01 and 1.00 for data of Table 2.

Figure 1.

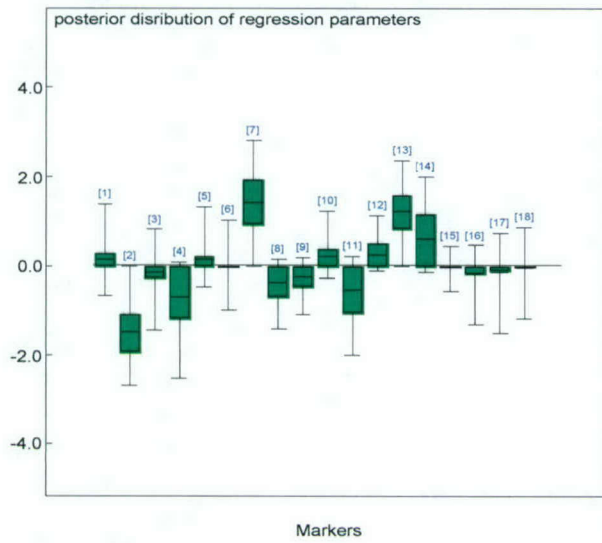


Figure 2.

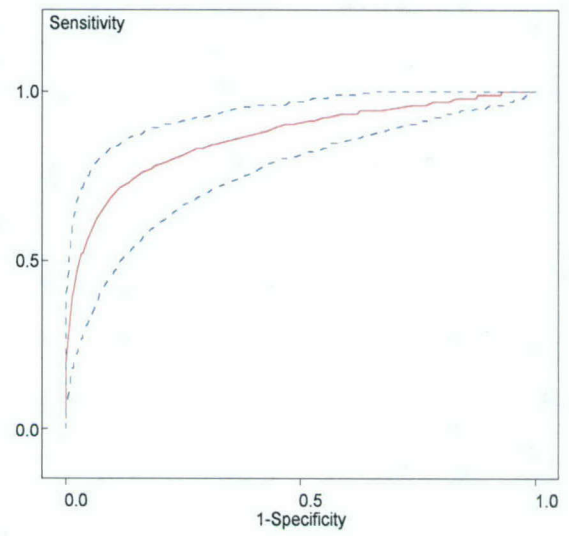


Figure 3.

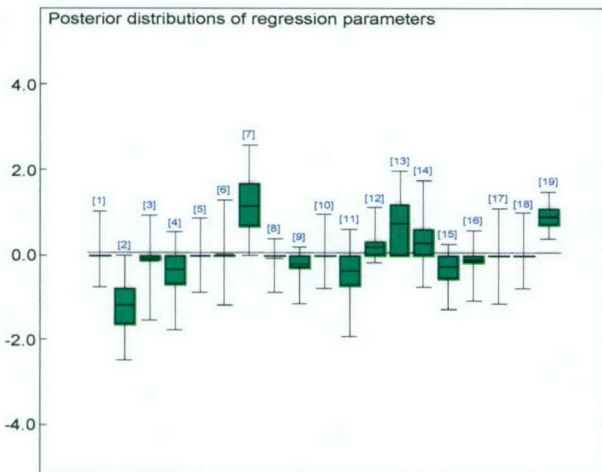
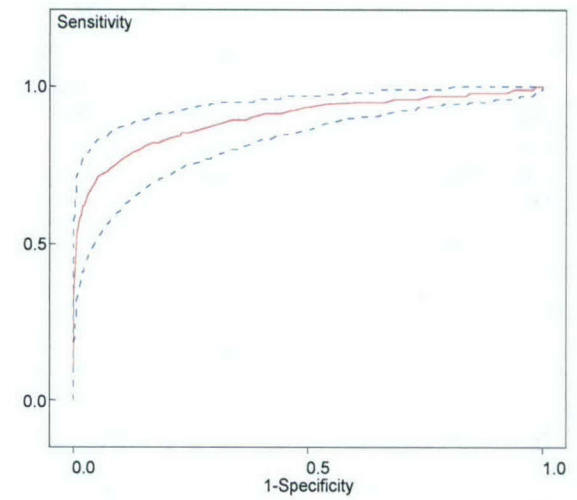


Figure 4.



Elevated expression of the General Cell UNC-45 isoform associates with high grade invasive ovarian carcinoma

Martina Bazzaro¹, Taylor Tang¹, Catherine J TurSKI¹, Robert E Bristow^{2,3}, Ie-Ming Shih^{1,2,3}, and Richard BS Roden^{1,2,3*}.

Departments of Pathology¹, Obstetrics and Gynecology², and Oncology³, The Johns Hopkins School of Medicine, Baltimore, MD 21205.

* Corresponding author. Mailing address: Ross Research Building, Room 512B, 720 Rutland Avenue, Baltimore, MD 21205 USA

Tel: 410 502 5161

Fax: 443 287 4295

email: roden@jhmi.edu)

Grant support was provided by the US Department of Defense Grant OC010017 (to R.B., I.-M. S. and R.B.S.R.) and the HERA foundation (to M.B.). We gratefully acknowledge the support of Sean Patrick, Robert Kurman and the Richard TeLinde Endowment.

Running title: GC-UNC-45 expression in ovarian carcinoma (36 of 40 word maximum)

Abstract (185 of 200 word maximum)

New tumor-associated antigens have promise as biomarkers and therapeutic targets that are urgently needed for epithelial ovarian cancer. In this report we derived a cell line from a patient with low grade serous carcinoma of the ovary and immunoprecipitated tumor associated antigens from tumor lysate using autologous patient antibody. Two novel tumor associated antigens, the General Cell isoform of UNC-45 (GC-UNC-45) and KIAA1529, were identified by matrix-assisted laser desorption ionization time-of-flight analysis. GC-UNC-45 is a cytoplasmic 100kDa protein that is a member of the UCS (UNC-45/CRO1/She4p) family of chaperones, but no significant homologies to KIAA1529 were found. Ectopic over-expression of GC-UNC-45 enhanced the rate of cell proliferation in vitro. Although GC-UNC-45 is present in normal surface epithelium, benign cystadenoma and low-grade serous carcinoma, elevated GC-UNC-45 expression was associated with high grade and advanced stage ovarian serous carcinomas. *GC-UNC-45* transcripts were higher in high grade disease than immortalized ovarian surface epithelium. However only 2/81 sera from patients with serous carcinoma and 0/50 controls reacted with GC-UNC-45. Thus, we describe GC-UNC-45 as a novel immunogenic biomarker of high-grade advanced disease that enhances the rate of cell proliferation.

Introduction

While the pathogenesis of ovarian serous carcinoma is poorly understood, a dualistic ovarian tumor progression model has recently been proposed based upon morphologic and molecular genetic analyses ¹. In this model, surface epithelial tumors are divided into low-grade neoplasms that arise stepwise from borderline tumors and high-grade neoplasms that lack precursor lesions recognizable by morphology. The indolent, low-grade neoplasms generally respond poorly to chemotherapy but they may, we speculate, be more amenable to immunotherapeutic approaches. Thus, while genetic and proteomic techniques are frequently used to identify candidate molecular biomarkers, we isolated tumor associated antigen (TAAs) by immunoprecipitation using autologous antibody from a patient with low-grade serous carcinoma ². Herein, we describe mammalian general cell (GC) isoform of UNC-45 as a new ovarian cancer TAA. UNC-45 is a member of the UCS (UNC-45/cro1/She4p) family involved in a variety of myosin- and actin-dependent functions in eukaryotic organisms ³. Elevation of GC-UNC-45 levels via ectopic expression increases the rate of cell proliferation. Significantly, elevated GC-UNC-45 expression is associated with high-grade relative to low-grade ovarian carcinoma and its precursors. Further, GC-UNC-45 expression was significantly higher in more advanced stage disease.

Methods

Antigen identification by matrix-assisted laser desorption ionization time-of-flight analysis. IgG from 0.5ml of 0.2 μ m-filtered sera from patient JH514 was bound to a protein G spin column (Seize-X, Pierce) and cross-linked with disuccinimidyl suberate

according to the manufacturers' instructions. Cultured JH514 cells were lysed in M-PER (Pierce) and clarified by centrifugation and passage through a protein G spin column. JH514 lysate (10mg/ml) was reacted with the autologous antibody column for 1h at 4°C. After extensive washing, the column was eluted at pH2.5. Eluates were precipitated in 10% (w/v) trichloroacetic acid and analyzed by SDS-PAGE with Coomassie staining. The ~100 kDa and ~200kDa protein bands were excised and digested with TPCK-treated sequencing grade trypsin (Worthington Biochemical Corp., Lakewood, NJ) as previously described⁴. Masses of the resulting peptides were measured by matrix-assisted laser desorption ionization time-of-flight (MALDI-TOF) on a Voyager DE STR (Applied Biosystems, Foster City, Ca). Positive ion mass spectra were analyzed using Data Explorer (version 3.5). Mass accuracy was better than 100 ppm. GC-UNC-45 was identified by searching the monoisotopic masses acquired from the 100kDa protein against the NCBI non-redundant database using the MS-Fit search engine on the protein Prospector web site (prospector.ucsf.edu).

Generation of GC-UNC-45 transient transfectants. Full-length *GC-UNC-45* cDNA was subcloned from MGC-999 (ATCC) into the mammalian vectors pcDNA3.1 (Invitrogen) and pEGFP-C1 (Clontech). Subconfluent cultures of 293T were transfected with plasmids DNA by using Lipofectamine 2000 reagent (Life Technologies).

Cellular localization of GC-UNC-45. 293T cells were seeded 12 hours after transfection at 2,000 cells/500 ml per well in Lab-Tek II chambered coverglass (Nalge Nunc International) and nuclei were visualized by Hoersch 33342 staining. Mounted samples were analyzed under a Nikon Eclipse TE 200 inverted fluorescence microscope and

captured with an RT monochrome digital camera. Twelve bit images were merged and analyzed with the Ultraview acquisition software, and pseudocolored.

Proliferation assay. Fluorescent 293T and HeLa (ATCC) cells were imaged and manually counted in six 20X power field under a Nikon Eclipse TE 200 inverted fluorescence microscope 12, 24 and 36 hours after transfection.

Prokaryotic expression and purification of recombinant GC-UNC-45 protein. Full length human GC-UNC-45 coding sequence was subcloned from MGC-999 (ATCC) into pProExHTc vector (Invitrogen). After transformation the bacteria were grown to an OD₆₀₀ of 0.6 and induced with 1mM isopropylthio- β -D-galactoside. 6His-tagged protein was purified on nickel-nitriloacetic acid resin columns under denaturing conditions according to the manufacturer (Qiagen).

Generation of rabbit antisera. Rabbits were immunized with 250 μ g of antigen in Freund's Complete Adjuvant and boosted with 125 μ g of antigen in Freund's Incomplete Adjuvant on days 14, 28 and 35. Rabbits were inoculated with the following antigens: full length 6His-tagged human GC-UNC-45 and KLH-coupled peptide HTSAASPAVSLLSGLPLQ of human GC-UNC-45. Immunizations and peptide affinity purification were performed by Proteintech Laboratories using their standard protocol.

Immunohistochemistry. Sections (5 μ m) from paraffin-embedded tissue were used for immunohistochemistry. Slides were deparaffinized in fresh xylenes and rehydrated through sequential graded ethanol steps. Antigen retrieval was performed by citrate buffer

incubation [18mM citric acid/8 mM sodium citrate (pH 6)] using a household vegetable steamer (Black and Decker) for 60 min. Slides were incubated for 5 min with 3% hydrogen peroxide; washed in 20mM Tris, 140 mM NaCl, and 0.1% Tween 20 (pH 7.6); and incubated in antibody dilution 1:250 for 60 min at room temperature. The avidin-biotin-peroxidase complex method from DAKO (Glostrup, Denmark) was used to visualize antibody binding, and slides were subsequently counterstained with hematoxylin.

Cell Extracts and Western Blotting. Cells were extracted in 62.5 mM Tris-HCl (pH 6.8), 2% w/v SDS, 10% glycerol, 50 mM DTT, and 0.01% w/v bromphenol blue. The samples were sonicated for three 10-s intervals and boiled for 5 min. Proteins were fractionated on SDS-polyacrylamide gels containing 12% acrylamide/0.4% bis-acrylamide and transferred to Immobilon-P membranes (Millipore, Bedford, MA) in 25 mM Tris-HCl (pH 8.5), 200 mM glycine, and 20% methanol for 2 h at 100 mA. Blots were blocked with 5% non-fat dried milk diluted in 50 mM Tris-HCl (pH 7.5) and 150 mM NaCl containing 0.1% Tween 20, incubated in a 1:1000 dilution of the GC-UNC-45 antibody and rinsed. Blots were then incubated for 1 h with horseradish peroxidase-conjugated rabbit anti- IgG antibody (1:10000; Amersham Corp.) and visualized using the Enhanced Chemiluminescence Kit (Amersham Corp.). Exposure times ranged from 30 s to 2 min.

Cell Lines. The cell line JH514 was maintained in Dulbecco's modified Eagles's medium (DMEM) supplemented with 10% fetal calf serum, penicillin (100IU/ml, and

streptomycin (100 μ g/ml) at 95% air/5% CO₂. 293T and HeLa cell lines were obtained from American Type Culture Collection and cultured according to their specifications.

Results

Identification of GC-UNC-45 as an ovarian TAA

To identify ovarian TAAs, we derived a cell line JH514 from tumor excised from an 83 year old woman with metastatic low grade serous carcinoma of the ovary (Figure 1a). Western blot analysis with AE1/AE3 and anti-CK19 confirmed cytokeratin expression by the JH514 cell line (not shown). Autologous serum antibodies were covalently coupled to a protein G-Sepharose minicolumn and used to immunoprecipitate antigens from detergent lysate of the JH514 cell line. Bound antigens were eluted with low pH and analyzed by SDS-PAGE. The serum antibody from this patient immunoprecipitated two antigens of approximately 100kDa and 200kDa (Figure 1b). Each band was excised from the gel and subjected to trypsin digestion. The charge/mass ratio for the tryptic peptides of the ~100kDa (figure 1c and Table 1) and ~200kDa (not shown) antigens was determined by matrix-assisted laser desorption ionization time-of-flight analysis. The prospector website was used to search for proteins with matching peptides. The ~200kDa antigen was identified as KIAA1529 (195kDa). Nothing is known about the KIAA1529 antigen and no significant homologies or domains were identified. The ~100kDa was identified as GC-UNC-45 (SMAP-1 Genbank AB014729) which has a predicted mass of 101kDa (Table 1). Matched peptides cover 12% of the GC-UNC-45 protein (Table 1).

Effect of GC-UNC-45 over-expression on cell proliferation

Prior studies indicate that skeletal myogenic cell proliferation is retarded when levels of GC-UNC-45 mRNA are reduced⁵. Therefore, we asked whether over-expression of GC-UNC-45 influences proliferation rate. Initially, we compared the proliferation of 293T cells upon transient transfection with pEGFP-C1-GC-UNC-45 or pcDNA3.1-GC-UNC-45 versus vector control (Figures 2a and b). The efficiency of transfection was estimated at 50-70% by fluorescence microscopy. By fluorescence microscopy, GFP alone was present partially in the nucleus and predominantly in cytoplasm (Figure 2c), whereas the GFP-GC-UNC45 protein was localized exclusively to the cytoplasm (Figure 2d). We further confirmed the expression of GFP-GC-UNC-45 by Western blot using rabbit antiserum to GC-UNC-45 produced as a 6His fusion protein in *E. coli* (Figure 3a). Rabbit antiserum to GFP specifically reacted with ~130kDa and ~30kDa proteins in pEGFP-C1-GC-UNC-45 and pEGFP-C1 transfected cells respectively (Figure 3b). Upon counting the number of fluorescent cells at 12, 24 and 36h after transfection we noted a significantly greater proliferation rate in cells transfected with pEGFP-C1-GC-UNC-45 as compared to pEGFP-C1 ($p=0.0001$ at both 24h and 36h post transfection, Figure 2a). To exclude the possibility that GFP fusion affects the function of GC-UNC-45 or potential toxic effects of GFP expression, we transiently transfected 293T cells with pEGFP-C1 and pcDNA3.1 (vector control) or with pEGFP-C1 and pcDNA3.1-GC-UNC-45 and the proliferation rate was followed by counting the number of fluorescent cells 12, 24 and 36 hours post-transfection (Figure 2b). Again, there was an increase in cell proliferation in 293T cells transfected with pcDNA3.1-GC-UNC-45 versus pcDNA3.1 vector control, noticeable from 24 hours after transfection ($p=0.0001$, Figure 2b). Similar results were

obtained in HeLa cells (not shown) and Western blot analysis using antisera to full-length human GC-UNC-45 confirmed GC-UNC-45 over expression after transfection with pcDNA3.1-GC-UNC-45 (not shown).

GC-UNC-45 over-expression is associated with high grade, advanced stage ovarian serous carcinoma

In order to evaluate GC-UNC-45 expression in ovarian tumors and normal tissue we generated rabbit antisera against KLH coupled to a peptide comprising the final 18 residues of human GC-UNC-45. Peptide binding antibody was affinity purified on a peptide column. The specificity of the affinity purified peptide antibody was analysed by Western blot using 6His-Tagged human GC-UNC-45 purified from *E.coli* (not shown) and 293T cells transfected with pEGFP-C1-GC-UNC-45 or pEGFP-C1 (Figure 3c). The antibody specifically recognized recombinant GC-UNC-45 with either the 6His or GFP tags (Figure 3c). We optimized conditions for detection of GC-UNC-45 in paraffin-embedded human tissue using the affinity purified peptide antibody.

Immunohistochemical staining suggested a cytoplasmic localization for GC-UNC-45 (Figure 4), consistent with our *in vitro* studies using GFP-GC-UNC-45 (Figure 2d). A similar immunohistochemical staining pattern was observed using the rabbit antiserum to full length GC-UNC-45 (not shown).

In order to assess whether GC-UNC-45 is differentially expressed in ovarian serous carcinoma, we performed immunohistochemical staining of tissue microarrays using GC-UNC-45-specific antibody for low grade (14 cases) and high grade (32 cases) serous

carcinoma. Staining was scored blind as absent=0, weak=1, intermediate=2, and intense=3. Using this scoring system we observed that high grade serous carcinomas stained more intensely than low grade serous carcinoma ($p=0.027$, Figure 5). Conversely, staining of normal ovarian surface epithelium (12 cases) and benign serous cystadenoma ($n=4$) were not significantly different from each other ($p=0.29$, Figure 5) or from low grade serous carcinoma ($p=0.48$ and $p=0.21$ respectively). In contrast, staining of normal ovarian surface epithelium (12 cases) and benign serous cystadenoma ($n=4$) was significantly weaker than for high grade serous carcinoma (32 cases, $p=0.0028$ and $p=0.0065$ respectively, Figure 5). The GC-UNC-45 antibody staining of low stage (stages 1-2) serous carcinoma (18 cases) was also significantly weaker than for high stage (stages 3-4) serous carcinoma (32 cases, $P=0.0021$, Figure 6).

To assess whether the lower expression of GC-UNC-45 in normal surface epithelium is reflected at the transcriptional level, we compared the expression of GC-UNC-45 transcripts relative to the house keeping gene GAPDH using Q-PCR and expressed the ratio in relative units (Table 2). We noted that 7/15 high grade serous carcinoma expresses GC-UNC-45 mRNA at a >2-fold higher level than an immortalized ovarian surface epithelial cell line, IOSE-29 (a mean of 0.081 ± 0.107 for high grade disease versus 0.025 relative units for IOSE-29). In an attempt to control for culture effects upon GC-UNC-45 mRNA level we compared expression in both the primary low grade serous carcinoma from patient JH514 with and the cell line derived from the same tumor. We observed similar expression levels of GC-UNC-45 mRNA in both the JH514 primary

tissue and the cell line (0.044 and 0.050 relative units respectively) both of which are lower than for high grade serous carcinoma (mean of 0.081 relative units).

Discussion

We describe the first cell line derived from a low-grade serous carcinoma of the ovary which may have utility in dissecting the relationship between this pathologic entity and high grade serous carcinoma ¹. Furthermore, we identify a new ovarian TAA, GC-UNC-45. Several lines of evidence suggest that GC-UNC-45 is involved in tissue proliferation. GC-UNC-45 transcripts are generally abundant during the first stages of development but decrease during differentiation processes ⁵. For example, GC-UNC-45 transcripts are expressed at high levels in all tissues of 8-day mouse embryos whereas by 9.75 days the most robust expression was confined to regions of intense development such as bronchial arches and forelimb. Moreover, studies of C2C12 myoblast differentiation showed that the highest levels of GC-UNC-45 were associated with non-differentiated, highly proliferating cells whereas in differentiating myoblast the GC-UNC-45 levels were significantly lower ⁵. Furthermore, a 68-75% decrease in cell proliferation was observed in cells treated with antisense oligonucleotides that specifically reduce the level of GC-UNC-45 GC mRNA ⁵. We find that over-expression of GC-UNC-45 in 293T cells enhances the rate of cell proliferation. Furthermore, GC-UNC-45 is expressed at higher levels in high grade ovarian carcinoma as compared to low grade disease and its putative precursors, benign serous cystadenomas and normal ovarian surface epithelium ¹.

GC-UNC-45 possesses three TPR domains and a single UCS domain ³. The TPR domains resemble those that interact with molecular chaperones such as Hsp70 and

Hsp90⁶. The N-terminal TPR domain of *C. elegans* UNC-45 binds directly to the C-terminal MEEVD motif of Hsp90. Indeed, the murine and human GC-UNC-45 co-immunoprecipitated with Hsp90 (not shown). Interestingly, inhibitors of Hsp90 molecular chaperone exhibit potent toxicity toward ovarian cancer^{7,8}. UCS protein family members, which include GC-UNC-45, are necessary for a variety of myosin and actin-dependent processes in lower eukaryotes such as fungi^{9,10} and nematodes¹¹ through to humans^{3,5}. The central and UCS domain of UNC-45 also has chaperone activity for myosin S1 and the standard chaperone substrate citrate synthetase⁶. Humans and mice express two forms of UNC-45; a smooth muscle (SM) and a general cell (GC) form with ~55% identity between the isoforms and >90% identity between homologues⁵. The SM UNC-45 is critical to sarcomere assembly, but the GC-UNC-45 isoform likely functions in cytoskeletal motility and polarization by interaction with non-muscle myosins. In light of the elevated expression of GC-UNC-45 in advanced stage disease, it is noteworthy that elevated expression of myosin VI is associated with increased metastatic potential of ovarian cancer¹². However, despite these observations, we failed to observe a clear pattern of co-localization between GFP-fused GC-UNC-45 and either actin or tubulin (not shown).

The original patient with antibodies for GC-UNC-45 had low grade serous carcinoma although her disease was advanced. Interestingly, we identified an additional serum reactive to GC-UNC-45 from a patient with high grade ovarian carcinoma. Thus GC-UNC-45-specific antibodies were detected by ELISA using full length 6His-tagged recombinant protein in only 2/82 sera of patients with ovarian carcinoma, and 0/50 patients with non-malignant gynecologic disorders, suggesting that it is not highly

immunogenic. Like many other TAAs identified by autologous antibodies, GC-UNC-45 expression is not confined to the tumor and it is unclear why immunologic tolerance against such TAAs is broken. One possibility is an association of GC-UNC-45 with heat shock proteins⁶. Extracellular presentation of heat shock protein, including hsp70 and hsp90, has been associated with dendritic cell activation and autoimmune disease^{13,14}.

Acknowledgements

We thank Robert Cole of the Johns Hopkins Mass Spectrometry Core and Mike Delannoy of the Johns Hopkins Imaging Core for expert mass spectroscopy and confocal microscopy for protein identification and imaging.

References

1. Shih Ie M, Kurman RJ: Ovarian tumorigenesis: a proposed model based on morphological and molecular genetic analysis. *Am J Pathol* 2004, 164:1511-1518
2. Chinni SR, Falchetto R, Gercel-Taylor C, Shabanowitz J, Hunt DF, Taylor DD: Humoral immune responses to cathepsin D and glucose-regulated protein 78 in ovarian cancer patients. *Clin Cancer Res* 1997, 3:1557-1564
3. Hutagalung AH, Landsverk ML, Price MG, Epstein HF: The UCS family of myosin chaperones. *J Cell Sci* 2002, 115:3983-3990
4. Shevchenko A, Wilm M, Vorm O, Jensen ON, Podtelejnikov AV, Neubauer G, Mortensen P, Mann M: A strategy for identifying gel-separated

proteins in sequence databases by MS alone. *Biochem Soc Trans* 1996, 24:893-896

5. Price MG, Landsverk ML, Barral JM, Epstein HF: Two mammalian UNC-45 isoforms are related to distinct cytoskeletal and muscle-specific functions. *J Cell Sci* 2002, 115:4013-4023

6. Barral JM, Hutagalung AH, Brinker A, Hartl FU, Epstein HF: Role of the myosin assembly protein UNC-45 as a molecular chaperone for myosin. *Science* 2002, 295:669-671

7. Kelland LR, Sharp SY, Rogers PM, Myers TG, Workman P: DT-Diaphorase expression and tumor cell sensitivity to 17-allylamino, 17-demethoxygeldanamycin, an inhibitor of heat shock protein 90. *J Natl Cancer Inst* 1999, 91:1940-1949

8. Neckers L, Ivy SP: Heat shock protein 90. *Curr Opin Oncol* 2003, 15:419-424

9. Toi H, Fujimura-Kamada K, Irie K, Takai Y, Todo S, Tanaka K: She4p/Dim1p interacts with the motor domain of unconventional myosins in the budding yeast, *Saccharomyces cerevisiae*. *Mol Biol Cell* 2003, 14:2237-2249

10. Wesche S, Arnold M, Jansen RP: The UCS domain protein She4p binds to myosin motor domains and is essential for class I and class V myosin function. *Curr Biol* 2003, 13:715-724

11. Barral JM, Bauer CC, Ortiz I, Epstein HF: Unc-45 mutations in *Caenorhabditis elegans* implicate a CRO1/She4p-like domain in myosin assembly. *J Cell Biol* 1998, 143:1215-1225

12. Yoshida H, Cheng W, Hung J, Montell D, Geisbrecht E, Rosen D, Liu J, Naora H: Lessons from border cell migration in the *Drosophila* ovary: A role for myosin VI in dissemination of human ovarian cancer. *Proc Natl Acad Sci U S A* 2004, 101:8144-8149
13. Liu B, Dai J, Zheng H, Stoilova D, Sun S, Li Z: Cell surface expression of an endoplasmic reticulum resident heat shock protein gp96 triggers MyD88-dependent systemic autoimmune diseases. *Proc Natl Acad Sci U S A* 2003, 100:15824-15829
14. Asea A, Rehli M, Kabingu E, Boch JA, Bare O, Auron PE, Stevenson MA, Calderwood SK: Novel signal transduction pathway utilized by extracellular HSP70: role of toll-like receptor (TLR) 2 and TLR4. *J Biol Chem* 2002, 277:15028-15034

Figure Legends

Figure 1. Identification of GC-UNC-45 by MALDI-TOF as a TAA from low grade serous carcinoma

a. Morphology of cell line JH514 viewed under phase contrast. **b.** Immunoaffinity purification of TAAs from low grade serous carcinoma using autologous IgG. The antigens of ~100kDa and ~200kDa were excised for mass spectrometry. **c.** MALDI-TOF analysis of tryptic peptides derived from the ~100kDa ovarian cancer-associated antigen.

Figure 2. Effect of GC-UNC-45 over-expression on cell proliferation. 293T cells transiently co-transfected with either a. pEGFP-C1 (vector control) or pEGFP-C1-UNC-45 expressing GFP fused to GC-UNC-45, or b. pEGFP-C1 and pcDNA3.1 (vector control) or pEGFP-C1 and pcDNA3.1-GC-UNC-45 expressing full length GC-UNC-45. The number of fluorescent cells per field of view was counted 12, 24 and 36 hours post-transfection. The localization of fluorescence in HeLa cells transiently transfected with pEGFP-C1 (c) or p-EGFP-C1-GC-UNC-45 (d).

Figure 3. Specificity of GC-UNC-45 antisera. Western blot analysis using antiserum to full length human GC-UNC-45 (a), rabbit antiserum to GFP (b) or rabbit serum against GC-UNC-45 peptide (c). Reactivity has been tested against 6His-tagged human GC-UNC-45 purified from *E. coli* and 293T cells transfected with pEGFP-C1-GC-UNC-45 or pEGFP-C1 vector alone.

Figure 4. Representative histological sections showing GC-UNC-45 immunostaining Immunohistochemical staining for GC-UNC-45 and hematoxylin counterstaining of **a.** Normal ovarian surface epithelium (160X), **b.** benign serous cystadenoma (160X), **c.** Low grade ovarian carcinoma (160X), and **d.** High grade ovarian carcinoma (100X) specimens on an ovarian tissue microarray.

Figure 5. GC-UNC-45 expression and ovarian cancer grade

Immunohistochemical staining intensity for GC-UNC-45 in normal ovarian surface epithelium (12 cases), benign serous cystadenoma (4 cases), low grade (14 cases) and

high grade (32 cases) serous carcinoma specimens was scored. GC-UNC-45 staining is not statistically different in normal or cystic epithelium or low grade ovarian carcinoma. However GC-UNC-45 staining is significantly elevated in high grade ovarian cancer ($p=0.0002$) versus low grade versus high grade ovarian cancer ($p=0.0275$).

Figure 6. GC-UNC-45 expression in serous carcinoma by stage

Immunohistochemical staining intensity for GC-UNC-45 in early (18 cases) and advanced stage (32 cases) serous carcinoma specimens was scored. GC-UNC-45 staining was significantly higher in advanced stage (3-4) versus early stage (1-2) ovarian carcinoma.

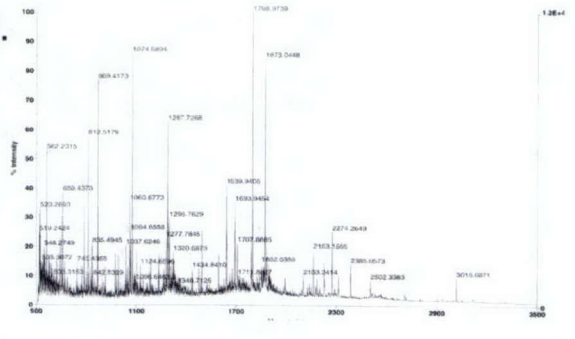
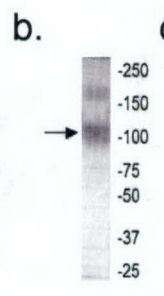
Table 1. Expected and observed M/z for peptides of GC-UNC-45 and the ~100kDa antigen.

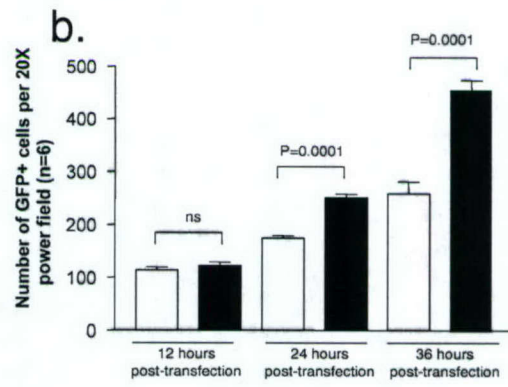
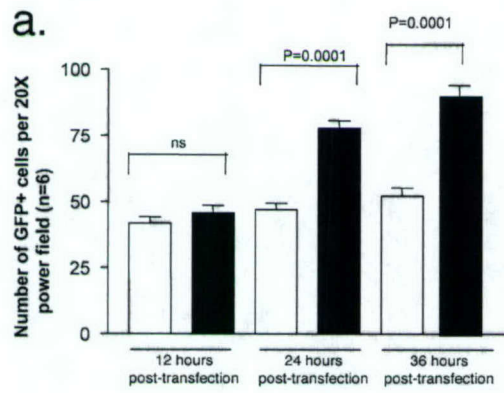
M/z submitted	MH+ matched	ΔDa	Missed cleavages	Database Sequence
523.2691	523.2186	0.050	0	(K)CSEK(D)
562.2315	562.3201	-0.089	1	(K)GTEKK(Q)
1074.6897	1074.5618	0.13	1	(R)CVSLEPKNK(V)
1179.6649	1179.5618	0.085	0	(K)SWFEGQGLAGK(L)
1186.7039	1186.5414	0.16	0/1Met-ox	(K)LGSAGGTDFSMK(Q)
1287.7267	1287.7749	-0.048	1	(R)TVATLSILGTRR(V)
1320.6865	1320.7527	-0.066	0	(R)ASFITANGVSLK(D)
1661.9771	1661.8606	0.12	0	(R)LLDMGETDLMLAALR(T)
1677.9307	1677.8556	0.075	0/1Met-ox	(R)LLDMGETDLMLAALR(T)
1693.9454	1693.8505	0.095	0/2Met-ox	(R)LLDMGETDLMLAALR(T)
1797.9774	1797.9063	0.071	0	(R)WAVEGLAYLTFDADV(E)
2225.2600	2225.1119	0.15	0	(R)EIASTLMESEMMEILSVLAK(G)
2273.2726	2273.0966	0.18	0/3Met-ox	(R)EIASTLMESEMMEILSVLAK(G)

Table 2. Q-PCR analysis of GC-UNC-45 mRNA level relative to GAPDH in ovarian carcinomas and cell lines. The expression level of GC-UNC-45 mRNA relative to that of GAPDH was expressed as $2^{([GAPDH\ Ct] - [GC-UNC-45\ Ct])}$

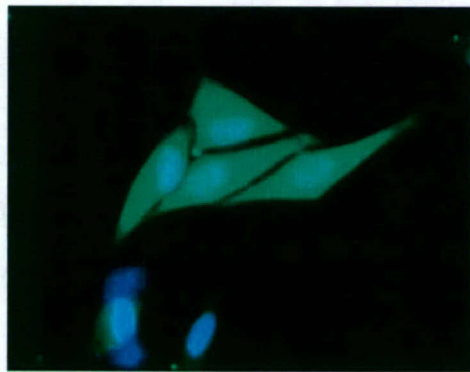
Sample	GC-UNC-45 Ct	GADPH Ct	Relative Expression	Tumor Grade
JH308	35	31	0.062	high
JH221	28.7	23	0.019	high
JH344	28.1	23	0.029	high
JH337	28.4	24.1	0.050	high
JH233	26.7	23.3	0.094	high
JH579	34.3	33.1	0.435	high
JH587	31.8	29.3	0.176	high
JH576	30.8	22.4	0.002	high
JH224	30	25.5	0.044	high
JH130	28.3	24.4	0.066	high
JH282	29	24.7	0.050	high
JH378	28.6	23.6	0.031	high
JH479	29.9	24.6	0.025	high
JH574	27.6	22.3	0.025	high
JH9	25.7	22.4	0.101	high
JH514	29.3	24.8	0.044	low

JH514 line	26.3	22	0.050	cell line
IOSE29	26.3	21	0.025	cell line

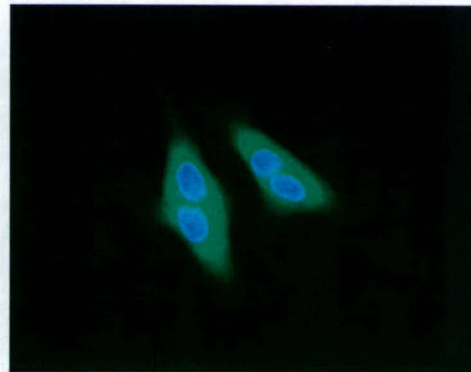


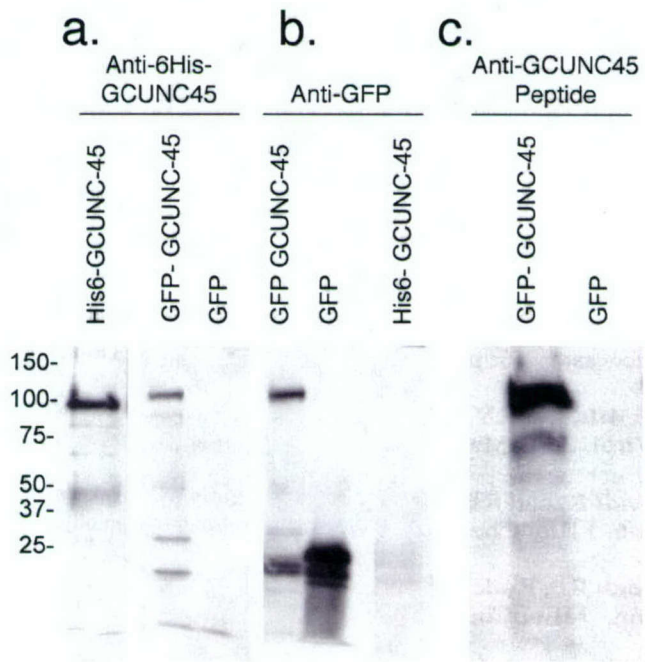


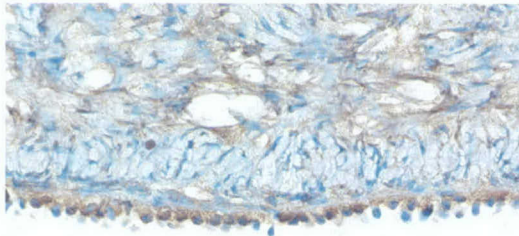
c.



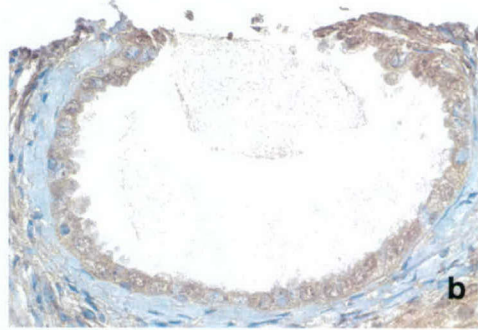
d.



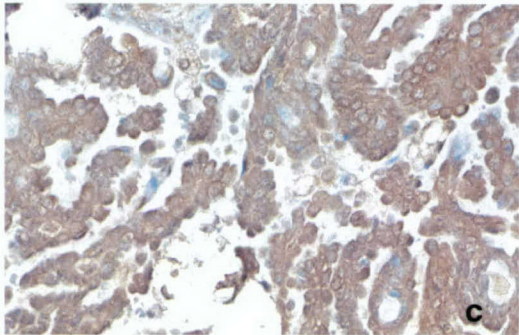




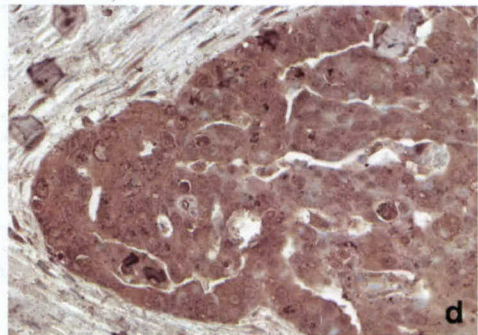
a



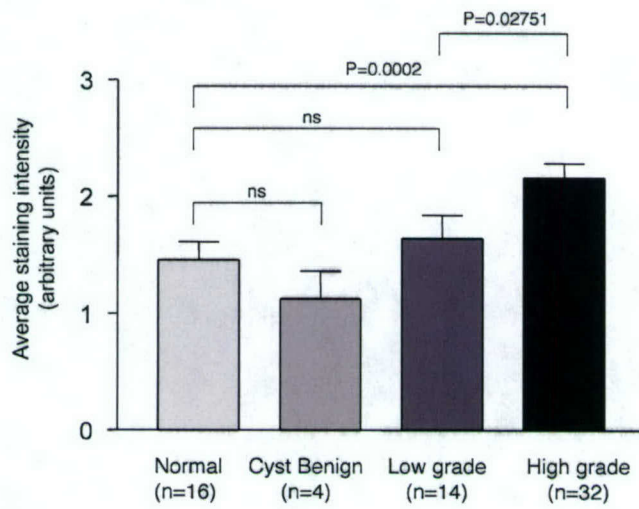
b

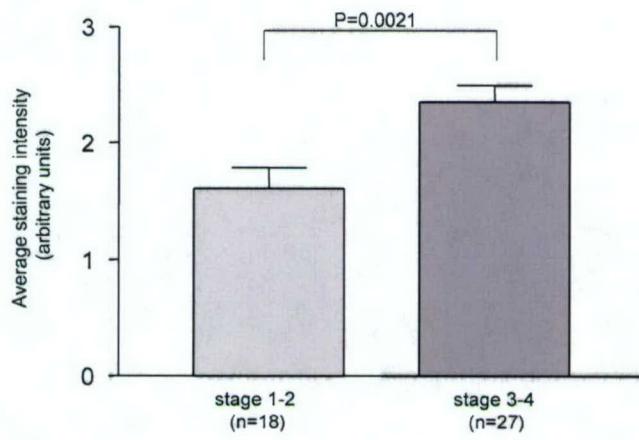


c



d





PROJECT 3 – DEVELOPMENT OF ANTIGEN-SPECIFIC CANCER VACCINES FOR
THE CONTROL OF OVARIAN CANCER

T-C Wu, M.D., Ph.D.

ABSTRACT:

Since over 95% of ovarian cancers express mesothelin, DNA vaccines encoding mesothelin represent a potential opportunity to control ovarian cancers. We have recently created a mesothelin-expressing peritoneal tumor from C57BL/6 mice. The tumor was capable of generating ascites and tumor growth in mice receiving intraperitoneal tumor challenge. Thus, this new peritoneal tumor model represents a suitable preclinical model for the development of DNA cancer vaccines against mesothelin-expressing tumors. Specifically we propose: Specific Aim 1: Generate and characterize the pcDNA3-BVP22, pcDNA3-MVP22, pcDNA3-mesothelin and pcDNA3-HVP22/mesothelin, pcDNA3-BVP22/mesothelin and pcDNA3-MVP22/mesothelin DNA constructs; Specific Aim 2: Characterize the ability of the various DNA vaccines to induce mesothelin-specific T cell-mediated immune responses in vaccinated mice; Specific Aim 3: Compare mesothelin-specific anti-tumor effects of the various DNA vaccines using mesothelin-expressing murine tumor models; Specific Aim 4: Compare pcDNA3-mesothelin/HSP70, pcDNA3-HVP22/mesothelin and pcDNA3-HVP22/mesothelin/HSP70 for their ability to induce mesothelin-specific cell-mediated immune responses and anti-tumor effects in vaccinated mice. The proposed studies will identify the best strategy for enhancing DNA vaccine potency. Since **Project 1** by Dr. Shih will identify new key molecules that are important for progression of serous tumors and **Project 2** by Dr. Roden will identify additional unique tumor antigens for ovarian serous tumors, these important and unique molecules can potentially serve as new targets for our vaccine development using the strategy developed in the current proposal.

Table of Contents

Cover.....	1
Abstract.....	2
Table of Contents.....	3
Introduction.....	4
Body.....	4
Key Research Accomplishments.....	7
Reportable Outcomes.....	8
Conclusions.....	8
References.....	8
Appendices.....	

Kim TW, Hung CF, Kim JW, Juang J, Chen PJ, He L, Boyd DA, Wu TC.
Vaccination with a DNA vaccine encoding herpes simplex virus type 1 VP22 linked to antigen generates long-term antigen-specific CD8-positive memory T cells and protective immunity. *Hum Gene Ther.* 2004 Feb; 15(2):167-77.

INTRODUCTION

There is a need to develop new therapies for ovarian cancer because current treatments, such as chemotherapy and radiation therapy, rarely result in a long-term cure for patients with local and metastatic disease. DNA vaccines represent an attractive approach to cancer therapy, but there are two major limitations to DNA vaccine potency. First, only a low percentage of professional antigen-presenting cells (dendritic cells) within the skin actually uptake the injected DNA. Second, DNA vaccines are unable to amplify and spread *in vivo* as viral vaccine vectors are able to do. Recently, we have enhanced DNA vaccine potency using herpes simplex virus (HSV-1) VP22 protein. VP22, an HSV-1 tegument protein, demonstrated the remarkable property of intercellular transport and is capable of distributing linked proteins to surrounding cells[1]. The linkage of HSV-1 VP22 (HVP22) to human papillomavirus-16 E7 protein led to dramatic increase in the number of E7-specific CD8⁺ T cell precursors in vaccinated mice (around 50-fold) and converted a less effective DNA vaccine into one with significant potency against E7-expressing tumors[2]. These results suggested that VP22 may be useful for development of new immunotherapies for ovarian cancer when linked to an ovarian tumor-specific antigen, such as mesothelin. We have therefore generated pcDNA3-HVP22, pcDNA3-BVP22, pcDNA3-MVP22, pcDNA3-mesothelin, pcDNA3-HVP22/mesothelin, pcDNA3-BVP22/mesothelin and pcDNA3-MVP22/mesothelin. The purpose of this study is to test whether greater VP22-mediated intercellular spreading of the encoded ovarian cancer antigen mesothelin will generate a higher degree of mesothelin-specific immunity.

Body:

We have generated pcDNA3-HVP22, pcDNA3-BVP22, pcDNA3-MVP22, pcDNA3-mesothelin, pcDNA3-HVP22/mesothelin, pcDNA3-BVP22/mesothelin and pcDNA3-MVP22/mesothelin. We have characterized the ability of the various DNA vaccines to induce mesothelin-specific T cell-mediated immune responses in vaccinated mice. We analyzed mesothelin-specific CD8⁺ and CD4⁺ T cells using CTL assays, ELISPOT assays, and intracellular cytokine staining with flow cytometry analysis. However, we failed to generate any detectable mesothelin-specific T cell responses after vaccination with DNA vaccines. This may be due to the fact that induction of immunity against self antigen mesothelin can be difficult because of immune tolerance. Several studies showed that heteroclitic analogs, which are single substitution analogs of an antigenic peptide at positions other than the main MHC anchor residues, are able to break tolerance and trigger immunity against self antigens. Because heteroclitic analogs have been shown to be associated with increased affinity of the epitope/MHC complex for the TCR molecule, they induce stronger T cell responses than the native epitope [3-8]. We therefore combined the heteroclitic strategy and our VP22 intercellular spreading strategy to develop a mesothelin-targeting DNA vaccine.

In the past few years, we have focused on the development of innovative strategies to enhance DNA vaccine potency using cervical cancer tumor-specific antigen E7. Increased understanding of intracellular pathways for antigen presentation has enabled the design of novel strategies to enhance MHC class I and class II presentation of antigens by DNA vaccine-transfected dendritic cells. Among the strategies that we have

tested, calreticulin (CRT) has emerged as a molecule of particular interest because of its ability to generate the strongest antigen-specific CD8⁺ T cell response when fused with a model antigen E7. Thus, we have combined the heteroclitic strategy and with the CRT strategy to develop another mesothelin-targeting DNA vaccine. To accomplish this, we first identified several potential candidate epitopes for mouse mesothelin protein (**Table 1**) using the BioInformatics & Molecular Analysis Section (BIMAS) for K^b peptide binding predictions (http://bimas.dcrt.nih.gov/molbio/hla_bind/). Second, because of the many potential epitopes of mesothelin, we focused on the mesothelin 343-351 epitope EIPFTYEQL (as it received the highest BIMAS prediction score) and substituted alanine at each position except anchor positions in the **Table 2** to generate heteroclitic analogs. Third, we generated DNA vaccine constructs using the pcDNA3 vector as shown in **Table 2**.

Table 1

Peptide name Start position	MHC class I	Peptide sequence	BIMAS score
meso343	H-2K^b	EIPFTYEQL	72
meso583	H-2K^b	GIPNGYLVL	72
meso17	H-2K^b	ICRSRFLLL	13
meso520	H-2K^b	MDIATFKRL	12
meso53	H-2K^b	LPTGLFLGL	11

Table 2

Names of Constructs	Peptide sequence
pcDNA3- 343W and pcDNA3-CRT/343W	EIPFTYEQL
pcDNA3- 343A1 and pcDNA3-CRT/343A1	AIPFTYEQL
pcDNA3- 343A2 and pcDNA3-CRT/343A2	EAPFTYEQL
pcDNA3- 343A3 and pcDNA3-CRT/343A3	EIAFTYEQL
pcDNA3- 343A4 and pcDNA3-CRT/343A4	EIPATYEQL
pcDNA3- 343A5 and pcDNA3-CRT/343A5	EIPFAYEQL
pcDNA3- 343A6 and pcDNA3-CRT/343A6	EIPFTYAQL
pcDNA3- 343A7 and pcDNA3-CRT/343A7	EIPFTYEAL

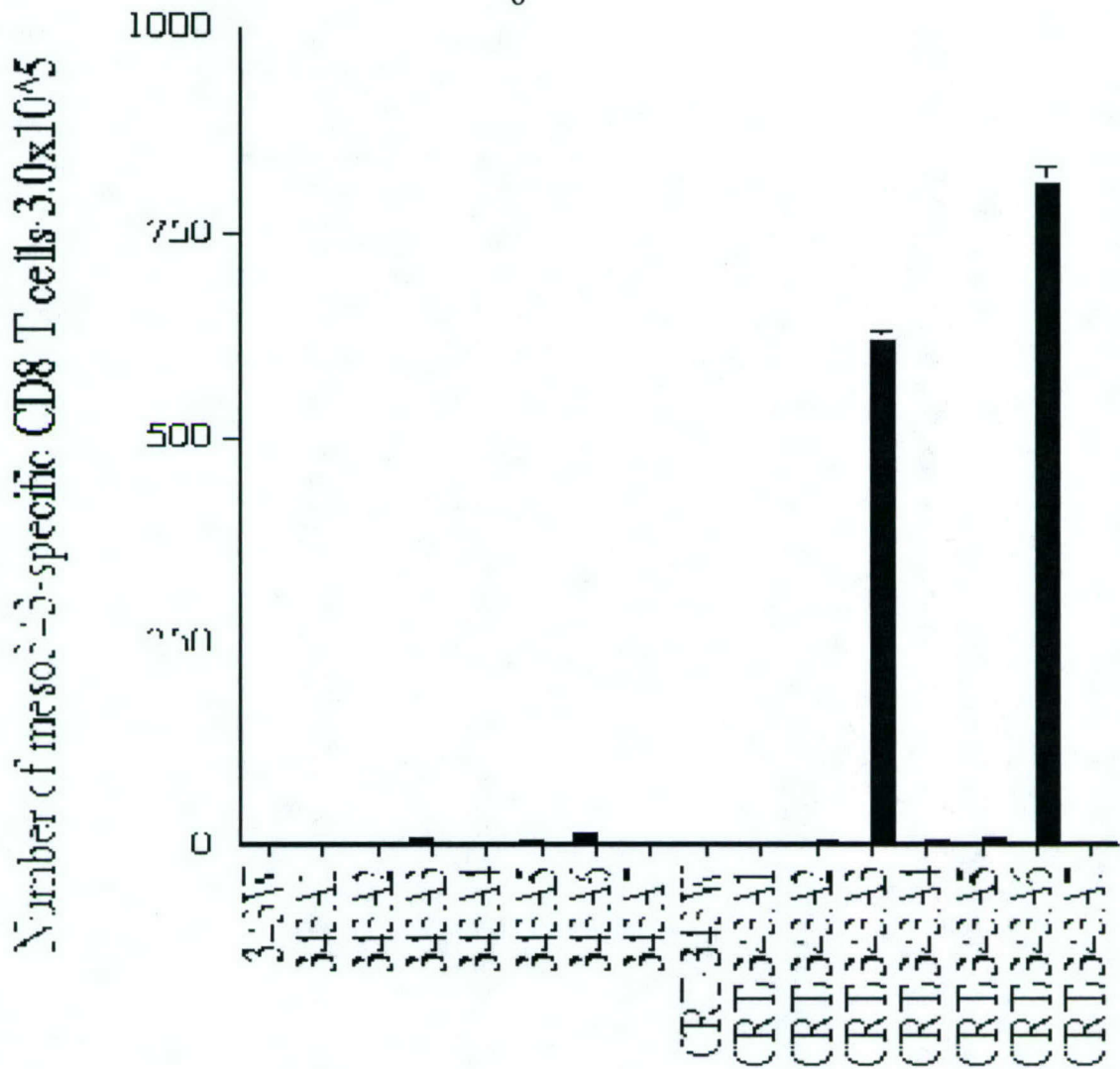


Figure 1. Characterization of mesothelin amino acid 343-351 -specific CD8⁺ T cell mediated immune responses in mice vaccinated with the various DNA vaccines. Intracellular cytokine staining followed by flow cytometry analysis was used to characterize the mesothelin-specific CD8⁺ T cell response to vaccination. Bar graph depicting the number of mesothelin 343-351 peptide-specific IFN- γ -secreting CD8⁺ T cell precursors / 3×10^5 splenocytes. Splenocytes harvested from mice vaccinated with DNA vaccines were incubated with wild type mesothelin amino acids 343-351 (EIPFTYEQL). Data are expressed as mean number of interferon-secreting T cells per 3×10^5 splenocytes \pm SEM. The data collected from all of the above experiments are from one representative experiment of two performed.

Mice were vaccinated with 2 μ g of DNA twice at a one-week interval by gene gun administration. As shown in **Figure 1**, mice vaccinated with DNA vaccines encoding CRT linked to heteroclitic epitopes 343A3 or 343A6 (pcDNA3-CRT/343A3 or pcDNA3-CRT/343A6) generated significantly higher numbers of antigen-specific CD8⁺ T cells against wild type mesothelin aa343-351 compared to DNA vaccines encoding CRT linked to wild type epitope 343 and others. In addition, DNA vaccines encoding wild type epitope 343 or heteroclitic epitopes 343A3, 343A6, and others can not generate significant numbers of antigen-specific CD8⁺ T cells against wild type mesothelin aa343-351. This suggests that a DNA vaccine encoding CRT linked to a heteroclitic

epitope of mesothelin enhances the epitope-specific CD8⁺ T cell response compared to a DNA vaccine encoding CRT linked to a wild type epitope or compared to a DNA vaccine encoding only an epitope of mesothelin.

We will test our DNA vaccines (pcDNA3-CRT/343A3 and pcDNA3-CRT/343A6) against the mesothelin-expressing tumor cell line WF-3 in tumor protection and tumor treatment experiments. If our DNA vaccines can significantly control WF-3 tumors, we will attempt to understand what effector cells contribute to the mechanism of the anti-tumor response using a CD8, CD4, or NK-depletion experiment. If these DNA vaccines generate strong antitumor effects against WF-3, we may expect to see autoimmune responses in vaccinated mice. We will confirm autoimmunity by biopsy of all organs in vaccinated mice.

KEY RESEARCH ACCOMPLISHMENTS:

- ◆ Mice vaccinated with pcDNA3-HVP22, pcDNA3-BVP22, pcDNA3-MVP22, pcDNA3-mesothelin, pcDNA3-HVP22/mesothelin, pcDNA3-BVP22/mesothelin and pcDNA3-MVP22/mesothelin exhibited no detectable mesothelin-specific T cell responses by using CTL assays, ELISPOT assays, and intracellular cytokine staining with flow cytometry analysis.
- ◆ DNA immunization with a calreticulin linked to heteroclitic epitope of mesothelin breaks tolerance and induces mesothelin specific immunity in mice

REPORTABLE OUTCOMES:

Kim TW, Hung CF, Kim JW, Juang J, Chen PJ, He L, Boyd DA, Wu TC.

Vaccination with a DNA vaccine encoding herpes simplex virus type 1 VP22 linked to antigen generates long-term antigen-specific CD8-positive memory T cells and protective immunity. *Hum Gene Ther.* 2004 Feb;15(2):167-77.

CONCLUSIONS:

A major hurdle of cancer immunotherapy is the issue of tolerance to self antigens by the host's immune system. This occurs because epitopes of the tumor antigens recognized by T cells are poor immunogens and are unable to induce activation and differentiation of effector T cells. A strategy that designs strong immunogenic variants (heteroclitic epitopes) of these epitopes would likely prime T cell responses that cross-react to the original targeting epitopes. This heteroclitic vaccine strategy has proved to be a powerful tool for breaking tolerance, generating strong immune responses and anti-tumor effects against self-antigens. We demonstrated that DNA immunization with a vaccine encoding CRT linked to a heteroclitic epitope of mesothelin breaks tolerance and induces mesothelin-specific immunity in mice

REFERENCES:

1. Elliott G and O'Hare P. 1997. Intercellular trafficking and protein delivery by a herpesvirus structural protein. *Cell*, 88: 223-33.
2. Hung CF, Cheng WF, Chai CY, Hsu KF, He L, Ling M, and Wu TC. 2001. Improving vaccine potency through intercellular spreading and enhanced MHC class I presentation of antigen. *J Immunol*, 166: 5733-40.
3. Ercolini AM, Machiels JP, Chen YC, Slansky JE, Giedlen M, Reilly RT, Jaffee EM. 2003. Identification and characterization of the immunodominant rat HER-2/neu MHC class I epitope presented by spontaneous mammary tumors from HER-2/neu-transgenic mice. *J Immunol* 170: 4273-80
4. Scardino A, Gross DA, Alves P, Schultze JL, Graff-Dubois S, Faure O, Tourdot S, Chouaib S, Nadler LM, Lemonnier FA, Vonderheide RH, Cardoso AA, Kosmatopoulos K. 2002. HER-2/neu and hTERT cryptic epitopes as novel targets for broad spectrum tumor immunotherapy. *J Immunol* 168: 5900-6
5. Hoffmann TK, Loftus DJ, Nakano K, Maeurer MJ, Chikamatsu K, Appella E, Whiteside TL, DeLeo AB. 2002. The ability of variant peptides to reverse the nonresponsiveness of T lymphocytes to the wild-type sequence p53(264-272) epitope. *J Immunol* 168: 1338-47
6. Gold JS, Ferrone CR, Guevara-Patino JA, Hawkins WG, Dyllal R, Engelhorn ME, Wolchok JD, Lewis JJ, Houghton AN. 2003. A single heteroclitic epitope determines cancer immunity after xenogeneic DNA immunization against a tumor differentiation antigen. *J Immunol* 170: 5188-94
7. Slansky JE, Rattis FM, Boyd LF, Fahmy T, Jaffee EM, Schneck JP, Margulies DH, Pardoll DM. 2000. Enhanced antigen-specific antitumor immunity with altered peptide ligands that stabilize the MHC-peptide-TCR complex. *Immunity* 13: 529-38
8. Dyllal R, Bowne WB, Weber LW, LeMaoult J, Szabo P, Moroi Y, Piskun G, Lewis JJ, Houghton AN, Nikolic-Zugic J. 1998. Heteroclitic immunization induces tumor immunity. *J Exp Med* 188: 1553-61

Vaccination with a DNA Vaccine Encoding Herpes Simplex Virus Type 1 VP22 Linked to Antigen Generates Long-Term Antigen-Specific CD8-Positive Memory T Cells and Protective Immunity

TAE WOO KIM,^{1,*} CHIEN-FU HUNG,^{1,*} JEONG WON KIM,¹ JEREMY JUANG,¹ PEI-JER CHEN,²
LIANGMEI HE,¹ DAVID A.K. BOYD,¹ and T.-C. WU^{1,3-5}

ABSTRACT

Intradermal vaccination with DNA encoding herpes simplex virus type 1 (HSV-1) VP22 linked to antigen leads to spread of antigen within the epithelium and results in enhanced antigen-specific CD8⁺ T cell immune responses in vaccinated mice. In this study, we characterized the number of antigen-expressing dendritic cells (DCs) in the draining lymph nodes of vaccinated mice and determined whether the linkage of VP22 to antigen would influence the ability of antigen-expressing DCs to activate antigen-specific CD8⁺ T cells *in vivo*. Vaccination with DNA encoding HSV-1 VP22 linked to human papillomavirus type 16 E7 antigen generated more antigen-expressing DCs in the draining lymph nodes of vaccinated mice than E7 alone. In addition, the linkage of VP22 to E7 improved the MHC class I presentation of E7 in transfected DCs and led to enhanced activation of E7-specific CD8⁺ T cells. We also observed that vaccination with DNA encoding VP22 linked to E7 generated more E7-specific CD8⁺ memory T cells, and enhanced long-term protective antitumor immunity against an E7-expressing tumor in vaccinated mice compared with vaccination with DNA encoding E7 alone. Thus, administration of DNA encoding VP22 linked to antigen represents a plausible approach for the development of protective DNA vaccines.

OVERVIEW SUMMARY

A limitation of DNA vaccination by gene gun is that the encoded antigen does not spread to neighboring cells as some replicating viral vaccine vectors do. We have previously showed that herpes simplex virus (HSV-1) VP22 linkage significantly enhanced the efficacy of vaccination against the human papillomavirus E7 protein. Here, we report evidence supporting that vaccination with DNA encoding HSV-1 VP22 linked to E7 antigen was capable of generating more antigen-expressing DCs in draining lymph nodes, more antigen-specific CD8⁺ memory T cells, and enhanced long-term protective antitumor immunity against an E7-expressing tumor in vaccinated mice compared with vaccination with

DNA encoding E7 alone. These findings may have an important impact on the development of protective DNA vaccines.

INTRODUCTION

DNA VACCINES have emerged as an attractive approach for generating antigen-specific immunotherapy (for reviews, see Donnelly *et al.*, 1997; Robinson, 1997). Because DNA is a relatively stable and pure molecule, it can be easily prepared and harvested in large quantities. In addition, naked plasmid DNA is relatively safe and therefore can be easily and repeatedly administered. However, naked DNA has no cell type speci-

¹Department of Pathology, Johns Hopkins Medical Institutions, Baltimore, MD 21205.

²Department of Medicine, National Taiwan University, Taipei 106, Taiwan.

³Department of Molecular Microbiology and Immunology, Johns Hopkins Medical Institutions, Baltimore, MD 21205.

⁴Department of Oncology, Johns Hopkins Medical Institutions, Baltimore, MD 21205.

⁵Department of Obstetrics and Gynecology, Johns Hopkins Medical Institutions, Baltimore, MD 21205.

*Tae Woo Kim and Chien-Fu Hung contributed equally to this work.

ficity. Thus, it is important to find an efficient route for the administration of DNA vaccines into the appropriate target cells. Intradermal administration of DNA vaccines by gene gun represents a convenient way to deliver DNA vaccines into dendritic cells (DCs) *in vivo*. Skin contains numerous MHC class II⁺ bone marrow-derived antigen-presenting cells (APCs) called Langerhans cells, which are capable of moving into the lymphatic system via draining lymph nodes (Condon *et al.*, 1996). The gene gun delivery method allows for direct targeting of genes of interest into Langerhans cells *in vivo* and is therefore ideal for the administration of DNA vaccines. We have successfully used this method to deliver DNA constructs for our vaccine development (Chen *et al.*, 1999, 2000; Ji *et al.*, 1999; Hung *et al.*, 2001a-c).

We have previously used this system to test several intracellular targeting strategies that enhance MHC class I and/or class II presentation of antigen. For example, we have significantly enhanced MHC class I presentation of a model antigen, human papillomavirus type 16 (HPV-16) E7, using the linkage of *Mycobacterium tuberculosis* heat shock protein 70 (HSP70) (Chen *et al.*, 2000), calreticulin (CRT) (Cheng *et al.*, 2001), or the translocation domain (domain II) of *Pseudomonas aeruginosa* exotoxin A [ETA(dII)] (Hung *et al.*, 2001b) to E7 in the context of a DNA vaccine. The linkage of these molecules to E7 resulted in augmentation of the E7-specific CD8⁺ T cell immune response in vaccinated mice. Furthermore, to enhance MHC class II antigen processing, we have previously linked the sorting signals of lysosome-associated membrane protein (LAMP-1) to the E7 antigen, creating the Sig/E7/LAMP-1 chimera (Wu *et al.*, 1995). We found that expression of this DNA vaccine was able to target E7 to endosomal and lysosomal compartments and enhance MHC class II presentation to CD4⁺ T cells in mice vaccinated with Sig/E7/LAMP-1 DNA compared with DNA encoding wild-type E7 (Ji *et al.*, 1999).

Although DNA vaccines employing intracellular targeting strategies can significantly enhance MHC class I and class II presentation of antigen in transfected DCs, they can generate only a limited number of antigen-expressing DCs because naked DNA vaccines lack the intrinsic ability to amplify and spread *in vivo*. This significantly limits the potency of DNA vaccines. Therefore, a strategy that facilitates the spread of antigen to more DCs may significantly enhance the potency of naked DNA vaccines. We have augmented the potency of DNA vaccines by using herpes simplex virus type 1 (HSV-1) VP22, an HSV-1 tegument protein capable of intercellular transport (Elliott and O'Hare, 1997). We showed that HSV-1 VP22 (VP22) was capable of enhancing intercellular spreading of the linked protein to APCs (Hung *et al.*, 2001a). Furthermore, we demonstrated that mice vaccinated with VP22/E7 DNA generated a significantly greater number of E7-specific CD8⁺ T cell precursors than mice vaccinated with wild-type E7 DNA (Hung *et al.*, 2001a). We also found that vaccination with VP22/E7 DNA generated a stronger antitumor effect than wild-type E7 DNA (Hung *et al.*, 2001a). Several issues related to the administration of VP22/E7 DNA include whether the administration of chimeric VP22/E7 DNA is capable of generating more antigen-expressing dendritic cells in the draining lymph nodes, activating more antigen-specific CD8⁺ memory T cells, and generating long-term protective antitumor immunity.

In this study, we demonstrated that vaccination of mice with pcDNA3-VP22/E7 led to more E7-expressing DCs in draining lymph nodes, more E7-specific CD8⁺ memory T cells, and enhanced long-term protective immunity against E7-expressing tumors in the vaccinated mice. Thus, administration of DNA vaccines with DNA encoding VP22 proteins represents a viable approach for the development of protective DNA vaccines.

MATERIALS AND METHODS

Plasmid DNA constructs and DNA preparation

We chose to use the pcDNA3 expression vector, which has been used effectively to investigate the correlation between the E7-specific T cell-mediated immune response and the antitumor effect generated by various DNA vaccines (Chen *et al.*, 2000). The generation of pcDNA3-E7 (Chen *et al.*, 2000), pcDNA3-VP22/E7 (Hung *et al.*, 2001a), pcDNA3-VP22/E7/GFP (Hung *et al.*, 2001a), pcDNA3-E7/GFP (Hung *et al.*, 2001c), pcDNA3-E7/HSP70 (Chen *et al.*, 2000), pcDNA3-CRT/E7 (Cheng *et al.*, 2001), pcDNA3-Sig/E7/LAMP-1 (Kim *et al.*, 2003), and pcDNA3-ETA(dII)/E7 (Hung *et al.*, 2001b) has been described previously. The accuracy of these constructs was confirmed by DNA sequencing. The DNA was amplified in *Escherichia coli* DH5 α and purified as described previously (Chen *et al.*, 2000).

Mice

Six- to 8-week-old female C57BL/6 mice were purchased from the National Cancer Institute (Frederick, MD) and kept in the oncology animal facility of the Johns Hopkins Hospital (Baltimore, MD). All animal procedures were performed according to approved protocols and in accordance with recommendations for the proper use and care of laboratory animals.

DNA vaccination

DNA-coated gold particles were prepared and gene gun particle-mediated DNA vaccination was performed with a helium-driven gene gun (Bio-Rad, Hercules, CA) according to a previously described protocol (Chen *et al.*, 2000). DNA-coated gold particles (1 μ g of DNA per bullet) were delivered to the shaved abdominal region of C57BL/6 mice, using a helium-driven gene gun (Bio-Rad) with a discharge pressure of 400 lb/in². C57BL/6 mice were vaccinated via gene gun with 2 μ g of pcDNA3, pcDNA3-E7, pcDNA3-E7/HSP70, pcDNA3-CRT/E7, pcDNA3-Sig/E7/LAMP-1, pcDNA3-ETA(dII)/E7, or pcDNA3-VP22/E7 in our mouse *in vivo* immunologic response experiment. These mice received a booster with the same regimen 1 week later.

Intracellular cytokine staining and flow cytometry analysis

Cell surface marker staining of CD8 and intracellular cytokine staining for interferon γ (IFN- γ) as well as FACScan analysis were performed under conditions described previously (Chen *et al.*, 2000). Before flow cytometry, splenocytes from different vaccinated groups of mice were collected and incubated for 20 hr with E7 peptide (amino acids 49–57, RAHYNIVTF, at 1

$\mu\text{g/ml}$) (Feltkamp *et al.*, 1993) containing an MHC class I epitope for detecting E7-specific CD8^+ T cell precursors. The number of IFN- γ -secreting CD8^+ T cells was analyzed by flow cytometry. Analysis was performed on a BD FACScan with CellQuest software (BD Biosciences Immunocytometry Systems, Mountain View, CA).

Preparation of CD11c^+ cells in inguinal lymph nodes from vaccinated mice

C57BL/6 mice (3 per group) received 12 inoculations (nonoverlapping intradermal administration) in the abdominal region via gene gun. Gold particles used for each inoculation were coated with $1 \mu\text{g}$ of pcDNA3-E7/GFP DNA, pcDNA3-VP22/E7/GFP, or no insert (used as a control). Inguinal lymph nodes were harvested from vaccinated mice 1, 3, or 5 days after vaccination via gene gun. A single-cell suspension from isolated inguinal lymph nodes was prepared. CD11c^+ cells were enriched from lymph nodes, using CD11c (N418) microbeads (Miltenyi Biotec, Auburn, CA). Enriched CD11c^+ cells were

analyzed by forward and side scatter and gated around a population of cells with size and granular characteristics of DCs. The percentage of CD11c^+ cells in the gated area was characterized by flow cytometry analysis, using phycoerythrin (PE)-conjugated anti- CD11c antibody (BD Biosciences Pharmingen, San Diego, CA). Green fluorescent protein (GFP)-positive cells were analyzed by flow cytometry analysis, using a protocol described previously (Lappin *et al.*, 1999). Data are expressed as the percentage of CD11c^+ GFP $^+$ cells among gated monocytes.

Activation of E7-specific CD8^+ T cell line by CD11c -enriched cells from vaccinated mice

Mice were vaccinated, and enriched CD11c^+ cells were collected as described above. CD11c -enriched cells (5×10^4) were incubated with 5×10^5 cells of the E7-specific CD8^+ T cell line (Wang *et al.*, 2000) for 16 hr. Activated IFN- γ -secreting E7-specific CD8^+ T cells were then determined by staining for both surface CD8 and intracellular IFN- γ and analyzed by flow cytometry analysis as described above.

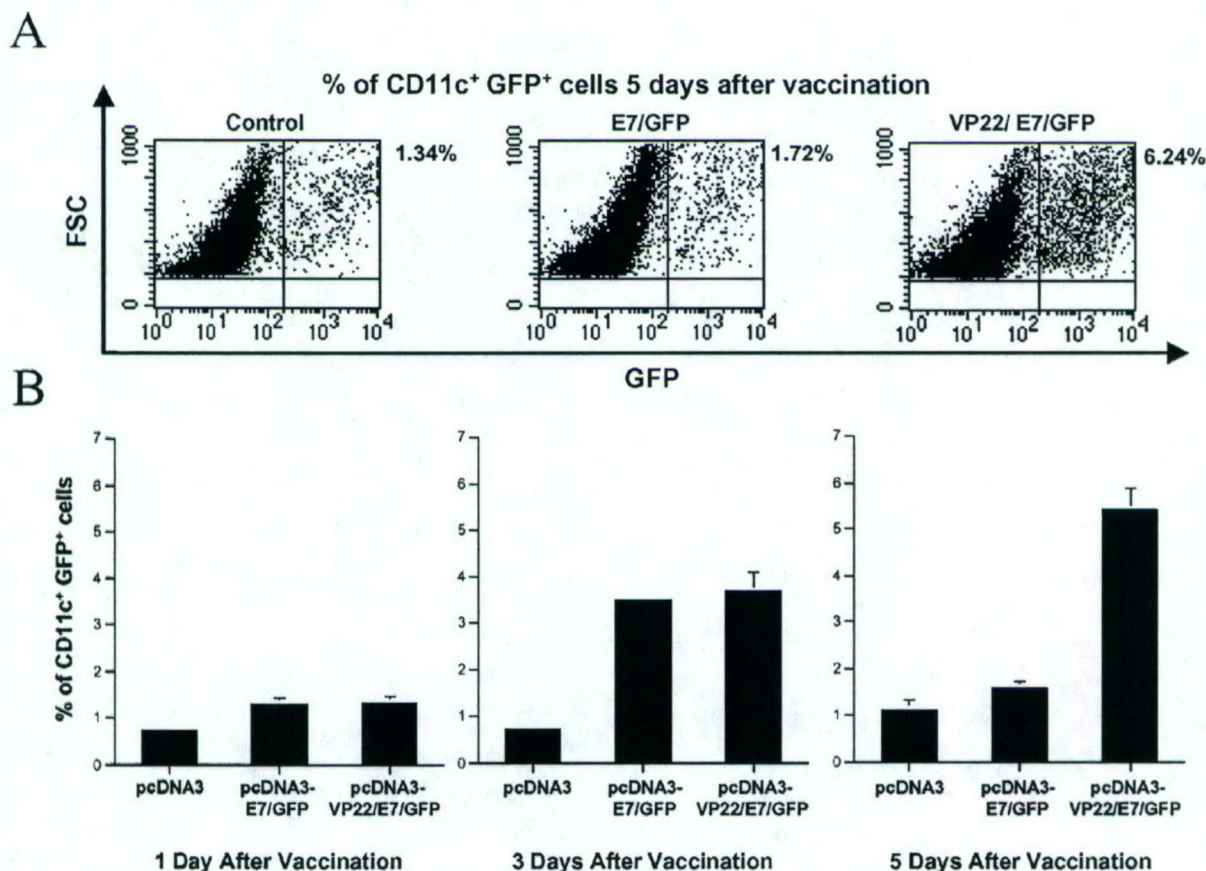


FIG. 1. Characterization of CD11c^+ GFP $^+$ DCs in the inguinal lymph nodes of vaccinated mice. Mice (three per group) were immunized with pcDNA3, pcDNA3-E7/GFP, or pcDNA3-VP22/E7/GFP DNA intradermally via gene gun. The inguinal lymph nodes were harvested from mice 1, 3, or 5 days after gene gun vaccination. DCs were enriched from a single-cell suspension of lymph nodes, using CD11c microbeads. (A) Representative flow cytometry data to determine the percentage of CD11c^+ GFP $^+$ cells among the gated monocytes 5 days after vaccination. The data presented are from one representative experiment of two performed. (B) Bar graphs depicting the percentage of CD11c^+ GFP $^+$ monocytes among the gated monocytes (mean \pm SD) in various vaccinated groups at various time points.

Characterizing expression of DC markers

We have used flow cytometry analysis to evaluate the expression of markers in DCs including MHC class I and class II, B7-1 and B7-2 costimulatory molecules, and CD40 as described previously (Wang *et al.*, 2000). The immortalized DC line used in this study was kindly provided by K. Rock (University of Massachusetts, Worcester, MA) (Shen *et al.*, 1997). DCs were transfected with GFP, E7/GFP, or VP22/E7/GFP DNA, using Lipofectamine 2000 (Life Technologies, Rockville, MD), and were collected 24 hr after transfection. DC surface marker staining for MHC class I and class II, B7-1 and B7-2 costimulatory molecules, and CD40 as well as FACScan analysis were performed under the conditions described previously (Chen *et al.*, 2000) after gating around a population of GFP⁺ cells.

Activation of E7-specific CD8⁺ T cell line by DNA-transfected DC line

A DC line was transfected with DNA encoding GFP, E7/GFP, or VP22/E7/GFP. The sorting of GFP⁺ DCs expressing GFP, E7/GFP, or VP22/E7/GFP was performed 24

hr after transfection, using a FACSVantage (BD Biosciences Immunocytometry Systems) according to the vendor's protocol. GFP⁺ DCs (1×10^5) were incubated with 1×10^6 cells of the E7-specific CD8⁺ T cell line (Wang *et al.*, 2000) for 4 hr. Cells were then stained for both surface CD8 and intracellular IFN- γ and analyzed by flow cytometry as described above. An E6-specific CD8⁺ T cell line was used as a negative control. The generation and characterization of this E6-specific CD8⁺ T cell line have been described previously (Peng *et al.*, 2003).

Determination of VP22-specific CD8⁺ T cells

CD8⁺ T cells were isolated from splenocytes of mice vaccinated with DNA encoding VP22/E7, harvested 1 week after the last vaccination. DC lines expressing DNA encoding GFP, E7/GFP, or VP22/GFP were prepared as described above. GFP⁺ DCs (1×10^5) were incubated with 1×10^6 CD8⁺ T cells for 6 hr. Cells were then stained for both surface CD8 and intracellular IFN- γ and analyzed by flow cytometry as described above.

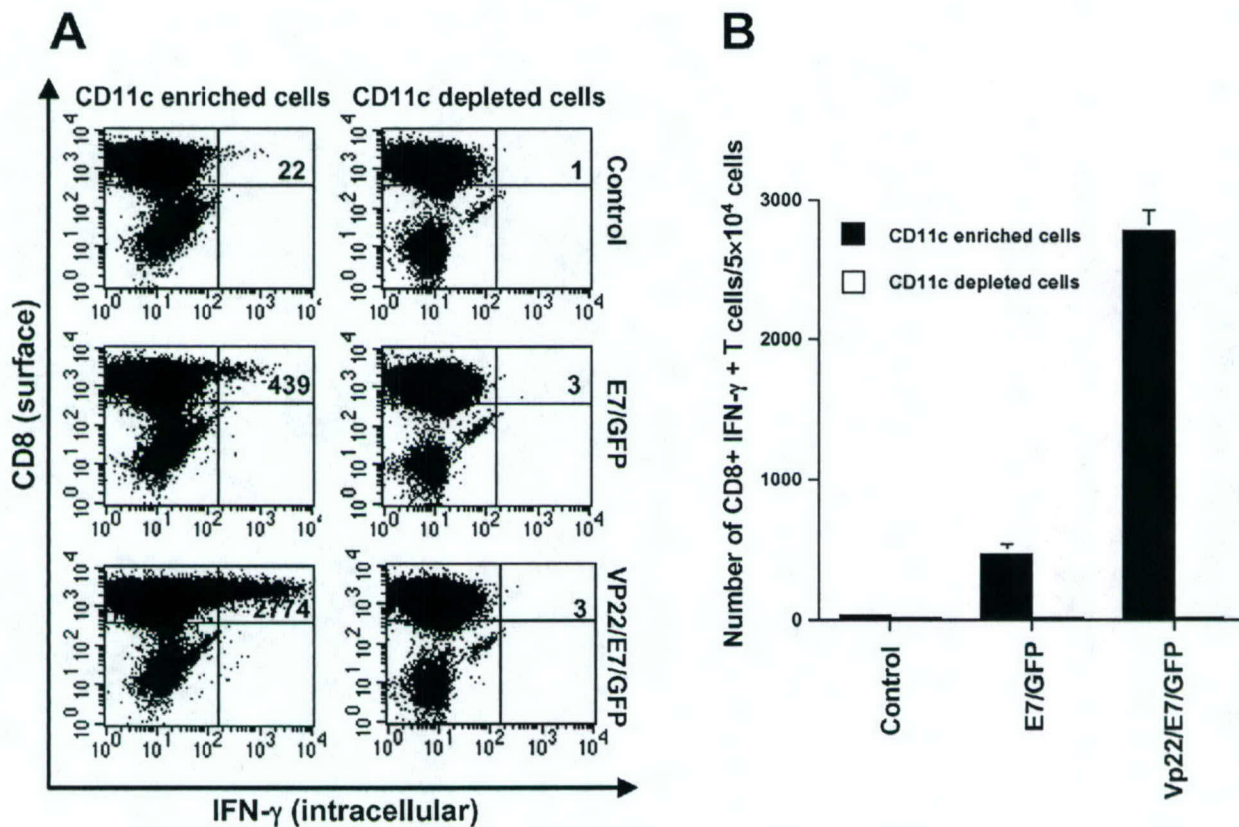


FIG. 2. Activation of an E7-specific CD8⁺ T cell line by CD11c-enriched cells isolated from the inguinal lymph nodes of vaccinated mice. Mice (three per group) were immunized with pcDNA3, pcDNA3-E7/GFP, or pcDNA3-VP22/E7/GFP DNA intradermally via gene gun. The inguinal lymph nodes were harvested from mice 3 days after gene gun vaccination. DCs were enriched from a single-cell suspension of lymph nodes, using CD11c microbeads. These CD11c-enriched cells were incubated with an E7-specific CD8⁺ T cell line (Wang *et al.*, 2000). The activating IFN- γ -secreting E7-specific CD8⁺ T cells were determined by staining for both CD8 and intracellular IFN- γ . (A) Representative flow cytometry data. The data presented are from one representative experiment of two performed. (B) Bar graph depicting the number of IFN- γ -secreting E7-specific CD8⁺ T cells per 5×10^4 E7-specific CD8⁺ T cells (mean \pm SD).

Eight-week long-term *in vivo* tumor protection experiment

For the long-term tumor protection experiment, mice (five per group) were vaccinated via gene gun with 2 μ g of pcDNA3, pcDNA3-E7, pcDNA3-VP22/E7, pcDNA3-E7/HSP70, pcDNA3-CRT/E7, pcDNA3-ETA(dII)/E7, or pcDNA3-Sig/E7/LAMP-1 DNA. One week later, mice were boosted by the same regimen as for the first vaccination. Seven weeks after the last vaccination, mice were intravenously challenged with TC-1 tumor cells (1×10^5 per mouse) via the tail vein. Mice were killed 28 days after tumor challenge and lung surface pulmonary nodules in each mouse were counted by experimenters blinded to sample identity as described previously (Ji *et al.*, 1998).

Statistical analysis

All data, expressed as means \pm SD, are representative of at least two different experiments. Data for intracellular cytokine staining with flow cytometry analysis and tumor treatment experiments were evaluated by analysis of variance (ANOVA).

Comparisons between individual data points were made by Student *t* test. All *p* values < 0.05 were considered significant.

RESULTS

Intradermal immunization with pcDNA3-VP22/E7 DNA led to a significant increase in E7-expressing DCs in draining lymph nodes of vaccinated mice

After intradermal immunization, DCs are known to migrate to draining lymph nodes, where they stimulate antigen-specific T cells (Condon *et al.*, 1996; Porgador *et al.*, 1998). We used GFP linked to E7 to serve as a fluorescent tag to identify DNA-transfected DCs in the inguinal lymph nodes. Inguinal lymph nodes were harvested from vaccinated mice 1, 3, or 5 days after gene gun immunization. Because there is a low quantity of DNA-transfected DCs in the inguinal lymph nodes, we enriched CD11c⁺ cells by means of CD11c (N418) microbeads. To reduce background and exclude CD11c⁺ cells that are not DCs, we gated around a population of cells consistent with DCs for

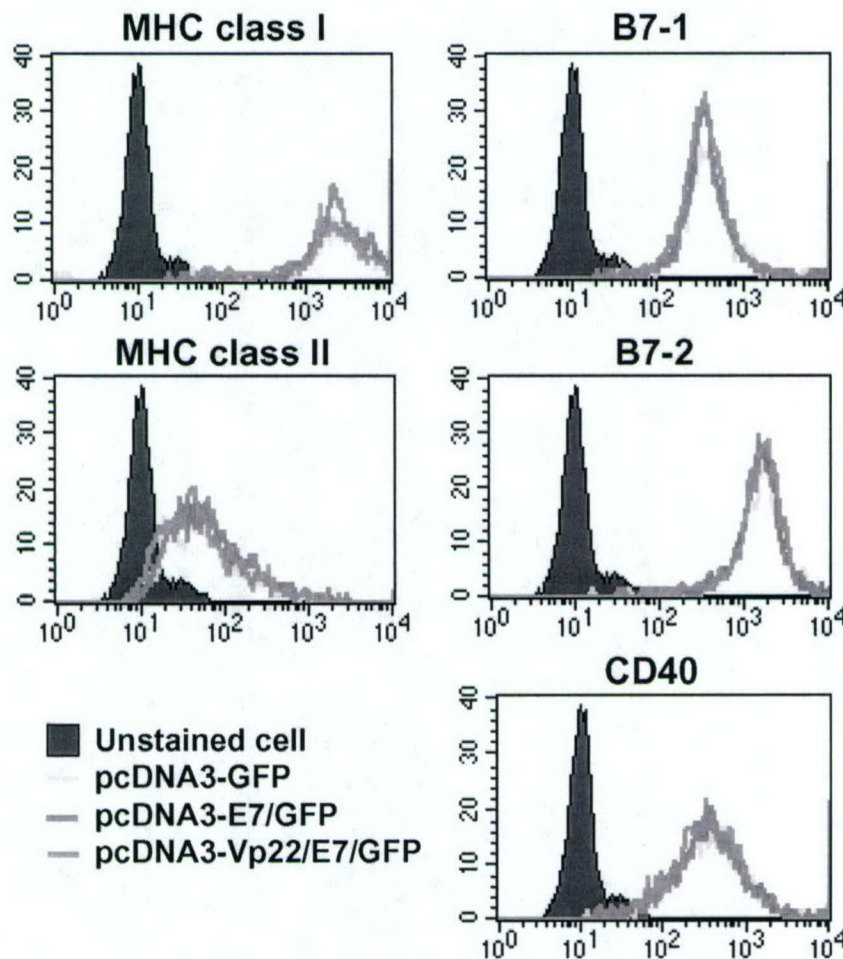


FIG. 3. Flow cytometry analysis to characterize the surface molecules in VP22/E7/GFP and E7/GFP DNA-transfected DCs. Flow cytometry analysis was performed on VP22/E7/GFP-transfected DCs and on E7/GFP-transfected DCs, using antibodies against MHC class I and class II molecules, B7-1 and B7-2 costimulatory molecules, and CD40. *Note:* We observed similar expression levels of these molecules on VP22/E7/GFP-transfected DCs and on E7/GFP-transfected DCs. The shaded areas represent cells stained only with secondary antibodies (negative control).

flow cytometry analysis. The percentage of CD11c⁺ cells among gated monocytes was more than 98% in each case (data not shown). Cells that were double-positive for GFP and CD11c likely represented antigen-expressing DCs, including DNA-transfected DCs, derived from vaccinated skin (Porgador *et al.*, 1998). We observed a significantly greater percentage of GFP⁺CD11c⁺ cells in lymph nodes harvested from mice vaccinated with VP22/E7/GFP DNA than in lymph nodes harvested from mice vaccinated with E7/GFP DNA ($p < 0.012$), or no insert ($p < 0.014$), 5 days after vaccination (Fig. 1A). There was some background of GFP⁺ cells in mice vaccinated with untagged pcDNA3. Interestingly, on day 1 and day 3 after vaccination, we did not observe a significant difference in the percentage of GFP⁺CD11c⁺ cells in inguinal lymph nodes between VP22/E7/GFP DNA- and E7/GFP DNA-vaccinated mice (Fig. 1B). These data suggested that the transfection efficiency of the E7/GFP DNA and VP22/E7/GFP DNA vaccines administered via gene gun is probably similar because the number of CD11c⁺GFP⁺ cells in mice vaccinated with GFP-containing DNA was similar 1 day or 3 days after vaccination. Our results also indicated that although the number of antigen-expressing DCs in the draining lymph nodes of VP22/E7/GFP- and E7/GFP-vaccinated mice is similar 3 days after vaccination, a significant increase

in antigen-expressing APCs in draining lymph nodes of VP22/E7/GFP DNA-vaccinated mice was detected only 5 days after vaccination, suggesting that intercellular spreading of antigen to APCs likely occurred later than 3 days after vaccination. In contrast, a significant decrease in antigen-expressing APCs in draining lymph nodes was observed in the E7/GFP DNA-vaccinated mice 5 days after vaccination when compared with 3 days after vaccination. Thus, we found that intercellular spreading of the marker protein within the epidermis resulted in a significantly increased number of antigen-expressing DCs in the draining lymph nodes of vaccinated mice.

Enhanced activation of E7-specific CD8⁺ T cell line by CD11c-enriched cells from VP22/E7 DNA-vaccinated mice

We then determined whether the linkage of VP22 to antigen would influence the ability of antigen-expressing DCs to activate antigen-specific CD8⁺ T cells *in vivo*. Because we observed that the number of antigen-expressing DCs in the draining lymph nodes of VP22/E7/GFP- and E7/GFP-vaccinated mice is similar 3 days after vaccination (Fig. 1B), inguinal lymph nodes were harvested from mice 3 days after gene gun

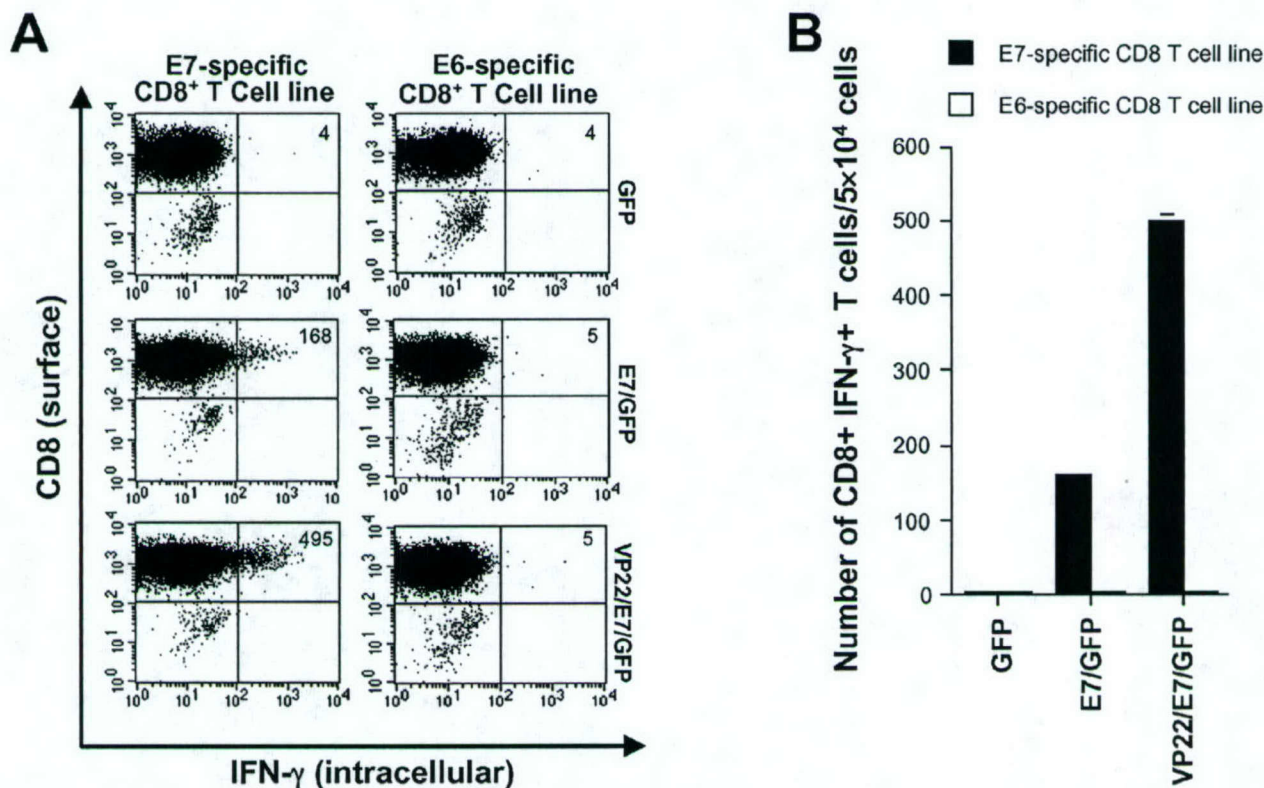


FIG. 4. Intracellular cytokine staining followed by flow cytometry analysis to determine the activation of E7-specific CD8⁺ T cells by DNA-transfected DCs. A DC line was transfected with GFP, E7/GFP, or VP22/E7/GFP plasmid DNA. The sorting of GFP⁺ DCs expressing GFP, E7/GFP, or VP22/E7/GFP was performed 24 hr after transfection. GFP⁺ DCs (1×10^5) were incubated with 1×10^6 cells from an E7-specific CD8⁺ T cell line (Wang *et al.*, 2000) for 4 hr. GFP⁺ DCs (1×10^5) were incubated with 1×10^6 cells from an E6-specific CD8⁺ T cell line for 4 hr as a negative control. Cells were then stained for both surface CD8 and intracellular IFN- γ and analyzed by flow cytometry. (A) Representative flow cytometry data. The data shown here are from one representative experiment of two performed. (B) Bar graph depicting the number of IFN- γ -secreting E7-specific CD8⁺ T cells per 1×10^6 E7-specific or E6-specific CD8⁺ T cells (mean \pm SD).

vaccination. CD11c⁺ cells were enriched from a single-cell suspension of lymph nodes, using CD11c microbeads (Miltenyi Biotec) as described above. CD11c-enriched cells were incubated with an E7-specific CD8⁺ T cell line (Wang *et al.*, 2000). Activated E7-specific CD8⁺ T cells were then stained for both surface CD8 and intracellular IFN- γ and analyzed by flow cytometry. As shown in Fig. 2A and B, CD11c-enriched cells isolated from mice vaccinated with pcDNA3-VP22/E7/GFP DNA were significantly more effective in activating the E7-specific CD8⁺ T cell line than were CD11c-enriched cells isolated from mice vaccinated with pcDNA3-E7/GFP ($p < 0.002$) or with pcDNA3-GFP ($p < 0.001$). Likewise, CD11c-enriched cells isolated from pcDNA3-VP22/E7/GFP-vaccinated mice 5 days after vaccination were more effective in activating the E7-specific CD8⁺ T cell line than were CD11c-enriched cells isolated from pcDNA3-E7/GFP- or pcDNA3-GFP-vaccinated mice 5 days after vaccination (data not shown). These results indicate that although there are a similar number of E7/GFP-expressing DCs in the draining lymph nodes of either E7/GFP DNA- or VP22/E7/GFP DNA-vaccinated mice 3 days after vaccination, there is significantly greater activation of E7-specific CD8⁺ T cells by DCs isolated from VP22/E7/GFP DNA-vaccinated mice. Our data suggest that the linkage of VP22 to antigen results in qualitative changes of antigen-expressing DCs and leads to enhanced activation of E7-specific CD8⁺ T cells.

No significant changes in DC surface markers of antigen-expressing DCs after transfection with VP22/E7/GFP DNA and with E7/GFP DNA

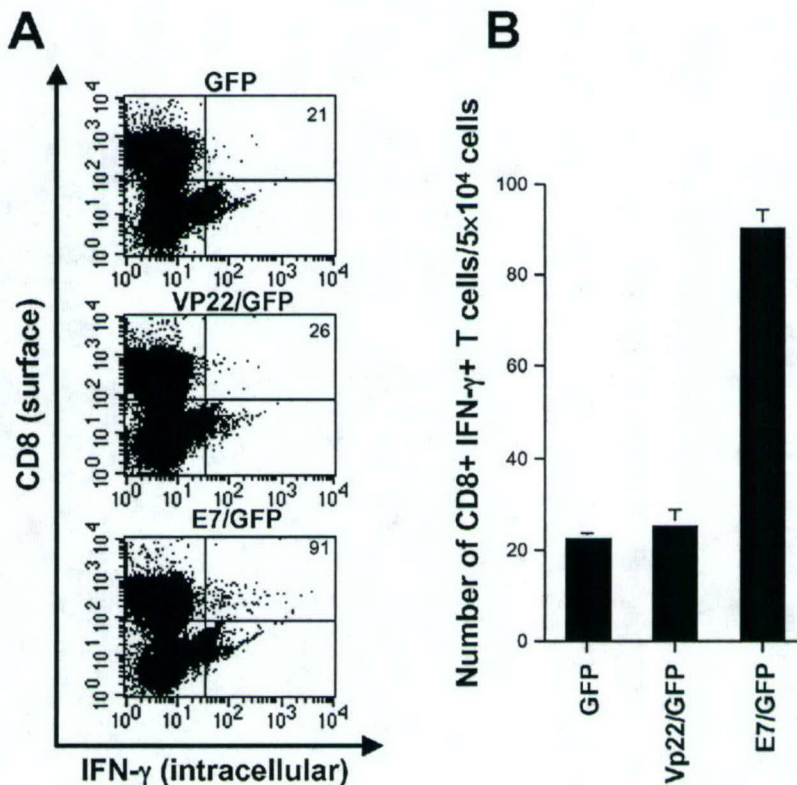
Because the qualitative changes of antigen-expressing DCs that led to enhanced activation of E7-specific CD8⁺ T cells

may be accounted for by an increase in expression of various DC surface molecules, we then determined whether the linkage of VP22 influences phenotypic changes of surface molecules (MHC class I, MHC class II, B7-1, B7-2, and CD40 molecules) on antigen-expressing DCs by flow cytometric analysis. We determined and compared the expression level of various DC markers in E7/GFP- and VP22/E7/GFP-transfected DCs. As shown in Fig. 3, we observed no significant differences between DNA-transfected DCs in terms of the expression of MHC class I, MHC class II, B7-1, B7-2, CD40, and other DC-specific markers. Our data suggest that the linkage of VP22 to antigen does not influence phenotypic changes in the characterized surface markers of antigen-expressing DCs.

Enhanced activation of E7-specific CD8⁺ T cells by pcDNA3-VP22/E7/GFP-transfected DCs

We determined whether the linkage of VP22 to E7 influenced the ability of DCs to activate an E7-specific CD8⁺ T cell line *in vitro*. DCs were transfected with DNA encoding GFP, E7/GFP, or VP22/E7/GFP. GFP⁺ DCs expressing GFP, E7/GFP, or VP22/E7/GFP were sorted by FACS advantage. GFP⁺ DCs were incubated with an E7-specific CD8⁺ T cell line. An E6-specific CD8⁺ T cell line was used as a negative control. IFN- γ -secreting E7-specific CD8⁺ T cells were determined by staining for both surface CD8 and intracellular IFN- γ and analyzed by flow cytometry. As shown in Fig. 4A and B, we observed a significant increase in the number of E7-specific IFN- γ -secreting CD8⁺ T cells from DCs transfected with VP22/E7/GFP DNA (260 ± 14.7) compared with DCs transfected with E7/GFP DNA (51 ± 9.6 ; $p < 0.001$), or no insert (2 ± 0.6 ; $p < 0.001$). Our data demonstrated that although ex-

FIG. 5. Intracellular cytokine staining and flow cytometry analysis to determine VP22-specific CD8⁺ T cells in mice vaccinated with VP22/E7 DNA. A DC line transfected with GFP, E7/GFP, or VP22/GFP plasmid DNA was used as a stimulator. CD8⁺ T cells (1×10^6), isolated from splenocytes of mice vaccinated with VP22/E7 DNA, were incubated for 6 hr with 1×10^5 GFP⁺ DCs. Cells were then stained for both surface CD8 and intracellular IFN- γ and analyzed by flow cytometry. (A) Representative flow cytometry data. The data shown here are from one representative experiment of two performed. (B) Bar graph depicting the number of IFN- γ -secreting, GFP-, VP22-, or E7-specific CD8⁺ T cells per 5×10^4 CD8⁺ T cells (mean \pm SD).



pression levels of the surface markers on VP22/E7/GFP DNA- and E7/GFP DNA-transfected DCs were similar, VP22/E7/GFP DNA-transfected DCs were capable of activating more E7-specific CD8⁺ T cells. Taken together, the data suggest that the linkage of VP22 molecule may influence the processing of antigen in DNA-transfected DCs.

Vaccination with VP22/E7 DNA does not elicit appreciable VP22-specific CD8⁺ T cells

To determine whether mice vaccinated with VP22/E7 DNA generated VP22-specific CD8⁺ T cells, we transfected a DC line with DNA encoding GFP, VP22/GFP, or E7/GFP and incubated the GFP⁺ DCs with splenocytes from mice vaccinated with DNA encoding VP22/E7. As shown in Fig. 5, we found that DCs transfected with E7/GFP ($78 \pm 3.6/5 \times 10^4$ splenocytes) generated significantly more IFN- γ -secreting CD8⁺ T cells than did DCs transfected with VP22/GFP ($16 \pm 2.0/5 \times 10^4$ splenocytes; $p < 0.013$) or GFP ($12 \pm 2.0/5 \times 10^4$ splenocytes; $p < 0.012$), and that DCs transfected with VP22/GFP generated a minimal increase in IFN- γ -secreting CD8⁺ T cells compared with DCs transfected with GFP. These data suggest that vaccination with DNA encoding a VP22/E7 fusion protein

does not generate appreciable CD8⁺ T cell immune responses against epitopes derived from VP22.

Mice vaccinated with pcDNA3-VP22/E7 DNA generated long-term E7-specific CD8⁺ T cells

Several lines of evidence suggest that CD8⁺ T cell-mediated immune responses are important in controlling both HPV infections and HPV-associated neoplasms. It is therefore important to assess quantitative changes in the number of E7-specific CD8⁺ T cells in mice vaccinated with the various DNA vaccines. We determined the number of IFN- γ -secreting E7-specific CD8⁺ T cells, using splenocytes taken from vaccinated mice at intervals of 1 week, 4 weeks, and 8 weeks. These mice were vaccinated with one of the following DNA vaccine constructs: pcDNA3, pcDNA3-E7, pcDNA3-CRT/E7, pcDNA3-E7/HSP70, pcDNA3-ETA(dII), pcDNA3-Sig/E7/LAMP-1, and pcDNA3-VP22/E7. As shown in Fig. 6, whereas mice vaccinated with pcDNA3-CRT/E7 generated the highest E7-specific CD8⁺ T cell response 1 week after the last vaccination, pcDNA3-VP22/E7 DNA generated more E7-specific IFN- γ -secreting CD8⁺ memory T cells 8 weeks postvaccination compared with mice

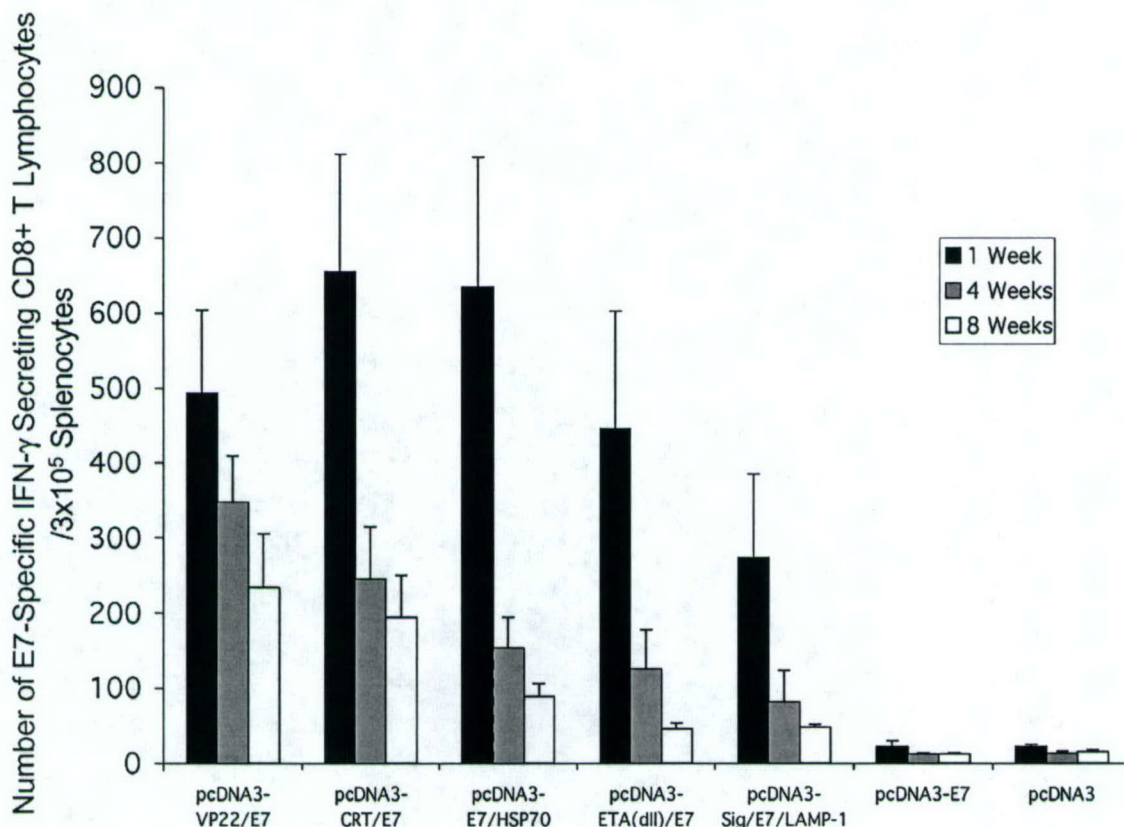


FIG. 6. Intracellular cytokine staining followed by flow cytometry analysis to determine the number of IFN- γ -secreting E7-specific CD8⁺ T cell precursors generated by various DNA vaccines at 1, 4, and 8 weeks after vaccination. Mice were immunized and splenocytes were collected and cultured as described in Materials and Methods. Splenocytes were collected 1, 4, and 8 weeks after initial vaccination. Bar graph depicting the numbers of E7-specific IFN- γ -secreting CD8⁺ T cells (mean \pm SD) generated by various recombinant DNA vaccines at 1 week, 4 weeks, and 8 weeks after vaccination. Note: Our data shows that at the end of the eight weeks, mice vaccinated with pcDNA3-VP22/E7 have the highest average number of E7-specific CD8⁺ T cell precursors.

vaccinated with the other vaccine constructs. Also, mice vaccinated with pcDNA3-VP22/E7 retained a greater percentage (~50%) of their initial E7-specific CD8⁺ T cell burst as memory cells than did mice vaccinated with the six other constructs. Our data suggest that mice vaccinated with pcDNA3-VP22/E7 DNA were capable of efficiently generating high levels of long-term E7-specific CD8⁺ memory T cells.

pcDNA3-VP22/E7 DNA vaccine provided enhanced long-term tumor protection in vaccinated mice

To determine whether the ensuing E7-specific CD8⁺ memory T cells generated by the pcDNA3-VP22/E7 vaccine translate to prolonged tumor protection against E7-expressing TC-1 tumor cells, we performed a long-term tumor protection experiment in mice vaccinated with pcDNA3, pcDNA3-E7, pcDNA3-CRT/E7, pcDNA3-E7/HSP70, pcDNA3-ETA(dII), pcDNA3-Sig/E7/LAMP-1, or pcDNA3-VP22/E7 DNA. Eight weeks after the first vaccination, mice were intravenously challenged with 1×10^5 TC-1 cells per mouse. As shown in Fig. 7, mice vaccinated with pcDNA3-VP22/E7 exhibited significantly fewer pulmonary nodules than mice vaccinated with pcDNA3-E7 ($p < 0.006$). In addition, mice vaccinated with pcDNA3-VP22/E7 or pcDNA3-CRT/E7 exhibited the lowest number of pulmonary nodules compared with mice vaccinated with the other five constructs. Our data indicate that

pcDNA3-VP22/E7 and pcDNA3-CRT/E7 provided enhanced long-term tumor protection in vaccinated mice.

DISCUSSION

In this study, we demonstrated that DNA vaccines employing the VP22 strategy generated marked increases in the number of antigen-expressing DCs in draining lymph nodes and more antigen-specific CD8⁺ memory T cells, and enhanced long-term antitumor effects in vaccinated mice. Furthermore, our data also suggest that the linkage of a VP22 molecule may influence the processing of linked antigen in DNA-transfected DCs, leading to enhanced activation of antigen-specific CD8⁺ T cells.

Our results indicated that, although the number of antigen-expressing DCs in the draining lymph nodes of VP22/E7GFP- and E7/GFP-vaccinated mice is similar 1 or 3 days after vaccination, a significant increase in antigen-expressing DCs in the draining lymph nodes of VP22/E7/GFP DNA-vaccinated mice was detected 5 days after vaccination compared with E7/GFP-vaccinated mice or mice vaccinated with empty vector (Fig. 1). This increase was likely due to VP22-mediated spreading of linked E7/GFP antigen to DCs postvaccination. The spreading of VP22-linked antigen from DNA-transfected cells to surrounding cells may be time dependent. Our previous study ob-

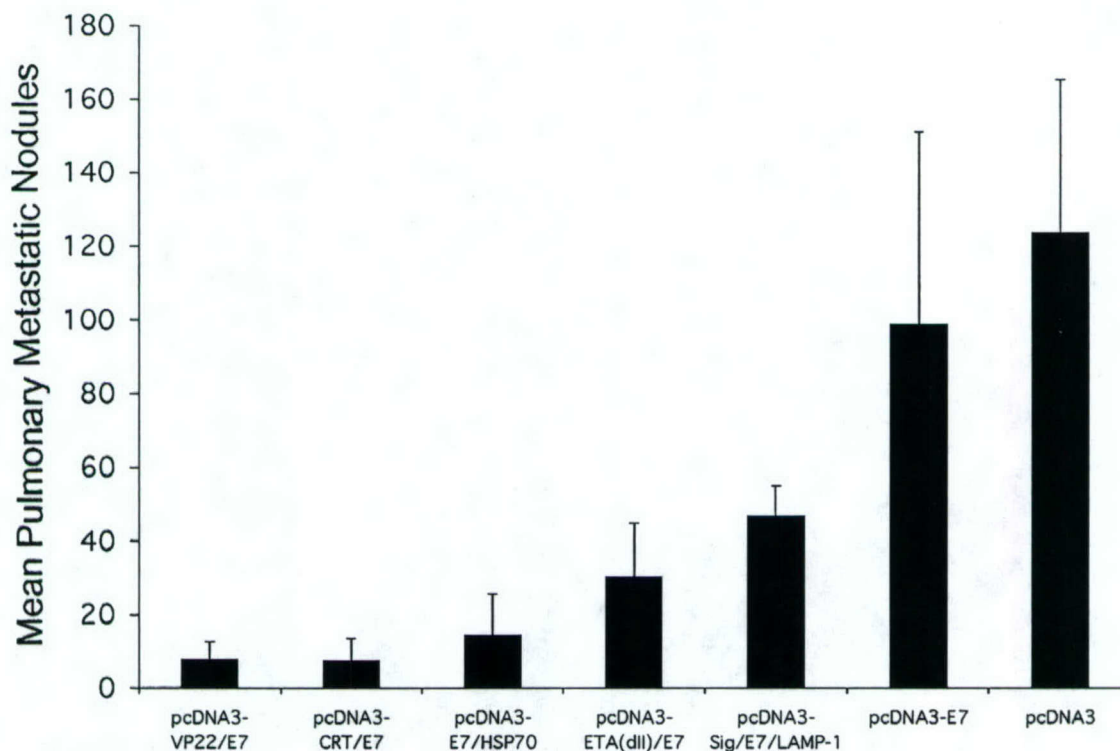


FIG. 7. Long-term *in vivo* tumor protection experiments to compare the antitumor effect generated by various DNA vaccine constructs in vaccinated mice eight weeks after initial vaccination. Mice were immunized with various DNA constructs and challenged with 1×10^5 TC-1 tumor cells/mouse 8 weeks after the initial DNA vaccination. Data are expressed as the mean number of lung nodules (mean \pm SD). Note: Mice vaccinated with pcDNA3-VP22/E7 and pcDNA3-CRT/E7 exhibited the lowest mean number of pulmonary metastatic nodules.

served that intercellular spreading mediated by VP22 did not take effect until 72 hr after gene transfer *in vitro* (Cheng *et al.*, 2002). Thus, the spreading of VP22-linked antigen may occur 3 days after gene transfer *in vivo*. Migration of antigen-expressing DCs as a result of VP22-mediated spreading 3 days postvaccination might contribute to the observed peak number of E7/GFP⁺ DCs 5 days postvaccination in mice vaccinated with VP22/E7/GFP DNA, although we cannot rule out other potential mechanisms.

We found that administration of DNA encoding VP22 linked to antigen resulted in an increased number of antigen-expressing DCs in draining lymph nodes and enhanced activation of E7-specific CD8⁺ T cells. We attribute this increase to intercellular spreading because the VP22 molecule likely facilitates the spreading of the linked antigen to surrounding DCs. However, we could not rule out the possibility that vaccination with DNA encoding VP22 may affect DC migration through chemokines or other factors that influence DC homing to draining lymph nodes after acquisition of antigen in the periphery. We also could not conclusively exclude the possibility that VP22 may affect the apoptotic or antiapoptotic functions of DCs by prolonging the survival of DCs, leading to more DCs in draining lymph nodes.

Our data indicated that the linkage of VP22 to antigen may potentially enhance MHC class I presentation of the linked antigen. Because we observed that the number of antigen-expressing DCs in the draining lymph nodes of VP22/E7/GFP- and E7/GFP-vaccinated mice is similar 3 days after vaccination (Fig. 1B), these DCs were isolated, enriched by means of CD11c microbeads, and incubated with an E7-specific CD8⁺ T cell line to compare their ability to activate E7-specific CD8⁺ T cells. As shown in Fig. 2, CD11c-enriched cells isolated from mice vaccinated with pcDNA3-VP22/E7/GFP DNA were more effective in generating significantly more IFN- γ -secreting E7-specific CD8⁺ T cells than were CD11c-enriched cells isolated from mice vaccinated with pcDNA3-E7/GFP DNA. The observed enhanced activation of E7-specific CD8⁺ T cells may be due to the phenotypic or functional changes of DCs expressing VP22/E7/GFP. However, we did not observe significant differences in MHC class I, MHC class II, B7-1, B7-2, or CD40 expression on the surface of an E7-expressing DC line (Fig. 3). Therefore, it is likely that the linkage of VP22 to E7 may lead to enhanced processing and presentation of E7 through the MHC class I pathway. Our data, based on the use of an E7-specific CD8⁺ T cell line incubated with a DC line transfected with the various DNA vaccines, were consistent with this notion (Fig. 4). We have previously observed that the linkage of VP22 to E7 antigen in transfected 293 cells also leads to enhanced MHC class I presentation of E7 (Hung *et al.*, 2001a). Thus, the data strongly suggest that the linkage of VP22 molecule to antigen may influence the processing of antigen in DNA-transfected DCs.

In vaccine development, CD8⁺ memory T cells are important for creating a vaccine that can elicit long-lived protection against viral infection and tumor in a vaccinated host. Immune response that is mediated by CD8⁺ memory T cells is more rapid and aggressive than the primary response. This response can control infections faster and can fully eliminate the pathogen. In the context of long-term CD8⁺ memory T cell responses, our results demonstrated that pcDNA3-VP22/E7-vac-

inated mice generated the highest number of E7-specific CD8⁺ memory T cells compared with other constructs. As shown in Fig. 6, we observed that at the end of 8 weeks, pcDNA3-VP22/E7 generated a higher level of E7-specific CD8⁺ memory T cells, more than 10-fold higher than pcDNA3-E7, in vaccinated mice. Interestingly, half of the initial CD8⁺ effector T cells survived to become CD8⁺ memory T cells. Furthermore, we observed that in our 8-week tumor protection experiment (Fig. 7), mice receiving the pcDNA3-VP22/E7 DNA vaccine exhibited the lowest number of pulmonary nodules after TC-1 challenge. Data from the experiments supported the importance of CD8⁺ memory T cells, in that a vaccine capable of generating higher levels of CD8⁺ memory T cells can more effectively provide long-term protection against pathogen in a vaccinated host.

In summary, our findings illustrate the promise of using the VP22 strategy to enhance vaccine potency by generating more antigen-expressing DCs in draining lymph nodes, more antigen-specific CD8⁺ memory T cells, and better long-term protective immunity in vaccinated mice. Thus, VP22 may facilitate future vaccine development for the control of cancers and infectious disease.

ACKNOWLEDGMENTS

We thank Drs. Robert J. Kurman and Drew M. Pardoll for helpful discussions. We also thank Drs. Ken-Yu Lin and Richard Roden for critical review of the manuscript. This work was supported by the National Cancer Institute, the Cancer Research Institutes, and the American Cancer Society.

REFERENCES

- CHEN, C.-H., JI, H., SUH, K.W., CHOTI, M.A., PARDOLL, D.M., and WU, T.C. (1999). Gene gun-mediated DNA vaccination induces antitumor immunity against human papillomavirus type 16 E7-expressing murine tumor metastases in the liver and lungs. *Gene Ther.* **6**, 1972-1981.
- CHEN, C.-H., WANG, T.-L., HUNG, C.-F., YANG, Y., YOUNG, R.A., PARDOLL, D.M., and WU, T.-C. (2000). Enhancement of DNA vaccine potency by linkage of antigen gene to an HSP70 gene. *Cancer Res.* **60**, 1035-1042.
- CHENG, W.-F., HUNG, C.-F., CHAI, C.-Y., HSU, K.-F., HE, L., LING, M., and WU, T.-C. (2001). Tumor-specific immunity and antiangiogenesis generated by a DNA vaccine encoding calreticulin linked to a tumor antigen. *J. Clin. Invest.* **108**, 669-678.
- CHENG, W.-F., HUNG, C.F., HSU, K.F., CHAI, C.Y., HE, L., POLO, J.M., SLATER, L.A., LING, M., and WU, T.C. (2002). Cancer immunotherapy using Sindbis virus replicon particles encoding a VP22-antigen fusion. *Hum. Gene Ther.* **13**, 553-568.
- CONDON, C., WATKINS, S.C., CELLUZZI, C.M., THOMPSON, K., and FALO, L.D., Jr. (1996). DNA-based immunization by *in vivo* transfection of dendritic cells. *Nat. Med.* **2**, 1122-1128.
- DONNELLY, J.J., ULMER, J.B., SHIVER, J.W., and LIU, M.A. (1997). DNA vaccines. *Annu. Rev. Immunol.* **15**, 617-648.
- ELLIOTT, G., and O'HARE, P. (1997). Intercellular trafficking and protein delivery by a herpesvirus structural protein. *Cell* **88**, 223-233.
- FELTKAMP, M.C., SMITS, H.L., VIERBOOM, M.P., MINNAAR, R.P., DE, J.B., DRIJFHOUT, J.W., TER, S.J., MELIEF, C.J., and KAST, W.M. (1993). Vaccination with cytotoxic T lymphocyte epi-

- tope-containing peptide protects against a tumor induced by human papillomavirus type 16-transformed cells. *Eur. J. Immunol.* **23**, 2242–2249.
- HUNG, C.-F., CHENG, W.-F., CHAI, C.-Y., HSU, K.-F., HE, L., LING, M., and WU, T.-C. (2001a). Improving vaccine potency through intercellular spreading and enhanced MHC class I presentation of antigen. *J. Immunol.* **166**, 5733–5740.
- HUNG, C.-F., CHENG, W.-F., HSU, K.-F., CHAI, C.-Y., HE, L., LING, M., and WU, T.-C. (2001b). Cancer immunotherapy using a DNA vaccine encoding the translocation domain of a bacterial toxin linked to a tumor antigen. *Cancer Res.* **61**, 3698–3703.
- HUNG, C.-F., HSU, K.-F., CHENG, W.-F., CHAI, C.-Y., HE, L., LING, M., and WU, T.-C. (2001c). Enhancement of DNA vaccine potency by linkage of antigen gene to a gene encoding the extracellular domain of Flt3-ligand. *Cancer Res.* **61**, 1080–1088.
- Jl, H., CHANG, E.Y., LIN, K.Y., KURMAN, R.J., PARDOLL, D.M., and WU, T.C. (1998). Antigen-specific immunotherapy for murine lung metastatic tumors expressing human papillomavirus type 16 E7 oncoprotein. *Int. J. Cancer* **78**, 41–45.
- Jl, H., WANG, T.-L., CHEN, C.-H., HUNG, C.-F., PAI, S., LIN, K.-Y., KURMAN, R.J., PARDOLL, D.M., and WU, T.-C. (1999). Targeting HPV-16 E7 to the endosomal/lysosomal compartment enhances the antitumor immunity of DNA vaccines against murine HPV-16 E7-expressing tumors. *Hum. Gene Ther.* **10**, 2727–2740.
- KIM, T.W., HUNG, C.F., LING, M., JUANG, J., HE, L., HARDWICK, J.M., KUMAR, S., and WU, T.C. (2003). Enhancing DNA vaccine potency by coadministration of DNA encoding antiapoptotic proteins. *J. Clin. Invest.* **112**, 109–117.
- LAPPIN, M.B., WEISS, J.M., DELATTRE, V., MAI, B., DITTMAR, H., MAIER, C., MANKE, K., GRABBE, S., MARTIN, S., and SIMON, J.C. (1999). Analysis of mouse dendritic cell migration in vivo upon subcutaneous and intravenous injection. *Immunology* **98**, 181–188.
- PENG, S., HUNG, C.F., TRIMBLE, C., HE, L., YEATERMEYER, J., and WU, T.C. (2003). Development of an HPV-16 DNA vaccine targeting E6. Submitted.
- PORGADOR, A., IRVINE, K.R., IWASAKI, A., BARBER, B.H., RESTIFO, N.P., and GERMAIN, R.N. (1998). Predominant role for directly transfected dendritic cells in antigen presentation to CD8⁺ T cells after gene gun immunization. *J. Exp. Med.* **188**, 1075–1082.
- ROBINSON, H.L. (1997). Nucleic acid vaccines: An overview. *Vaccine* **15**, 785–787.
- SHEN, Z., REZNIKOFF, G., DRANOFF, G., and ROCK, K.L. (1997). Cloned dendritic cells can present exogenous antigens on both MHC class I and class II molecules. *J. Immunol.* **158**, 2723–2730.
- WANG, T.-L., LING, M., SHIH, I.-M., PHAM, T., PAI, S.I., LU, L., KURMAN, R.J., PARDOLL, D.M., and WU, T.-C. (2000). Intramuscular administration of E7-transfected dendritic cells generates the most potent E7-specific anti-tumor immunity. *Gene Ther.* **7**, 726–733.
- WU, T.-C., GUARNIERI, F.G., STAVELEY-O'CARROLL, K.F., VISCIDI, R.P., LEVITSKY, H.I., HEDRICK, L., CHO, K.R., AUGUST, T., and PARDOLL, D.M. (1995). Engineering an intracellular pathway for MHC class II presentation of HPV-16 E7. *Proc. Natl. Acad. Sci. U.S.A.* **92**, 11671–11675.

Address reprint requests to:

Dr. T.-C. Wu
Department of Pathology
Johns Hopkins University School of Medicine
Ross 512H, 720 Rutland Avenue
Baltimore, MD 21205

E-mail: wutc@jhmi.edu.

Received for publication June 18, 2003; accepted after revision December 31, 2003.

Published online: January 21, 2004.